Elucidating the Role of WRNIP1 in the Protection of Stalled Replication Forks

DISSERTATION

ZUR

ERLANGUNG DER NATURWISSENSCHAFTLICHEN DOKTORWÜRDE

(Dr. sc. nat.)

VORGELEGT DER

MATHEMATISCH-NATURWISSENSCHAFTLICHEN FAKULTÄT

DER

UNIVERSITÄT ZÜRICH

VON

BARTLOMIEJ POREBSKI

AUS

POLEN

PROMOTIONSKOMMISSION:

PROF. DR. KERSTIN GARI (VORSITZ UND LEITUNG DER DISSERTATION)

PROF. DR. MASSIMO LOPES

PROF. DR. LORENZA PENENGO

PD. DR. MANUEL STUCKI

PROF. DR. PIERRE-HENRI GAILLARD

ZÜRICH, 2018

Contents

ABSTRACT

DNA is the blueprint of life. It contains all the information necessary for the synthesis of proteins – the building blocks and workhorses of the cell. Maintenance of DNA in an unchanged state is therefore of utmost importance, since any mutations or loss of the information it holds may lead to catastrophic events, such as cell death or tumorigenesis. DNA needs to be faithfully copied with every cell division, which is an enormous task, given its size and importance. DNA replication is constantly challenged by endogenous and exogenous factors, which have the potential to stall or stop replication – such a circumstance is called replication stress. While cells have evolved a number of mechanisms to deal with replication stress, e.g. checkpoint signaling that halts the cell cycle, DNA repair pathways that remove obstacles or factors that stabilise stalled replication forks, persisting replication stress inevitably leads to genomic instability and tumorigenesis. Interestingly, cancer cells, due to their unrestricted proliferation, have elevated level of replication stress, which makes them more susceptible to anti-cancer therapies that exacerbate genomic instability. It is thus obvious that dissecting the events and mechanisms leading to and following replication stress is important from a basic science and clinical research point of view.

Among the many aspects of replication stress, one that is gaining an increasing amount of attention is replication fork stability. Over the last years it was shown that a stalled replication fork is rapidly remodeled into a 4-way structure, an event that is believed to contribute to its stabilisation. However, such a structure needs to be carefully maintained, since lack of its protection may cause an unscheduled processing by nucleases, leading to genomic instability. Interestingly, among the factors that protect stalled replication forks are many proteins previously associated with other DNA repair pathways, such as homologous recombination or Fanconi anaemia. The most recent member of the 'protectosome' group is WRNIP1 (Werner helicase interacting protein 1), but its mode of action is unclear.

In this project, we attempted to characterise WRNIP1's biochemical activities and investigate further its cellular function. We have found that the protein exerts its protective function downstream of replication fork reversal, challenging the current model. Our in vitro data show that WRNIP1 binds specifically to 4-way DNA junctions, a structure resembling a reversed replication fork. We have also found that WRNIP1 interacts directly with the replication fork remodeler ZRANB3 and that it is able to limit its replication fork reversal activity in vitro. Combined with published data, our data led us to propose a mechanism in which WRNIP1 binds to reversed replication forks immediately after their generation, thus protecting them against unscheduled MRE11-dependent degradation.

ZUSAMMENFASSUNG

DNA ist der Bauplan des Lebens. Sie enthält alle notwendigen Informationen für die Synthese von Proteinen, den molekularen Werkzeugen der Zelle. Die Integrität der DNA ist äusserst wichtig, da Mutationen oder der Verlust von Erbinformation katastrophale Folgen, wie Zelltod oder Tumorentstehung, haben können. Mit jeder Zellteilung muss die DNA zuverlässig verdoppelt werden, was angesichts der Grösse des Genoms und seiner entscheidenden Bedeutung eine enorme Herausforderung darstellt. Die Replikation der DNA wird ständig durch endogene oder exogene Faktoren beeinträchtigt, was dazu führen kann, dass die Replikation blockiert oder abgebrochen wird. Diesen Zustand bezeichnet man als Replikationsstress. Die Zelle hat verschiedene Mechanismen entwickelt, um Replikationsstress entgegenzuwirken; diese umfassen zum Beispiel die Aktivierung von Checkpoints, die den Zellzyklus anhalten, oder Faktoren, die blockierte Replikationsgabeln stabilisieren. Trotz dieser Schutzmechanismen führt anhaltender Replikationsstress unausweichlich zu genomischer Instabilität und Tumorigenese. Interessanterweise sind Krebszellen aufgrund ihres unkontrollierten Wachstums inhärent erhöhten Levels an Replikationsstress ausgesetzt. Dies macht sie empfindlicher gegenüber Krebstherapien, die die genomische Instabilität weiter steigern. Daher ist es offensichtlich, dass die Analyse von Vorgängen, die Replikationsstress verursachen sowie entgegenwirken, nicht nur für die Grundlagenforschung, sondern auch für die klinische Forschung von grosser Bedeutung ist.

Einer der vielen Aspekte von Replikationsstress, der in den letzten Jahren wachsende Beachtung bekam, ist die Stabilisation von Replikationsgabeln. Es wurde gezeigt, dass blockierte Replikationsgabeln rasch zu vierarmigen Strukturen umgebaut werden, was vermutlich zu ihrer Stabilisation beiträgt. Jedoch müssen auch diese Strukturen geschützt werden, um zu vermeiden, dass sie von Nukleasen prozessiert werden, was wiederum zu genomischer Instabilität führen kann. Unter den Faktoren, die einen protektiven Effekt auf Replikationsgabeln haben, befinden sich erstaunlich viele Proteine, die zuvor mit dem DNA-Reparatursystem in Verbindung gebracht wurden. Diese umfassen unter anderem Fanconi-Anämie-Enzyme und Proteine, die an der homologen Rekombination beteiligt sind. Das zuletzt identifizierte Mitglied der sogenannten 'Protektosom'-Gruppe ist WRNIP1 (Werner helicase interacting protein 1), doch seine genaue Wirkungsweise ist unklar.

Ziel dieses Projektes war es, die biochemischen Aktivitäten von WRNIP1 zu charakterisieren und seine zelluläre Funktion zu untersuchen. Wir haben festgestellt, dass das Protein seine protektive Funktion erst nach der Umkehrung der Replikationsgabel ausführt, was ein bestehendes Modell in Frage stellt. Unsere in vitro-Daten zeigen ausserdem, dass WRNIP1 spezifisch an vierarmige DNA-Strukturen bindet, welche reversierten Replikationsgabeln ähneln. Wir haben auch eine direkte Interaktion zwischen WRNIP1 und ZRANB3 identifiziert und konnten zeigen, dass

WRNIP1 in vitro ZRANB3's Fähigkeit, Replikationsgabeln in vierarmige Strukturen umzubauen, reduziert. In Kombination mit publizierten Daten deuten unsere Ergebnisse auf einen Mechanismus hin, in dem WRNIP1 direkt nach der Reversierung an Replikationsgabeln bindet und sie so vor einer MRE11-abhängigen Degradation schützt.

ACKNOWLEDGEMENTS

I would like to express my gratitude to Prof. Dr. Kerstin Gari for giving me the opportunity of becoming a member of her group and for involving me in this interesting project that has, does and will continue to challenge and surprise me. Moreover, I would like to thank for the incredible support, which was a perfect blend of hands-on supervision and independence, allowing me to develop my scientific instincts, project management skills and to make and learn from my own mistakes. Regarding the latter, I want to thank for the patience and understanding. Above all that, I am grateful for showing me high scientific standards that I will do my best to follow in my scientific career.

I also want to thank all the members of my PhD Thesis Committee: Prof. Dr. Massimo Lopes, Prof. Dr. Lorenza Penengo, Prof. Dr. Pierre-Henri Gaillard and PD Dr. Manuel Stucki for useful discussions and support I received during my PhD thesis.

Furthermore, I would like to thank all the members of the Gari group for creating a work environment that made my lab experience challenging, stimulating, but also very smooth and humorous. I want to especially thank Sandra Kummer for contributing greatly to my project by establishing cell lines, expression systems and performing the interactome study.

Last, but not least, I want to thank the entire Institute of Molecular Cancer Research. The former and the present directors for fostering the family-like environment and the stimulating atmosphere, and the technical and administrative staff who keep the place operating seamlessly. Also, all other members of the institute for the exchange of knowledge and ideas, for all the help and expertise I was supported with, especially from PD. Dr. Stefano Ferrari, Dr. Kurt Jacobs and Dr. Sofija Mijic.

INTRODUCTION

1 Life cycle of a cell

A cell can be considered the most basic biological entity, due to its ability to perform all the activities being hallmarks of life, i.e. metabolism, growth, response to environmental stimuli and, most importantly, reproduction that ensures survival. All living organisms - from the simplest prokaryotes to the most complex eukaryotes - are composed of cells, which, despite fundamental differences between the two superdomains, follow a similar cycle of growth and reproduction that involves regulated duplication and equal division of cellular contents, yielding two identical daughter cells.

1.1 The eukaryotic cell cycle is divided into discrete phases

In contrast to prokaryotic cells, the eukaryotic cell cycle is divided into discrete phases, during which events, ultimately leading to cell division, happen in a sequential and highly regulated manner (Figure 1). The human cell cycle is generally divided into two main phases: mitosis and interphase, with the former being the moment when the cell physically divides and the latter consisting of cell growth and duplication of genetic material. Interphase starts after a cell has divided or received a signal that forces it to leave the quiescent state. In the first phase, G_1 (gap 1), the cell grows in size, synthesizing proteins necessary for subsequent stages, and, depending on internal and external cues, either commits to the cycle or leaves it, entering aforementioned quiescence phase (G_0).

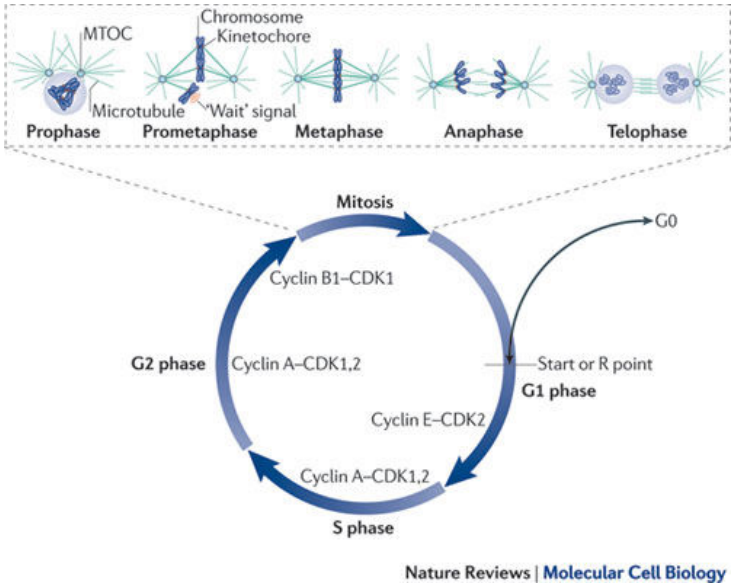

Figure 1: Eukaryotic cell cycle (Pines, 2011).

After G_1, which in human somatic cells can last up to 11 hours, the cell enters the S-phase (synthesis) when the blueprint of life – DNA – is replicated, which will be described in the next section. Cycling human cells allocate around one-third (approximately 8 hours) of the whole cell cycle to complete S-phase. Following is a second, shorter (approx. 4 hours), gap phase (G_2) when the cell continues to grow, synthesizes proteins necessary for mitosis

and ensures that it is ready to divide. In the final, shortest (approx. 1 hour) phase (M), the cell segregates its contents into two pools and undergoes cytokinesis, yielding two identical daughter cells (Alberts et al., 2002).

Due to its importance and complexity, the cell cycle is strictly regulated by both extra- and intra-cellular mechanisms. The former, including nutrient availability and the presence of growth factors, applies mainly to G_1. In cycling cells, nutrients shortage will cause entering quiescent state when the cell suspends growth until conditions become optimal again. On the other hand, cells that naturally remain in G_0, as is the case for many animal cell types, start cycling only if they receive an extracellular stimulus forcing them to proliferate, e.g. skin fibroblasts during wound healing. The intra-cellular mechanism of cell cycle control is built around so-called "checkpoints" - points during the cell cycle when it can be halted if certain conditions needed to progress to the next phase are not met. For instance, progression from G_1 to S is delayed when DNA is damaged, progression from G_2 to M requires completion of DNA replication, and mitosis is halted when chromosomes are not properly attached to the mitotic spindle (Alberts et al., 2002).

1.2 Strict regulation of the cell cycle is necessary to avoid unrestricted proliferation

While cell cycle control mechanisms are not absolutely required for the cell to commit to division, they are essential to ensure that the process is completed with a positive outcome, e.g. that chromosomes are separated properly, mutations in DNA are not passed on or that a cell does not go through more rounds of proliferation than it is supposed to. Unsurprisingly, the gene most frequently mutated in cancers, *TP53*, encodes a protein which negatively regulates entry into S-phase and, in case of DNA damage that is beyond repair, triggers apoptosis. Inactivation of *p53* allows cancer cells to replicate DNA that contains lesions, thus propagating genomic instability and leading to further deregulation of cellular processes. At the same time, loss of *p53* function prevents apoptosis, therefore cancer cells are not eliminated from the population, further committing to neoplasia (Alberts et al., 2002).

2 DNA Replication

As already mentioned, cells allocate around a third of the cell cycle to replicate DNA. Since DNA stores the information about, among others, how all the proteins are built, it is of utmost importance to ensure that the molecule is passed to the daughter cells intact, making DNA maintenance processes, like replication and repair, the most crucial ones in the life of a cell.

2.1 Genome duplication is initiated from replication origins in a highly regulated manner

While the bulk of DNA synthesis takes place in S-phase, the replication process already starts in G_1 when the pre-replicative complex (pre-RC) is loaded onto the chromatin at certain loci, called origins of replication (licensing) (Figure 2). In contrast to yeast *Saccharomyces cerevisiae*, features marking replication origins have not been precisely identified in metazoans, however there seems to be a preference for CpG islands and G-rich regions that can form G-quadruplexes. Importantly, DNA replication can only be triggered from the origins that have been licensed, which, when coupled to the fact that licensing is limited to G_1, provides a very elegant way to avoid re-replication of the genome. Upon G_1-S transition, additional factors are loaded to the pre-RC, including components of the replicative helicase CMG (Cdc45-GINS-MCM) and the replicative polymerases Polϵ, Polα and Polδ. Finally, with the entry to S-phase, the processivity factor Proliferating Cell Nuclear Antigen (PCNA) is loaded with the help of the Replication Factor C (RFC) complex, to complete the replisome – the functional unit of replication. Initiation of DNA synthesis, or origin firing, also undergoes strict control. First, only a subset of licensed origins is activated, the rest is kept dormant

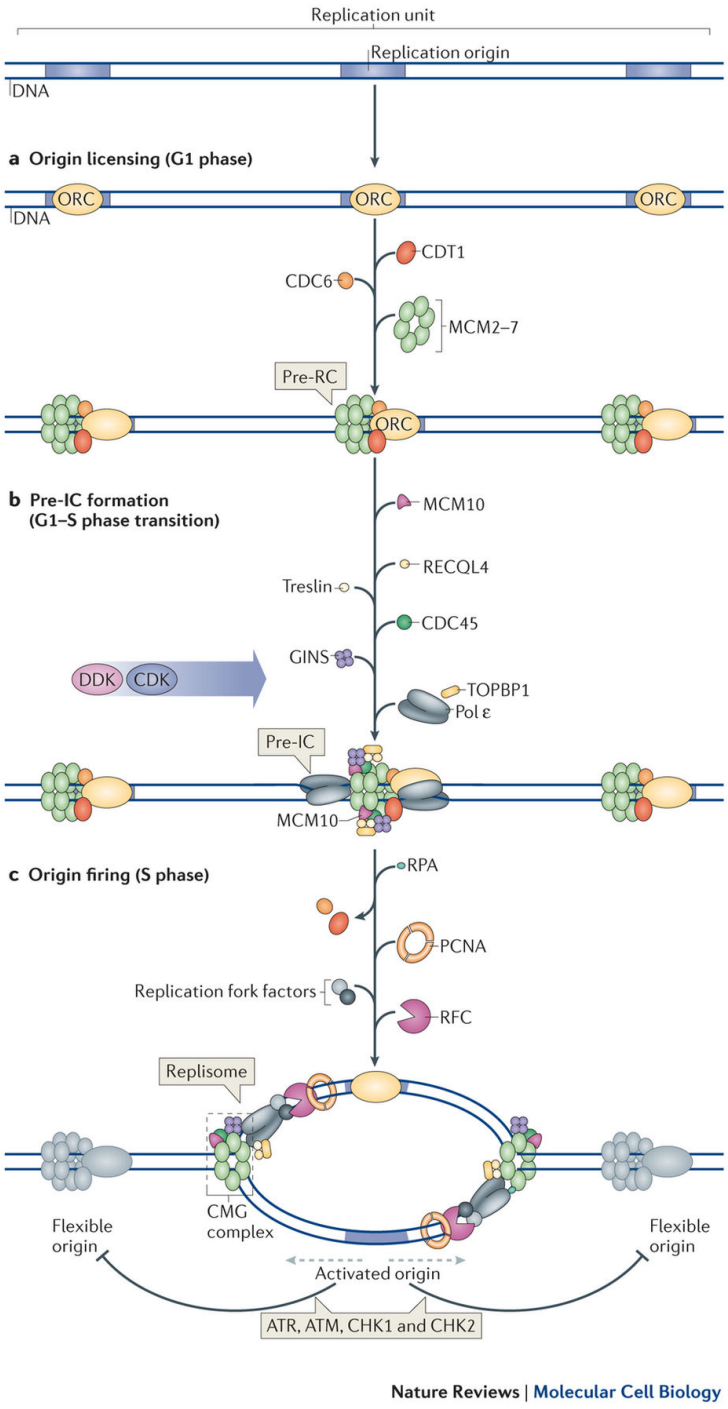

Figure 2: Overview of replication initiation (Fragkos et al., 2015). See text for explanation.

to serve as a backup, should active replisomes encounter a roadblock. Secondly, to avoid exhaustion of replication factors, not all origins are activated at the same time. It was found that euchromatin is being replicated in the early, while transcriptionally inactive heterochromatin in the late, stage of S-phase. On top of transcription, over the last years, chromatin topology has been recognised as an important determinant of replication origin usage, with chromosomal regions being in close proximity in space being replicated at the same time. Lastly, the intra-S-phase checkpoint plays an important role in the regulation of origin firing also during unperturbed replication, as discussed in the subsequent section (rev. in: Leonard and Méchali (2013), Fragkos et al. (2015)).

2.2 DNA replication is carried out by the replisome at replication forks

At a molecular level, DNA replication is a two-step process, consisting of unwinding of parental duplex to subsequently use both strands as templates for the synthesis of new ones; both activities are performed at the replication fork by distinct factors within the replisome in a concerted manner. The former function is provided by the CMG complex, which, upon origin firing, translocates on the parental DNA by virtue of its ATPase activity, prying two strands apart. The resulting positive supercoiling ahead of the replication fork is resolved by Topoisomerase I, which is indispensable for unhindered replication fork movement. Subsequent DNA synthesis is initiated by DNA primase (Polymerase Alpha subunit) synthesizing a short RNA primer, which is further extended by Polα's DNA polymerase activity. Afterwards, replicative polymerases Polδ and Polϵ take over, synthesizing long stretches of DNA with high fidelity, thanks to their processivity and proofreading capabilities. Due to the chemistry of DNA polymerisation that allows extension of the primer only at its 3' end, synthesis of one strand (leading) is continuous, while growth of the other (lagging) is achieved by repeated cycles of priming and extension, producing short (100-200 nt) Okazaki fragments that are processed and ligated together upon completion by DNA2, FEN1 and DNA Ligase I (rev. in: Branzei and Foiani (2010), Leman and Noguchi (2013)). According to the consensus view, there is a division of labour between the two replicases, with Polϵ synthesising the leading and Polδ the lagging strand. However, this view is being challenged over the last couple of years with studies presenting strong evidence for one polymerase doing the bulk of DNA replication and the other having an auxiliary role (Georgescu et al. (2014), Yeeles et al. (2015), Johnson et al. (2015), rev. in Lujan et al. (2016)). Although depictions of the replisome are usually simplified to the proteins performing the main enzymatic activities essential for DNA replication, which is in line with the recently established 'minimal replisome' (Yeeles et al., 2015), a number of targeted and unbiased proteomic studies show that the replisome is a far much more complex assembly consisting of DNA and RNA metabolising proteins, chromatin remodelers, components of signaling pathways, etc. (Alabert et al. (2014), Dungrawala et al. (2015), Ribeyre et al. (2016)).

2.3 DNA replication is challenged by a wide variety of exogenous and endogenous factors

What has also become evident is that the composition of the replication fork proteome changes in response to replication stress (Dungrawala et al. (2015), Ribeyre et al. (2016)), a circumstance when DNA synthesis is stalled or stopped. Replication stress can be caused by pathological conditions, like unrepaired DNA lesions, reduced dNTPs pools, DNA-protein cross-links or oncogene activation leading to de-regulation of origin firing, as well as by sources connected to normal cellular processes and features, such as metabolites, replication-transcription collisions, torsional stress, difficult-to-replicate sequences, secondary DNA structures or ribonucleotide misincorporation (Zeman and Cimprich, 2014). The multitude of potential sources suggests that cells are subjected to replication stress on a daily basis. Under normal conditions, it is efficiently dealt with by pathways dedicated to DNA damage signaling, repair and cell cycle control (rev. in Ciccia and Elledge (2010)); as already noted, if damage exceeds repair capacity, the cell may be forced to undergo apoptosis or enter senescence.

2.4 Replication stress is a potent driver, but also an Achilles heel, of tumorigenesis

Aforementioned replication stress response pathways were found to be activated in many precancerous lesions and to act, together with the tumour suppresor protein p53, as a barrier against tumorigenesis (Figure 3). It was proposed that these benign early lesions progress to malignancy when the DNA damage response pathways or p53 function are compromised, exacerbating genomic instability and evading apoptosis (Bartkova et al. (2005), Halazonetis et al. (2008)). On the other hand, counter-intuitively at first, cancer cells are more dependent on DDR pathways to sustain unrestricted proliferation. This is due to the fact that, while mild replication stress is a potent driver of tumorigenesis, high level leads to cell death by mitotic catastrophe, acting as an onco-

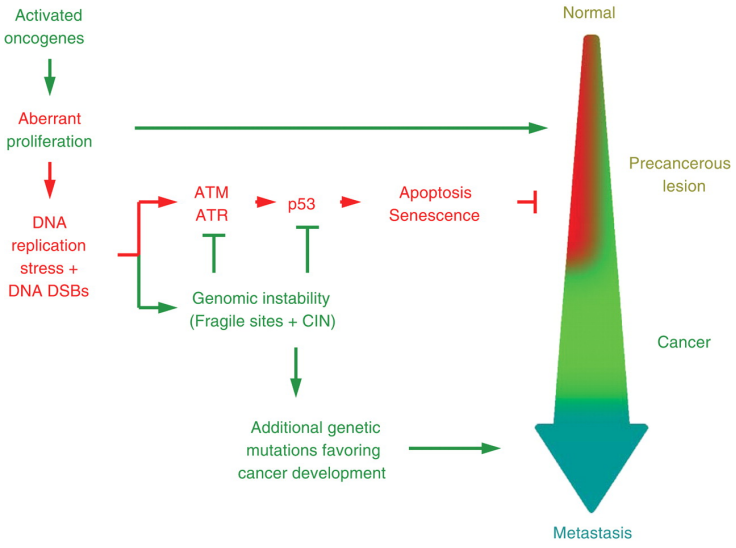

Figure 3: Model for contribution of replication stress and genome instability to tumorigenesis (Halazonetis et al., 2008).

suppresive mechanism. In fact, many anti-cancer therapies, intentionally or not, are based on aggravating replication stress to levels lethal for cancer cells, yet still tolerable for the healthy ones. Conventional approaches, like radiotherapy, alkylating agents or platinum-based compounds, introduce DNA lesions, nucleoside analogues reduce the pool of available dNTPs, and topoisomerases poisons elevate torsional stress - all these have been used as anti-cancer drugs for years, but only recently were linked to replication stress. Moreover, as our understanding of this phenomenon progresses, more targeted approaches are under development, for instance selective inhibitors of the ATR-Chk1 signaling cascade that signals replication stress ((Aguilera and Gómez-González, 2008), Gaillard et al. (2015), Zhang et al. (2016)). All in all, as our knowledge on the subject expands, it is becoming more evident that replication stress can and should be considered one of the hallmarks of cancer (Macheret and Halazonetis (2015), Hanahan and Weinberg (2011)).

3 Replication stress response

3.1 ATR initiates the cellular response to replication stress

3.1.1 Activation of ATR signaling cascade at stalled replication forks

The replication stress response may be considered a specific sub-pathway of the DNA damage response. It is not triggered directly by lesions, but is rather a consequence of the replication fork encountering an obstacle. Such an event causes fork stalling and leads to the generation of long stretches of ssDNA that, when coated with the ssDNA-binding protein RPA (Replication Protein A), contributes to the activation of ATR (Ataxia telangectasia and Rad3-related) – the kinase that orchestrates the replication stress response (Figure 4) (rev. in Saldivar et al. (2017)). Excess ssDNA can stem from functional uncoupling of the helicase and polymerase functions of the replisome (Byun et al., 2005). A second requirement for an efficient ATR activation is a 5'-ended ssDNA-dsDNA junction, arising either naturally on the lagging strand due to repeated priming or as a result of re-priming on the leading strand template e.g. by PrimPol (Mourón et al., 2013). Both of these structures can be also formed by stalled fork remodeling and processing, which will be described in subsequent sections. Important components necessary for triggering the ATR cascade are early activating factors: ATRIP (ATR-interacting protein), TOPBP1 (Topoisomerase II binding protein 1) and ETAA1 (Ewing tumour-associated antigen 1), which facilitate ATR recruitment to the ssDNA-RPA and engage its kinase activity (rev. in Saldivar et al. (2017)).

3.1.2 ATR-CHK1 cascade suppresses cell cycle progression and origin firing in response to replication stress

Two key effects of ATR - cell cycle arrest and suppression of late origin firing - are mediated via phosphorylation of its substrate, CHK1 (Checkpoint Kinase 1) (rev. in Saldivar et al. (2017)). While cell cycle arrest is presumed to simply prevent entry into mitosis with damaged or under-replicated DNA, ATR's role in origin firing regulation is more complex. Of note, ATR-CHK1 pathway prevents excessive origin firing in an unperturbed S-phase, presumably to ensure that the amount of active replisomes does not exceed the supply of replication factors. Indeed, it was shown that forcing unscheduled origin firing by ATR inhibition causes global fork breakage even in unchallenged cells and is exacerbated by the induction of replication stress; it was attributed to the exhaustion of RPA when too many replisomes are active at the same time (Toledo et al., 2014). On the other hand, the ATR pathway is believed to activate dormant origins in the vicinity of stalled replication forks to complete replication. While the mechanism of this local activation is enigmatic, it is suspected that all origins within a chromatin region that is being replicated are immune to inhibition by the checkpoint (rev. in Saldivar et al. (2017)).

3.1.3 ATR stabilises stalled replication forks by preventing RPA exhaustion and regulating fork-associated proteins

Another important role of ATR in the replication stress response is to stabilise the stalled replication fork, i.e. to ensure that the replisome is able to resume replication when the stress is dealt with, by preventing detrimental processing and promoting restart efforts. One way ATR achieves this is via the aforementioned inhibition of late origin firing, which prevents exhaustion of the cellular pool of RPA, a protein that when bound to ssDNA serves as a recruitment platform for many DDR proteins (Toledo et al., 2014). It is also plausible that excessive origin firing might deplete other factors necessary for stalled fork stabilisation. Also, ATR may exert its protective function by regulating enzymes that process stalled replication forks. Indeed ATR was shown to phosphorylate several replication fork remodelers, such as SMARCAL1 (SWI/SNF-related, matrix-associated, actin-dependent regulator of chromatin, subfamily-A-like 1) (Couch et al., 2013), WRN (Werner syndrome helicase) and BLM (Bloom syndrome helicase) (rev. in Urban et al. (2017)). It was shown that hyperactivation of SMARCAL1 caused by ATR-inhibition, may cause generation of SLX4 (Structure-specific endonuclease subunit SLX4)-dependent DNA breaks, suggesting that remodeling of stalled replication forks has to be strictly controlled (Couch et al., 2013). Importantly, while it was believed that fork breakage is associated with disassembly of the replisome, proteome-wide study using iPOND-SILAC (Isolation of Proteins on Nascent DNA-Stable Isotope Labeling with Amino Acids in Cell Culture) mass spectrometry showed that the core replisome proteins remain

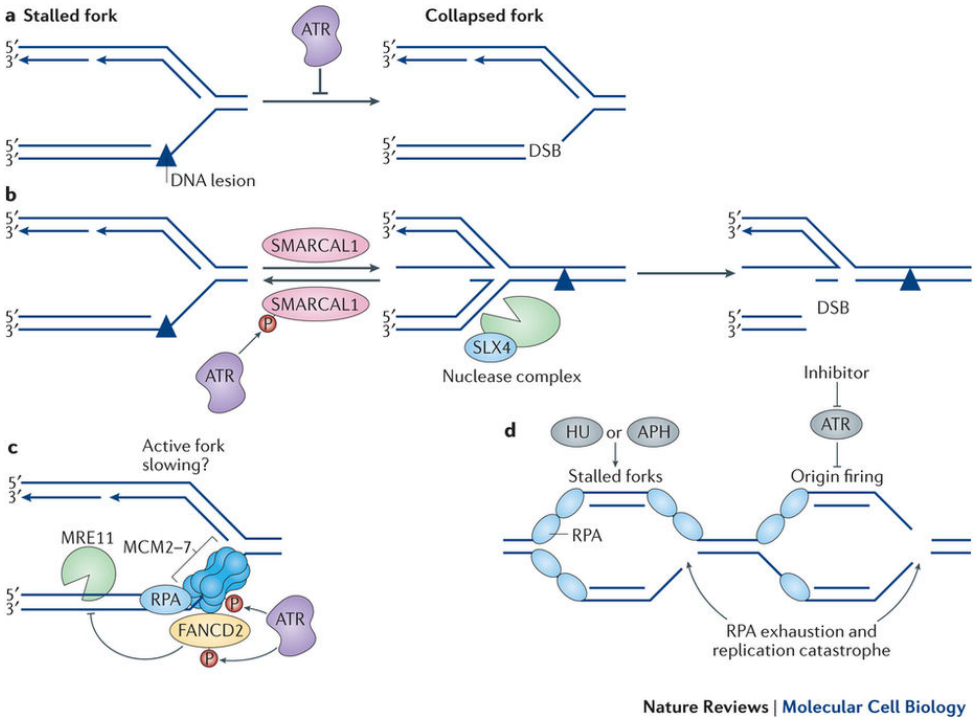

Figure 4: Proposed effects of ATR-mediated signaling in the replication stress response (Saldivar et al., 2017).

stably bound at stalled replication forks (Dungrawala et al., 2015). The same study also provided quantitative data about the proteome of stalled replication forks, strengthening the involvement of many proteins, conventionally linked to canonical DNA repair pathways, in the events at stalled replication forks. Interestingly, many of these factors are known ATR substrates (rev. in Toledo et al. (2017)).

3.2 PCNA orchestrates events at replication forks

A second important event that senses and signals replication stress is the modification of PCNA, induced when the replisome is stalled. PCNA is one of the main conductors of events at the replication fork. In unperturbed conditions, it stimulates processivity of replicative polymerases and acts as an interaction hub for enzymes processing Okazaki fragments (rev. in Moldovan et al. (2007)); all PCNA-interacting proteins have conserved binding motifs, with the PIP (PCNA-interacting protein)-box being the most common one.

3.2.1 Modification of PCNA by ubiquitin is decisive for replication stress response pathway choice

Besides its function in replication, PCNA coordinates the replication stress response at a stalled replisome, in a modification-dependent manner. Upon replication fork stalling, PCNA is either

mono-ubiquitylated at the conserved lysine 164 (K164) by Rad6/Rad18 (*S. cerevisiae* E2 ubiquitin-conjugating enzyme and E3 ubiquitin ligase, respectively) or poly-ubiquitylated by Rad5/Ubc13-Mms2 (*S. cerevisiae* E3 and E2, respectively), forming lysine-63-linked poly-Ub chains. In general, the ubiquitylation of PCNA triggers a DNA damage tolerance pathway, which, as the name suggests, allows replication to pass the lesion, without prior repair. The type of PCNA modification dictates the choice of subpathway. Mono-Ub recruits translesion synthesis (TLS) polymerases that are able to accommodate the damaged base in their catalytic centre and insert a nucleotide opposite. Frequently, the inserted nucleotide is incorrect, therefore TLS pathway is considered error-prone. On the other hand, poly-ubiquitylation of PCNA triggers an error-free pathway; it is thought to involve template switching or recombination-mediated replication, but the exact mechanism is still unknown. It is often suggested that replication fork reversal may be one of the transactions mediating it (rev. in Moldovan et al. (2007), Mailand et al. (2013)). While in yeast, poly-ubiquitylation of PCNA and its effects are well established, research in human cells proved to be more challenging. To induce and sustain the modification, acute genotoxic treatments or specific genetic conditions are required (Brun et al. (2010), Ciccia et al. (2012)). Moreover, there are two human homologues of Rad5 - HLTF (Helicase-like transcription factor) and SHPRH (SNF2 histone linker PHD ring helicase) (Motegi et al., 2008); the choice of the E3 ligase seems to be dependent on the type of DNA lesion (Lin et al., 2011). Recently, a third ubiquitin ligase able to modify PCNA was detected – TRAIP (TRAF interacting protein) (Hoffmann et al., 2016).

3.2.2 PCNA SUMOylation regulates recombination at replication forks

Apart from ubiquitylation, PCNA can be also modified by SUMO (Small ubiquitin-like modifier) at the same residue – Lys164. The majority of discoveries on this subject were made in yeast, where SUMOylation of PCNA is well established, in contrast to human cells. In yeast, a portion of PCNA was found to be constitutively SUMOylated during the S-phase. The modification serves as a recruitment platform for SUMO-PCNA readers that have a SIM (SUMO-interacting motif) domain, such as Srs2 – a helicase that prevents unscheduled recombination by destabilising Rad51 nucleofilaments (rev. in Mailand et al. (2013)). Several human orthologues of Srs2 have been proposed based on their ability to disrupt RAD51-ssDNA complexes, e.g. RTEL1 (Barber et al., 2008), FBH1 (F-box DNA helicase 1) (Fugger et al., 2009), however only one of them – PARI (PCNA-interacting partner) – was shown to bind SUMO-PCNA (Moldovan et al., 2012). It has to be noted though, that SUMOylation of PCNA in human cells cannot be detected unless a tagged ectopic allele of SUMO is overexpressed (Gali et al., 2012), rendering the presence of such a modification on human PCNA a subject of ongoing debate.

4 Transactions at stalled replication forks

4.1 Importance of stalled fork stabilisation

Ensuring the stability of a stalled replication fork is of great importance, since failure to do so results in replication fork breakage, or collapse. Fork collapse is defined as a loss of capacity to perform DNA synthesis; such a general definition allows accommodating multiple proposed events leading to the collapse, e.g. replisome disassembly or nucleolytic degradation. Irrespective of the cause, fork collapse can lead to incomplete or aberrant DNA replication, which may result in the loss of genetic information, chromosomal aberrations, aneuploidy, etc. Thus, replication fork collapse can be considered as the molecular event underlying genomic instability, emphasising the importance of fork stabilisation (Zeman and Cimprich (2014), Cortez (2015), Gaillard et al. (2015)).

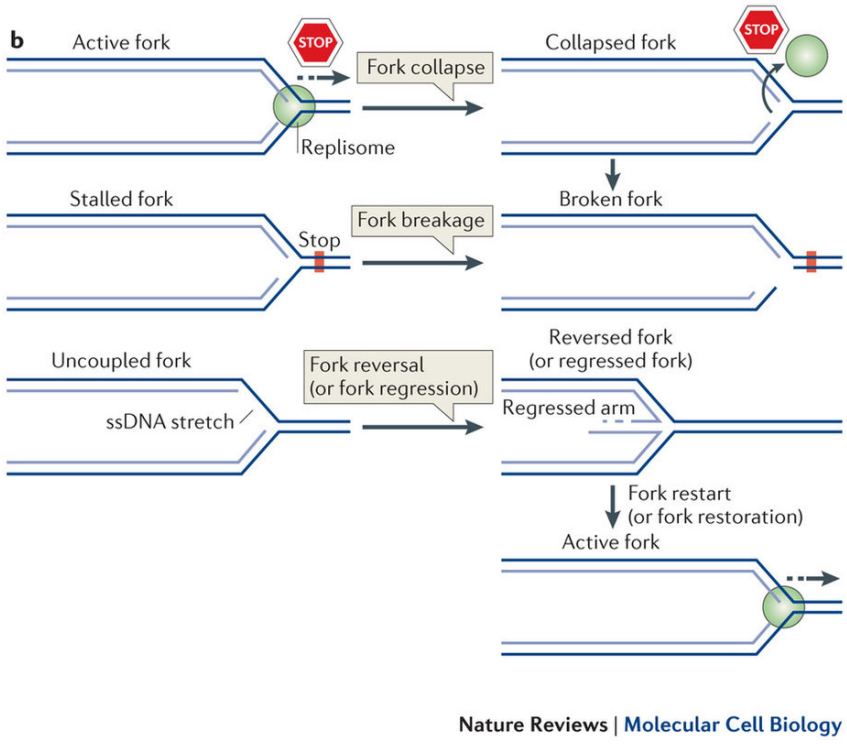

Figure 5: A general overview of possible transactions at replication forks following genotoxic stress. Stalled replicaiton fork regression into a 4-way structure may prevent fork collapse (loss of replicative potential) or fork breakage (DSB formation at a fork) and enable restoration of an active replication fork when replication stress subsides. Modified from (Neelsen and Lopes, 2015).

4.2 Replication fork reversal is an early response to replication stress

In order to avoid replication fork breakage, it is intuitive to imagine that response mechanisms should be in place that would enable recruitment of canonical DNA repair factors and allow them to process the lesion, while, at the same time, provide a way to restart the fork, after the damage is repaired, or to by-pass the lesion. One such mechanism was proposed in 1976; it assumed remodeling of the fork stalled by a single-strand lesion into a four-way junction by fork reversal, which would cause the two nascent strands to anneal. Such a transaction would create an alternative template for the stalled strand, therefore allowing replication without the need to remove the lesion (Higgins et al., 1976). In another scenario, fork reversal could facilitate the repair of the damage by relocating it back into the dsDNA region, which could make it more accessible to DNA repair enzymes. Despite being an appealing idea, it was subsequently discredited due to technical concerns. Two decades later, a study in *Escherichia coli* showed that replication-associated double-strand breaks are dependent on the activity of the RuvAB complex, which is able to generate four-way junctions (Holliday junctions) by means of its branch migration activity, reviving the idea of stalled fork reversal (Seigneur et al., 1998). Several years afterwards, studies in *S. cerevisiae* showed that replication stalling with hydroxyurea (HU) in checkpoint-deficient cells causes accumulation of four-way replication intermediates (Lopes et al., 2001). The intermediates were further identified as reversed forks with the use of electron microscopy (Sogo et al., 2002).

Interestingly, while fork reversal observed in bacteria was thought to be a way to avoid excessive fork breakage and ensure fork restart (rev. in Michel and Sandler (2017)), evidence from yeast suggested that the regressed fork is a pathological structure that only occurs when the replication checkpoint is defective (Lopes et al. (2001), Sogo et al. (2002)). Over the next ten years, multiple studies showed that fork reversal could be catalysed by several enzymes in vitro (rev. in Neelsen and Lopes (2015) and see below). The first evidence for replication fork reversal in human cells came in 2012, when it was reported that mild Topoisomerase I inhibition by CPT (camptothecin) causes fork regression in a PARP1 (Poly [ADP-Ribose] Polymerase 1)-dependent manner. The fact that this remodeling event was necessary to limit CPT-induced double-strand breaks was a strong argument in favour of replication fork reversal being a protective, rather than a deleterious event (Ray Chaudhuri et al., 2012). Further work from the same lab has shown that replication forks are regressed also in response to oncogene over-expression (Neelsen et al., 2013), on repetitive sequences (Follonier et al., 2013) and, finally, by induction of replication stress with several commonly used genotoxins (Zellweger et al., 2015). Moreover, in the cited studies, a small amount of regressed forks was reproducibly found in unchallenged cells. All these data strongly suggest that replication fork reversal is a general response to replication stress and is needed to prevent replication fork collapse (Figure 5).

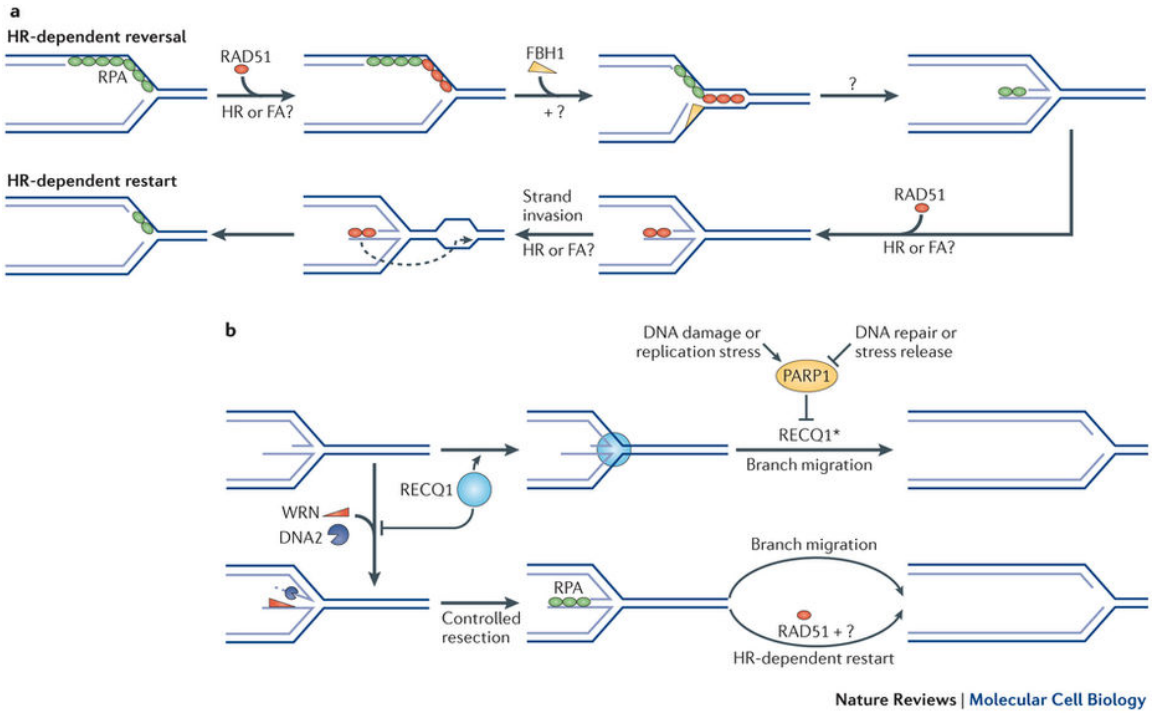

Figure 6: A general view on formation and processing of reversed replication forks (Neelsen and Lopes, 2015). See text for explanation

4.3 Factors involved in replication fork remodeling

The mechanism of stalled fork reversal is still a subject of research and discussion, however early work in bacteria suggests an involvement of homologous recombination (HR) factors, conventionally thought to act exclusively in double-strand break repair (Seigneur et al., 1998). In this study, the authors concluded that HR proteins act on a RuvAB-reversed fork to protect it from nucleolytic cleavage and assist replication restart. Further studies in human cells implicate more homologous recombination proteins, such as RAD51 (Hashimoto et al. (2010), Petermann et al. (2010)), BRCA2 (Lomonosov et al. (2003), Schlacher et al. (2011)), BRCA1 (Schlacher et al., 2012) and MRE11 (Hashimoto et al. (2010), Schlacher et al. (2011), Schlacher et al. (2012)), in the events at a stalled replication fork. Also, recent data shows that polyubiquitylation of PCNA that initiates the recombination-dependent PRR pathway, as described earlier, is necessary for replication fork reversal in human cells (Vujanovic et al., 2017).

4.3.1 RAD51 is a central node in replication fork reversal

The exact molecular events leading to replication fork reversal are yet to be elucidated, but RAD51 seems to play a central role in the process. It was found to be indispensable for replication fork reversal induced by a panel of genotoxins in human U2OS cells (Zellweger et al., 2015). RNAi-mediated depletion of RAD51 completely abrogated replication fork reversal, directly assayed by

electron microscopy, along with reverting other phenotypical features associated with the reversal: slowdown of replication fork progression, ssDNA accumulation at the stalled fork and a lack of double-strand breaks induction. Since RAD51 associates with replication forks even in unperturbed conditions (Zellweger et al., 2015), its activity has to be controlled to avoid unscheduled recombination. Recently, RADX (RPA-related, RAD51-antagonist on X-chromosome), a ssDNA- and RAD51-binding protein, was shown to limit RAD51's recruitment to replication forks, thus limiting remodeling events (Dungrawala et al., 2017).

4.3.2 ATPases mediating replication fork reversal in vitro and in cells

Apart from RAD51, a number of enzymes were suggested to mediate replication fork remodeling (rev. in Neelsen and Lopes (2015)). All these enzymes use the energy from ATP hydrolysis to either first unwind and then anneal DNA strands (canonical helicases) or migrate the branch point (translocases).

DNA helicases So far, 5 helicases able to remodel fork-like structures were identified in human cells: the RECQ helicases BLM, WRN, RECQL5 (RECQ-like helicase 5) (rev. in Urban et al. (2017)) and RECQL1 (Berti et al., 2013) and FBH1 (Fugger et al., 2015).

RECQ helicases Among these, the best studied are BLM and WRN. While in vitro, both proteins can mediate fork regression, as well as fork restoration reactions, their functions in cells are not clear. Both are recruited to replication forks under stress conditions, where they are targets for ATR-dependent phosphorylation. Apart from being a target, WRN was also found to promote activation of the ATR cascade. Cells lacking or expressing a mutant allele of WRN are highly sensitive to replication-stress-inducing agents, have impaired replication fork restoration and elevated frequency of replication fork reversal (rev. in Urban et al. (2017)). All these phenotypes could be explained with data suggesting that WRN co-operates with DNA2 in the controlled resection of reversed replication forks to facilitate their restart (Thangavel et al., 2015). Reports about BLM helicase suggest that it may be involved in the control of RAD51-mediated recombination at the fork - on the one hand the two proteins co-operate in the restoration of replication forks, but on the other, Bloom-syndrome-patient-derived cells have an elevated frequency of sister chromatid exchanges (SCEs), which are thought to result from unrestricted recombination events (rev. in Urban et al. (2017)).

The third member of the human RECQ family, RECQ5, is also able to regress replication-fork-like structures in vitro (rev. in Neelsen and Lopes (2015)). The cellular function of RECQ5 is not clear, however existing evidence shows that it is involved in the prevention or resolution of

replication intermediates that arise from transcription-replication collisions (rev. in Urban et al. (2017)).

FBH1 FBH1, one of the putative functional homologues of yeast Srs2, FBH1 was initially identified as a suppressor of RAD51-mediated recombination following replication stress, by displacing RAD51 from chromatin in a helicase-activity-dependent fashion (Fugger et al. (2009), Simandlova et al. (2013)). Moreover, FBH1 can directly ubiquitylate RAD51, which prevents its association with DNA (Chu et al. (2015)). FBH1 also co-operates with MUS81 in the generation of DSBs after prolonged replication fork stalling, which triggers apoptosis, thus eliminating cells with high levels of genomic instability (Fugger et al., 2013). On the other hand, FBH1 has been later shown to mediate replication fork reversal, both in vitro and, as the first human enzyme, in cells (Fugger et al., 2015). Nonetheless, these somewhat contradictory data can be explained by a model where FBH1 does promote replication fork regression immediately after fork stalling, however, if the fork is not recovered within a certain time, FBH1 displaces RAD51 from the reversed fork, which enables MUS81-dependent DSB formation. Indeed, the duration of genotoxic treatments used in the cited studies supports this hypothesis, demonstrating how dynamic the events at stalled replication forks are and underscoring the necessity for a careful experimental design.

DNA translocases Apart from DNA helicases, several dsDNA translocases were proposed as good candidates for mediating replication fork reversal (rev. in Neelsen and Lopes (2015), Poole and Cortez (2017)). These enzymes recognise the branch point of a fork and are able to migrate it, so that the parental strands are wound back and the nascent ones annealed together, forming the regressed arm. So far, five dsDNA translocases have been implicated in replication fork reversal – RAD54 (DNA repair and recombination protein RAD54), FANCM (Fanconi anaemia group M protein), SMARCAL1, ZRANB3 (Zinc finger, RAN-binding domain containing 3) and HLTF.

RAD54 RAD54 activities have been analysed mainly in vitro, where it was identified as a dsDNA translocase that is able to perform branch migration of 3- and 4-way junctions, with a preference for fork reversal over restoration. Additionally, RAD54 interacts with RAD51 and promotes its association with DNA. Even though biochemical activities of RAD54 make it a perfect candidate for mediating fork reversal, there is no data from experiments in cells that would support this hypothesis (rev. in Mazin et al. (2010)).

FANCM The Fanconi anaemia translocase FANCM was shown to drive replication fork reversal in vitro (Gari et al., 2008b), maintain replication in cells in an ATP-dependent manner (Blackford et al., 2012) and activate ATR signaling upon replication stress (Collis et al., 2008). Also,

recent data suggest a role of FANCM at the replisome stalled by an ICL, where the protein is suspected to drive fork regression that would facilitate either ICL repair or its traverse (Walter lab, unpublished, Mutreja and Lopes, unpublished).

HLTF, SMARCAL1, ZRANB3 The next two translocases - SMARCAL1 and ZRANB3 - were identified as the first enzymes that are able to rewind complementary DNA strands and were termed "annealing helicases" (Yusufzai and Kadonaga (2008), Yusufzai and Kadonaga (2010)). It was then shown that the proteins use this activity to mediate branch migration reactions in vitro, in a similar way to HLTF. All three enzymes can catalyse fork regression, as well as fork restoration reactions, albeit the former seems to be the preferable one in vitro (Bétous et al. (2012), Blastyak et al. (2010)). All three enzymes were implicated in replication fork reversal in cells by the use of electron microscopy or DNA fibres (Kile et al. (2015), Vujanovic et al. (2017), Taglialatela et al. (2017)).

Interestingly, while the enzymatic activities were assayed in the same way and rely on ATP hydrolysis, the three proteins seem to use different conserved structural features to facilitate DNA binding and mediate the reaction. SMARCAL1 uses a HARP (HepA-related protein) domain to recognise branched DNA containing both dsDNA and ssDNA (Bétous et al., 2012). HLTF has a preference for branched DNA substrates and depends on its HIRAN domain's (HIP116 Rad5p N-terminal) ability to bind a 3'OH-ended DNA. In contrast to the other two, the 3D-structure of ZRANB3 has not been determined yet, however it was recently shown that its HARP-like domain is necessary for DNA binding and its ATPase and branch migration activities (Badu-Nkansah et al., 2016). Such different ways of binding seemingly the same substrate may confer specificity to these enzymes for a particular structure that arises at a blocked replication fork, e.g. HLTF may act when the tip of the leading strand is in close proximity to the branch point, while SMARCAL1 can reverse the fork if there is an accumulation of ssDNA on both template strands. In addition to fork remodeling, all three enzymes are able to metabolise D-loops and ZRANB3 possesses a unique ATP-dependent endonuclease activity, however its role remains unclear (Weston et al., 2012).

At a cellular level, all three proteins are involved in the replication stress response, since their depletion causes typical phenotypes, such as altered replication dynamics under stress, defects in replication restart, replication-associated DNA breaks and a sensitivity to genotoxins (rev. in Poole and Cortez (2017)). Importantly, some of these phenotypes are non-overlapping, suggesting non-redundancy of the enzymes. This is further supported by the fact that co-depletion of ZRANB3 and SMARCAL1 sensitises cells to genotoxins more than individual knockdowns (Ciccia et al., 2012). Also the way cells regulate the activity of these enzymes differs significantly. SMARCAL1 was shown to be recruited to replication sites by an interaction with RPA (Yusufzai et al. (2009), Bansbach et al. (2009)), which is enhanced upon HU-treatment (Bétous et al., 2012). RPA also reg-

ulates SMARCAL1 branch migration activity in vitro by providing a preference for forks with a leading-strand gap, which reflects a pathological situation, in contrast to a physiological lagging-strand gap (Bétous et al., 2013). SMARCAL1's branch migration activity is also negatively regulated by stress-induced phosphorylation mediated by ATR, ATM and DNA-PKcs (DNA protein kinase, catalytic subunit). Phosphorylation is necessary to avoid replication fork collapse, demonstrating that fork reversal, while needed for stalled fork stabilisation, has to be kept under a strict control to avoid genomic instability (Couch et al., 2013). In contrast to SMARCAL1, ZRANB3 does not interact with RPA (Yusufzai and Kadonaga, 2010), but is rather recruited to the stalled forks by modified PCNA. ZRANB3 contains two motifs that mediate interaction with unmodified PCNA – the PIP box and APIM (AlkB homolog 2 PCNA-interaction motif) – and an NZF (Npl4 zinc finger) motif that binds to poly-ubiquitylated PCNA; all three domains are necessary for the efficient recruitment of ZRANB3 to foci after DNA damage (Ciccia et al., 2012) and for mediating fork reversal in cells (Vujanovic et al., 2017). Although not much is known about any post-translational modifications, inhibition of DDR kinases by caffeine prolongs ZRANB3's retention in DNA damage foci, suggesting a potential regulatory mechanism similar to SMARCAL1 (Ciccia et al., 2012).

HLTF shares the architecture and activities with its better-investigated yeast homologue, Rad5. Both proteins have a RING (Really Interesting New Gene) domain, which confers the ubiquitin E3 ligase activity that mediates poly-ubiquitylation of PCNA upon replication stress (Motegi et al., 2008); this modification is thought to trigger an error-free, recombination-based pathway to stabilise or restart replication forks. HLTF possesses an ATP-dependent dsDNA translocase activity that drives branch migration. Depletion of HLTF sensitises the cells to genotoxins (Motegi et al., 2008) and changes replication dynamics under stress conditions, which was attributed to the lack of protective fork reversal catalysed by HLTF (Kile et al., 2015). Regulation of the protein's activity or its cellular behaviour have remained unclear.

Several recent reports suggest that SMARCAL1, ZRANB3 and HLTF comprise the trio that is solely responsible for replication fork reversal upon HU treatment in BRAC1/2-deficient background and each of them is equally important for the process. The studies also suggest that the regressed replication fork, if left unprotected, is an entry point for detrimental nucleolytic overprocessing (Mijic et al. (2017), Lemaçon et al. (2017), Taglialatela et al. (2017), Kolinjivadi et al. (2017)).

4.4 Replication fork restart

There are several proposed models for the restart of replication forks stalled by conditions that do not modify the template strand, such as hydroxyurea or aphidicolin (Petermann and Helleday (2010), Berti and Vindigni (2016)). Since RAD51 was found to be necessary for stalled replication

forks restart, both with and without the generation of double-strand breaks (Petermann et al., 2010), the above-mentioned models predict recombination reactions to be involved. Indeed, the first report on the mechanism of replication fork restart in vivo shows that upon mild topoisomerase inhibition, RECQ1 helicase (a.k.a. RECQL1 - RECQ-like helicase 1) restarts replication by converting a 4-way junction into a 3-way one. The activity of RECQ1 is controlled by PARP1-mediated PARylation – upon replication stress PARP1 modifies the helicase, thereby inhibiting its fork restart activity and stabilising the fork in the regressed state (Berti et al., 2013). In the second model, the regressed arm is processed to generate a 3'-tail, which is then used for the RAD51-mediated strand invasion downstream of the branch point. Indeed, recent results suggest that nucleolytic processing of the reversed fork by DNA2 (DNA replication ATP-dependent helicase/nuclease) is needed for efficient replication restart (Thangavel et al., 2015). The two studies were done using short genotoxic treatment, however long lasting replication fork stalling was proposed to elicit replication restart pathways that are mediated via a transient double-strand break, generated at the fork by MUS81 endonuclease (Hanada et al. (2007), Pepe and West (2014)). Subsequently, replication may be restarted via RAD51-mediated HR-like strand invasion downstream of the branch point, followed either by resolution of the resulting D-loop to restore functional a replication fork or by break-induced replication (Petermann and Helleday, 2010). Recent studies confirmed the latter hypothesis, showing that in lack of adequate protection, even short fork stalling may lead to MUS81-mediated cleavage of the fork and initiation of break-induced replication. However, such a fork restart pathway ultimately leads to genomic instability, suggesting that resuming replication via DSB formation is a last resort mechanism to complete genome duplication if safer measures fail (Lemaçon et al., 2017).

4.5 Open questions regarding replication fork remodeling

Fate of the replisome

Among the many open questions regarding the mechanism of stalled fork reversal is what happens with the replisome during this transaction. The replisome is a multi-protein assembly, with many proteins physically bound to newly synthesised, template or both DNA strands. It is difficult to imagine a scenario in which all these proteins stay bound, while the parental stands are being wound back and nascent ones annealed and extruded from the branch-point. On the other hand, recent iPOND data suggest that the abundance of the core replisome components does not decrease upon replication fork stalling with hydroxyurea (Dungrawala et al., 2015). A simple solution to these contradicting ideas would be the existence of factors that displaces replisome proteins from DNA, while being retained at the reversed replication fork, ready to help re-assemble a functional replisome when replication has to be restarted. In 2012, such a process was observed

in vitro for T4 bacteriophage UvsW (Ultraviolet sensitive W) helicase, which was able to reverse a stalled replication fork, shift the replisome proteins to the regressed arm and then help restore a functional replication fork (Manosas et al., 2012).

Signaling events in the response to replication fork reversal

Another facet of replication fork reversal that is being debated, is whether or not it involves any signaling cascade. Given the requirement of extensive ssDNA at the fork, it can be assumed that canonical ATR signaling precedes the reversal. However, the question if the 4-way junction elicits a distinct response is open. One study suggests that replication fork reversal mediated by the helicase FBH1 initiated DSB signaling that involves ATM (Ataxia telengectasia mutated)-dependent phosphorylation of CHK2 (Checkpoint kinase 2) and RPA (Fugger et al., 2015). It could be explained by the fact that the regressed arm is essentially a one-ended double strand break. These results were then challenged by a study analysing replication fork reversal in response to a panel of genotoxins; although all compounds caused ssDNA accumulation and fork reversal, activation of ATM and ATR signaling cascades differed greatly. Importantly, none of the analysed drugs caused the previously reported phosphorylation of CHK2 and RPA (Zellweger et al., 2015).

4.6 Potential roles of replication fork reversal

In the original model, fork reversal was envisioned as a way to assist repair or bypass of the template-strand lesion (Higgins et al., 1976). Although the mechanistic role of fork regression is still lacking, it is undoubtedly more complex than initially proposed. First of all, among compounds that elicit fork reversal are hydroxyurea and aphidicolin (Zellweger et al., 2015), which modes of action do not generate physical lesions, but rather prevent DNA synthesis by limiting the pool of available deoxyribonucleotides and inhibiting the replicative polymerases, respectively. A possible role for replication fork reversal in these conditions would be to limit the functional uncoupling of helicase and polymerases, thus preventing accumulation of ssDNA at the stalled fork. Fork reversal can be also triggered by reagents that induce inter-strand crosslinks (ICL), such as cisplatin and mitomycin C (Zellweger et al., 2015). The potential role of fork regression in response to ICL is even more elusive, since there is no consensus on how cells deal with these lesions. One model suggests that ICLs are absolute roadblocks for the replisome and their repair requires two incoming replication forks to converge on both sides of an ICL (Zhang et al., 2015); after the convergence, CMG helicase is evicted by VCP (Valosin-containing protein, a.k.a. p97) from one of the forks, which triggers its reversal by FANCM (Fanconi anemia complementation group M) (Walter lab, unpublished). The role for fork reversal in this context was not discussed, but it can be speculated that moving the branch-point away from the ICL by rewinding the parental

duplex could facilitate repair of the lesion. A different model suggests that, in the majority of cases, the replisome does not stop at the ICL, but rather is able to traverse it in a FANCM-dependent manner, without the necessity for convergence (Huang et al., 2013). Interestingly, replication forks encountering and traversing ICLs (local forks) are not reversed, in contrast to distal ones (global forks) (Mutreja and Lopes, unpublished). A possible explanation for these data is that the progression of global forks has to be halted to give the local ones enough time to traverse; otherwise, the supercoiling generated by an incoming fork could hinder the efficient traverse (Mutreja, personal communication).

Apart from the potential positive effects, stalled fork regression can also contribute to - rather than prevent - genomic instability, for instance by causing expansion of tri-nucleotide repeats (Follonier et al., 2013). Also, a four way junction formed by the regression could be a perfect substrate for structure-specific nucleases, like MUS81 (Methyl methanesulfonate and UV-sensitive clone 81), what will be elaborated on in the subsequent section.

4.7 Nucleolytic processing of stalled replication forks

The importance of stalled replication fork stabilisation to avoid genomic instability is very well established. However, still very little is known about the events taking place directly at the stalled fork that ensure its protection against collapse. Over the last several years, the idea of a 'protectosome' emerged, referring to a group of proteins that protect the stalled replication fork from unscheduled nucleolytic degradation by nucleases conventionally connected to DSB repair by homologous recombination (Figure 7) (rev. in Higgs and Stewart (2016)). Among these proteins there are several factors belonging to the HR or Fanconi anaemia repair pathways, such as RAD51 (Hashimoto et al., 2010), BRCA1/2 (Schlacher et al. (2011), Schlacher et al. (2012)), REV1 (Yang et al., 2015), FANCD2 (Schlacher et al., 2012) and BOD1L (Higgs et al., 2015). All these were found to protect the nascent DNA at replication forks from degradation mediated by MRE11 or DNA2 under mild replication stress conditions that do not generate DSBs. The exact protective mechanism is not known for any of them, but all seem to be important for RAD51 stabilisation at the fork, and failure to do so leads to nascent DNA degradation and ensuing chromosomal aberrations. The importance of dissecting the stalled replication fork stabilisation pathway was recently underscored by the finding that restoration of stalled fork protection is one way BRCA1/2-deficient tumours can acquire resistance towards the PARP1 inhibitor Olaparib (Chaudhuri et al., 2016).

As noted, the mechanistic insights into stalled fork protection and degradation are largely unknown. It was originally speculated that a reversed replication fork could be the structure targeted by the nucleases (Schlacher et al., 2011), which was further supported by findings suggesting that, upon mild replication stress, stalled forks are immediately regressed in a RAD51-dependent

fashion (Zellweger et al., 2015). Indeed, recently, several groups found that, at least in BRCA1/2-deficient background, RAD51-, ZRANB3-, SMARCAL1- or HLTF-mediated replication fork reversal is necessary for the unscheduled MRE11-dependent degradation to occur (Mijic et al. (2017), Lemaçon et al. (2017), Taglialatela et al. (2017), Kolinjivadi et al. (2017)). However, although RAD51 is indispensable for replication fork regression, this step is different than loading of the recombinase during HR since it does not depend on BRCA2 (Mijic et al., 2017). In contrast, the resection of an unprotected fork was found to follow the same process as in the canonical HR (rev. in Cejka (2015)), i.e. nascent DNA degradation is initiated by CtIP (CtBP-interacting protein) together with MRE11 and then continued by a more potent exonuclease, EXO1 (Exonuclease 1) (Lemaçon et al., 2017). In agreement with a number of reports unequivocally stating that unscheduled nascent DNA resection is deleterious to the cell (rev. in Higgs and Stewart (2016)), fork degradation was found to cause an elevated number of chromosomal aberrations (Lemaçon et al. (2017), Mijic et al. (2017), Taglialatela et al. (2017)). However, a surprising discrepancy was reported with regard to fork reversal - one of the studies shows that preventing resection by blocking fork reversal exacerbates genomic instability (Mijic et al., 2017), while the other reports an alleviation (Taglialatela et al., 2017). While this difference is difficult to reconcile, the necessity of proper maintenance of stalled replication forks is obvious and may explain the growing number of factors found required for this process. Apart from the already listed HR/FA-pathway components, very recently WRNIP1 (Werner helicase interacting protein 1) – a protein of uncharacterised activity was found to co-operate with BRCA2 in the protection of stalled replication forks from MRE11-dependent degradation (Leuzzi et al., 2016) (Figure 8A).

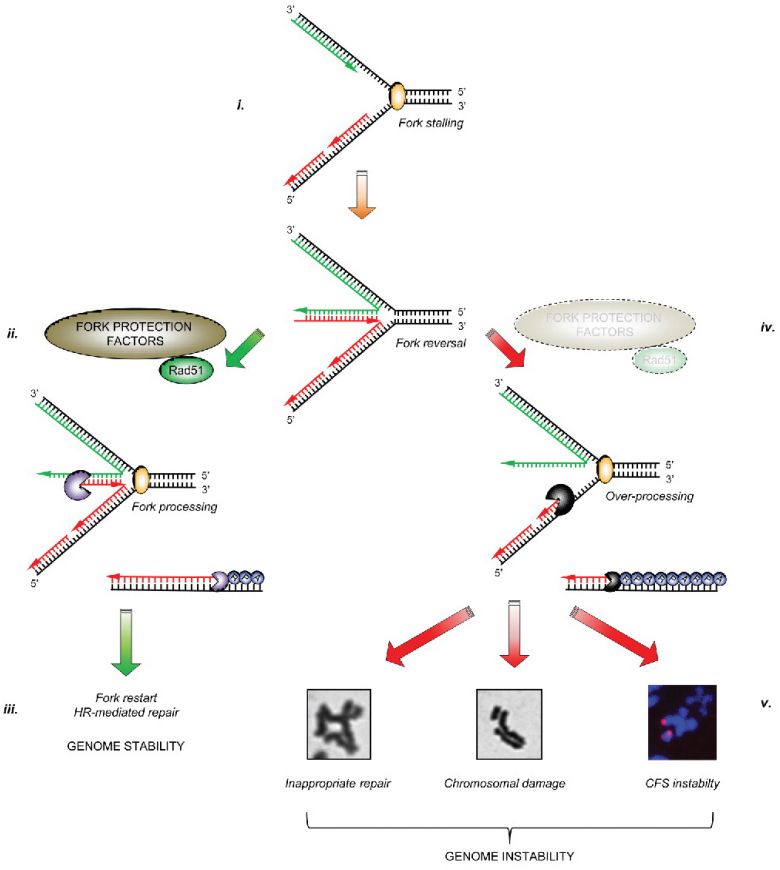

Figure 7: The importance of stalled replication fork protection for ensuring genomic stability (Higgs and Stewart, 2016).

5 WRNIP1

WRNIP1 was identified in 2001 as an interactor of WRN in a yeast two-hybrid screen and in vitro pull-down experiments (Kawabe et al., 2001). The protein is ubiquitously and evenly expressed in human tissues, with some databases reporting an elevated abundance in the brain (The Human Protein Atlas). There are two transcript variants of WRNIP1 present in cells, resulting from an alternative splicing event – putatively activation of an alternative 3' splice site in exon 3, which produces a protein that has an internal truncation of 25 amino acids. Genome-wide mRNA sequencing data show that the shorter transcript is present at very low levels, both in healthy and cancerous tissues (0-5% of total WRNIP1 transcripts) (ISOexpresso database).

5.1 Structural features of WRNIP1

WRNIP1 homologues are found from humans to prokaryotes, with 35% sequence identity between most divergent species, suggesting a very high evolutionary conservation of the protein (Kawabe et al., 2001). In silico analysis of WRNIP1's sequence revealed two conserved domains: an N-terminal UBZ (ubiquitin-binding zinc finger) and a central ATPase domain of the AAA+ type (ATPases associated with various cellular activities) (Kawabe et al., 2001). The UBZ domain is characteristic for proteins of the post-replicative repair pathways, such as TLS polymerases or RAD18 that use it to recognise modified PCNA. Structural studies of the UBZ motif showed that it is identical to the one found in RAD18, but different to Polη (Suzuki et al., 2016). WRNIP1's UBZ was found to be important for binding ubiquitin, with a preference for poly-chains, and for monoubiquitylation of the protein itself in a process called coupled monoubiquitylation (Bish and Myers, 2007). The second conserved domain of WRNIP1, the AAA+ ATPase, shares homology with clamp loader proteins, such as RFC, or bacterial RuvB – a component of already mentioned RuvAB complex involved in replication fork reversal in bacteria. The domain possesses motifs characteristic for the family – Walker A, Walker B and arginine finger, all of which are necessary for the ATP hydrolysis reaction (Wendler et al., 2012). WRNIP1, similarly to most AAA+ ATPases, forms oligomers, presumably homo-octamers (Tsurimoto et al., 2005), which seems to be important for nuclear foci formation (Crosetto et al., 2008).

5.2 Cellular behaviour of WRNIP1

When analysed by immunofluorescence microscopy, WRNIP1 localises almost exclusively to the nucleus, where it shows a mainly diffuse staining with several puncta. Upon genotoxic treatment, WRNIP1 re-localises to damage sites, which depends on its UBZ domain and a C-terminal third of the protein, suggested to be important for oligomerisation (Crosetto et al. (2008), Nomura et al.

(2012), Kanu et al. (2016)). More importantly, WRNIP1 was found to associate with replication forks in two independent unbiased proteomic screens (Alabert et al. (2014), Dungrawala et al. (2015)); the latter also showed that WRNIP1's abundance increases immediately after replication fork stalling by hydroxyurea, peaking at the 15 minutes' time-point, suggesting that the protein performs its function at an early stage of the replication stress response. Apart from functional domains important for WRNIP1's localisation to damage-induced foci, recruitment of the protein seems to depend on ATMIN (ATM-interacting protein) and the ubiquitylation of PCNA, since depletion of the E3 Ub ligase RAD18 or expression of the PCNA K164R mutant abrogates WRNIP1 foci formation after long aphidicolin treatment (Kanu et al., 2016).

5.3 WRNIP1 interacts with proteins involved in replication and the replication stress response

In support of Ub-PCNA-dependent recruitment, the yeast homologoue of WRNIP1, Mgs1, was found to interact with modified PCNA in a UBZ-dependent manner and this interaction was important for Mgs1's cellular function (Saugar et al., 2012). Other putative interactors that further put WRNIP1 at the replisome include the replicative polymerase Polδ (Tsurimoto et al., 2005), the replication fork remodeler ZRANB3 (Ciccia et al., 2012), the E3 ubiquitin ligase Rad18 (Yoshimura et al., 2009) and TLS polymerase Polη (Yoshimura et al., 2014).

5.4 Involvement of WRNIP1 in replication stress response pathways

Apart from localisation studies and suggested interactors, there is a significant body of evidence from research in yeast that implicates WRNIP1/Mgs1 in the DNA damage response. While Mgs1 knock-out alone is neither lethal to cells, nor causes growth retardation or sensitivity to genotoxins, it is synthetic lethal or sick with the loss of any of the error-free PRR pathway factors – Rad6, Rad18 or Rad5. The phenotype can be suppressed by boosting homologous recombination, either via over-expression of Rad52 or blocking the Srs2-dependent anti-recombination (Hishida and Ohno, 2002). Interestingly, the same study found that deletion of Mgs1 restores the growth of a yeast strain, which has a replication-stress-inducing mutation in Polδ and over-expresses Holliday junction resolvase RuvC, indicating that Mgs1 may be involved in the formation of 4-way junctions at challenged replication forks. These findings suggest that Mgs1 acts in a replication stress response pathway that is based on replication-coupled recombination. On the other hand, overexpression of Mgs1 leads to hyper-recombination and sensitivity to MMS and HU, indicating that the activity of the protein has to be carefully controlled (Hishida et al., 2001).

5.5 Biochemical activities of WRNIP1

There were several attempts to characterise WRNIP1/Mgs1 activities in vitro. It was shown that the yeast protein has a weak ATPase activity that is stimulated by the presence of DNA; ssDNA stimulated the protein better than dsDNA. The study also reports that Mgs1 is able to anneal complementary DNA strands, however, surprisingly, the presence of ATP inhibits the process (Hishida et al., 2001). It should be noted though that the ssDNA molecule used in these experiments was either M13 bacteriophage DNA or a single-stranded plasmid, both of which can contain secondary structures that may have been recognised by Mgs1. Two other studies report binding of human WRNIP1 to DNA substrates mimicking a primer-template or a 3-way junction (Yoshimura et al. (2009), Kanamori et al. (2011)). Interestingly, while WRNIP1 does not seem to have a strong activity on its own, the protein was found to stimulate biochemical activities of two of its interactors – Polδ and Fen1. In both cases, the stimulation was either not dependent or even negatively influenced by WRNIP1's ATPase activity (Kim et al. (2005), Tsurimoto et al. (2005)). These biochemical data may suggest that WRNIP1 acts as an auxiliary factor, assisting other proteins in their activities rather than doing the work itself, partially explaining why its function is so problematic to pinpoint.

5.6 WRNIP1 promotes ATM signaling in response to replication stress and protects stalled replication forks from nucleolytic processing

Two very recent studies shed some light on WRNIP1's cellular function. In 2015, WRNIP1 was shown to be a part of the ATM signaling pathway activated in the response to replication stress by bridging signaling from poly-ubiquitylated PCNA to the ATM cascade (Figure 8B). Interestingly, ATM signaling activation in response to ionizing radiation was not affected, raising the question about the type of structure or event that triggers the cascade specifically upon replication fork stalling. The authors proposed that a reversed fork might be a good candidate, based on the findings showing FBH1-dependent ATM signaling in response to hydroxyurea (Kanu et al. (2016), Fugger et al. (2015)).

The second study, published in 2016, reported the first specific cellular function of WRNIP1. It was found that WRNIP1 is yet another factor ensuring the stability of a stalled replication fork, protecting nascent DNA from MRE11-dependent degradation (Figure 8A). Using a combination of DNA fibres and proximity ligation assay, the authors propose that WRNIP1 acts epistatically with BRCA2 in loading RAD51 onto ssDNA and then ensures its stability by counteracting the anti-recombinogenic activity of FBH1. It was also shown that the ATPase activity of WRNIP1 is not needed for the protection of stalled forks, but is required for the efficient restart of a subset of forks (Leuzzi et al., 2016).

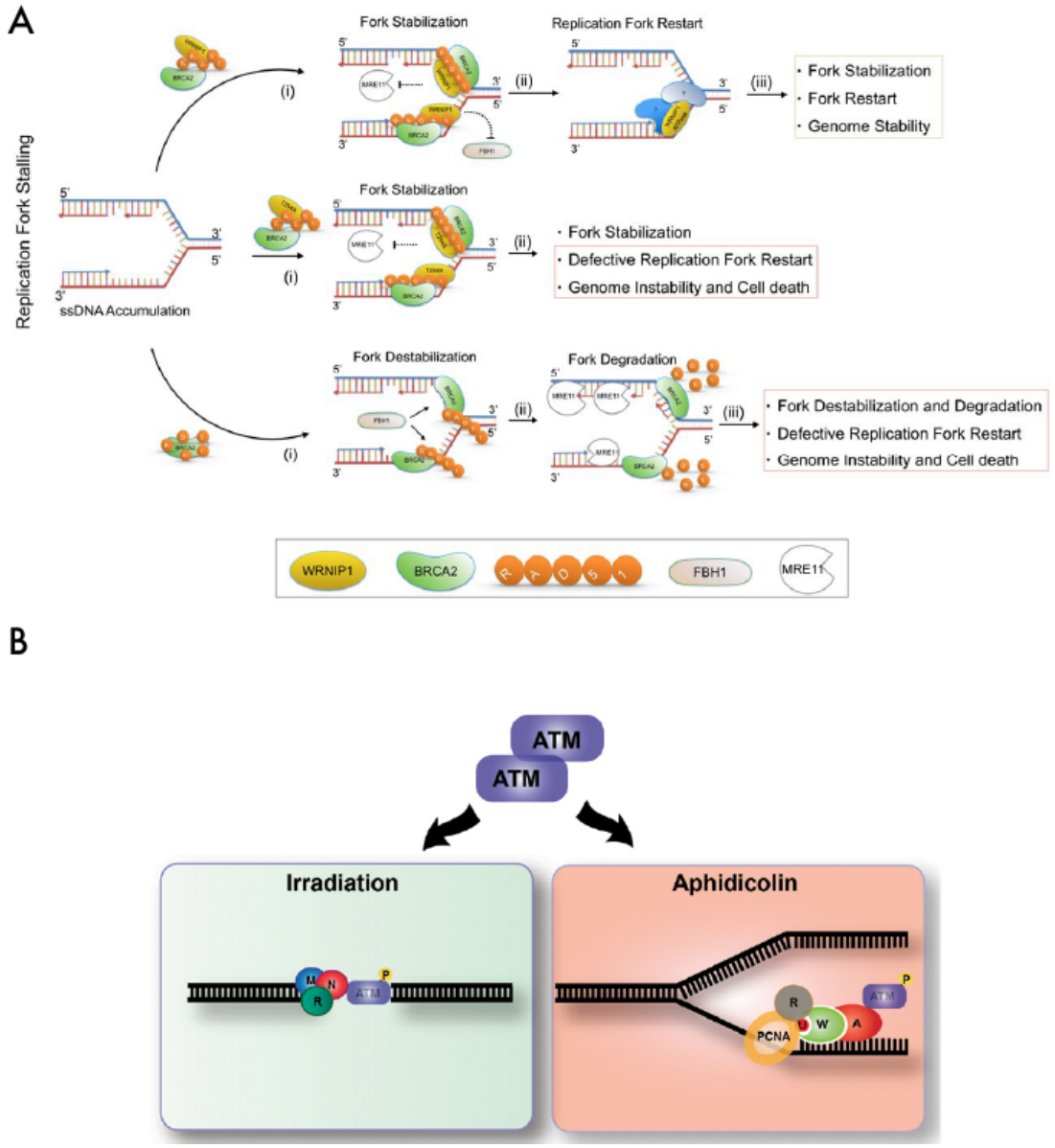

Figure 8: Proposed models for the cellular function of WRNIP1. (A) The role of WRNIP1 in stalled fork protection (Leuzzi et al., 2016). (B) The role of WRNIP1 in ATM signaling following replication stress (Kanu et al., 2016).

Despite presenting a compelling set of data implicating WRNIP1 in the protection of stalled replication forks, the suggested mechanism has several shortcomings. First, while FBH1 has been shown to disrupt RAD51-ssDNA complexes, it was also shown to have pro-recombinogenic activities and, above all, directly regress replication forks in response to HU (Fugger et al., 2015). This could offer an alternative explanation to the rescue of the fork protection that the authors see when WRNIP1-deficient cells are depleted of FBH1, namely that WRNIP1 protects the stalled fork downstream of its reversal. The study addresses this by showing that in HU-treated WRNIP1-deficient cells, there is an accumulation of exposed parental, rather than newly synthesised, ssDNA resulting from fork degradation, which the authors interpret as an indication that stalled replica-

tion forks are not reversed prior to degradation. It is however possible, that prolonged stalling of a reversed fork causes its degradation beyond the branch point, which is difficult to detect without looking at the replication intermediates directly. Lastly, while the authors propose an ATPase-dependent role of WRNIP1 in replication fork restart, the ATPase-dead mutant used in the study has never been shown to have compromised ATP hydrolysis activity (Tsurimoto et al., 2005).

6 Hypothesis - WRNIP1 contributes to replication fork reversal

Since WRNIP1 was discovered sixteen years ago many attempts to understand its function have been undertaken, however the picture is still far from coherent. Even though the protein is not essential for survival in unperturbed conditions, it becomes essential when the replication fork deals with replication stress. WRNIP1 then helps to avoid detrimental fork over-processing and, putatively, is involved in fork restart, possibly by somehow influencing Polδ.

As a focus of this PhD Thesis project, we decided to investigate the cellular function of WRNIP1 in the context of the DNA damage response, by performing an extensive characterisation of the protein in vitro and challenging these findings in cells. The project was initiated in 2013 when the function of WRNIP1 was still completely unknown. By analysing available data, especially from yeast genetic studies, at the time we came up with a hypothesis proposing that WRNIP1 is involved in the remodeling of stalled replication forks, either mediating the transaction directly or assisting other factors in doing so. We based the hypothesis on the aforementioned observation that loss of Mgs1 rescues the growth defect of a yeast pol3-13 strain over-expressing RuvC. It is assumed that, due to a mutation in the catalytic subunit of the DNA Polδ, the *pol3-13* strain experiences an elevated level of replication stress, which leads to a higher incidence of remodeling events at the fork, including fork regression into a 4-way junction. Such structures can then be processed by the bacterial RuvC nuclease, causing replication fork collapse and, consequently, inviability of the strain. Since deletion of Mgs1 alleviates this growth defects, we reasoned that the protein has to somehow contribute to the generation of RuvC-cleavable structures. Moreover, it was reported that Mgs1 has DNA annealing activity and possesses an ATPase domain. Based on all these observations, we reasoned that the protein could be a perfect candidate to reverse stalled replication forks.

METHODS

7 Genetic engineering methods

Transformation of bacteria

Chemically competent *Escherichia coli* DH10b/DH10bac cells were prepared by growing suspension culture in LB medium until OD_{600} = 0.5-0.6, followed by centrifugation to pellet the cells. The pellet was suspended in an appropriate volume of ice-cold TSB buffer (10% PEG-3350, 5% DMSO, 10 mM $MgCl_2$, 10 mM $MgSO_4$ in LB; filtered). The transformation was done by mixing 1-100 ng DNA with the KCM buffer (100 mM KCl, 30 mM $CaCl_2$, 50 mM $MgCl_2$ in water; filtered) and competent bacteria, followed by 10 min. incubation on ice and subsequent 15 min. incubation at RT. Afterwards, 400 μl S.O.C. medium was added, the cells were incubated at 37 °C with shaking (45 min for DH10b, 4 h for DH10bac), plated on an LB-agar plate and incubated overnight at 37 °C.

Propagation of plasmids

After transformation, several transformant clones were grown over-night in liquid LB medium supplied with appropriate antibiotics. Plasmid DNA was extracted using the QIAprep Spin Miniprep Kit or QIAGEN Plasmid Plus Kit (Qiagen).

Polymerase chain reaction

Unless otherwise stated, the polymerase chain reaction (PCR) was assembled according to the Figure 9A and performed using a protocol outlined in Figure 9B. In general, the analytical PCR was done using GoTaq® G2 DNA Polymerase (Promega) with extension time 60 s/kbp, while preparative and SDM (site-directed mutagenesis) PCR using the Phusion® Hot Start II DNA Polymerase (New England Biolabs) with the extension time 20 s/kbp.

A

Component	Amount and/or final conc./amount
Polymerase buffer (5X)	5 µl
dNTPs (10 mM each)	0.5 µl (= 0.2 mM each)
DMSO	0.5-1.25 µl (= 2-5 %)
forward primer (10 uM)	1 µl (= 0.4 µM)
reverse primer (10 µM)	1 µl (= 0.4 µM)
template DNA	25-100 ng
polymerase	0.25 µl (= 0.5 U)
nuclease-free water	up to 25 µl

B

Step	Temperature (°C)	Duration (seconds)	Comment
Initial denaturation	95	300	95
Denaturation	95	45	analytical - 35 cycles; preparative and SDM - 18 cycles
Annealing	var.	45	
Extension	72	var.	
Final extension	72	72	72
Pause	4	4	4

Figure 9: Conditions of PCR reactions. (A) PCR reaction mix. (B) PCR reaction program

Name	Sequence (5' - 3')
oBP03	GGGCCGCCGGGCTGCGGCGCGACCACTCTGGCTCACATC
oBP04	GATGTGAGCCAGAGTGGTCGCGCCGCAGCCCGGCGGCCC
oBP07	CACATCAACTCGCACCTGGAC
oBP15	GAAAACCATCCTTTTTATTGATCAAATTCATCGGTTCAATAAATCTC
oBP16	GAGATTTATTGAACCGATGAATTTGATCAATAAAAAGGATGGTTTTC
oBP19	CGGTTCAATAAATCTCAGCAGGACACTTTCCTTCCTCACGTGGAATGTGGGACGATCA CTCTGATTGGGGCAACCACTGAAAACCCTTCCTTCCAGGTCAACGCTGCTCTTCTG
oBP20	CAGAAGAGCAGCGTTGACCTGGAAGGAAGGGTTTTCAGTGGTTGCCCCAATCAGA GTGATCGTCCCACATTCCACGTGAGGAAGGAAAGTGTCCTGCTGAGATTTATTGAACC
oBP21	GGGGACAAGTTTGTACAAAAAAGCAGGCTTCACCATGGAGGTGAGCGGGCCGG
oBP22	CGTGAGGAAGGAAAGTGTCCTGCTGAGATTTATTGAAC
oBP23	CTGAAAACCCTTCCTTCCAGGTCAACGCTGCTCTTCTGAG
oBP24	GGGGACCACTTTGTACAAGAAAGCTGGGTCTCAGCACCTCCTCTGCTTGAAG
oBP28	CATCAACTCGCACCTGGCCCGCTGTCTGCTGCTCC
oBP29	GGAGCAGCAGACAGCGGGCCAGGTGCGAGTTGATG
oBP31	CTCGCCGCAGCCCGGCG
oBP37	CCAAGACAAATGATGTGCG
oBP38	ATCCTCTATGAACATGGCGG
oBP49	CTCGGCGCTGGCCCAGCCAGCCACCCCGACGGCAGCCGAGAG
oBP50	GCTGGCTGGGCCAGCGCCGAGCTCTCCGACAGCCGCCGCCTCTTG
oBP56	GCCGGGGAGCGGGCCGCGGGGCCCTCGCCGCCC
oBP57	GGGCGGCGAGGGCCCCGCGGCCCGCTCCCCGGC
oBP58	CACAGAGAATGACGTGGCGGAGGGCCTACAGCGATC
oBP59	GATCGCTGTAGGCCCTCCGCCACGTCATTCTCTGTG

Figure 10: List of primers used in this study

cDNA cloning

WRNIP1S, ZRANB3 and HLTF cDNA were purchased from the Mammalian Gene Collection (Dharmacon) as bacterial stabs (clone IDs: WRNIP1, no data; ZRANB3, 3077975; HLTF, 6015181). Subsequently, the cDNA was amplified by PCR using appropriate pair of primers flanked by attB recombination sites. The PCR product was isolated by TBE-agarose gel electrophoresis and purified using the QIAquick Gel Extraction Kit (Qiagen). Next, attB-cDNA was cloned into the pDONR221™ GATEWAY® entry vector (Invitrogen) according to the manufacturer's protocol and transformed into competent bacteria. Cloning of WRNIP1-L cDNA was done by series of PCR reactions on WRNIP1S-pDONR221 vector. Briefly, in the first step regions flanking the insertion

were amplified using primer pairs oBP21+22 and oBP23+24; PCR products were purified as described above. Second PCR reaction was done using both amplicons mixed with oligonucleotides oBP19+20. The full product was isolated and cloned into pDONR221 vector as described above.

Site-directed mutagenesis

Site-directed mutagenesis was performed according to the original idea of Stratagene (QuikChange® Site-Directed Mutagenesis, Stratagene). Briefly, PCR on a cDNA-pDONR221 vector was performed using long primers containing desired mutation in the middle; primers annealed to the same fragment of cDNA, therefore the whole vector was amplified. High-fidelity polymerase was used to avoid any extra mutations. Afterwards, 10 U of DpnI (New England Biolabs) restriction enzyme was added to degrade parental DNA and the mixture was incubated for 1-2 h at 37 °C. The DNA was purified using the QIAquick PCR Purification Kit (Qiagen) and transfected and propagated in bacteria as described above. Isolated plasmid DNA was checked for desired and extra mutations by sequencing (Microsynth).

Generation of destination vectors

GATEWAY® destination vectors were generated according to manufacturer's protocol (Invitrogen) and propagated in bacteria as described above.

RT-PCR

For WRNIP1 mRNA analysis, the total RNA was extracted from U2OS cells using the RNeasy Mini Kit (Qiagen). Then, the cDNA synthesis was done using the High Capacity RNA-to-cDNA Kit (Applied Biosystems) according to the manufacturer's protocol, followed by a PCR with WRNIP1-specific primers oBP37+oBP38.

8 General mammalian cells methods

Cell culture

All human cell lines were grown in DMEM (Dulbecco's Modified Eagle Medium, Gibco) supplied with 10% fetal bovine serum (Gibco) at 37 °C and 5% CO_2. Cells were split into a fresh medium upon reaching sub-confluency (2-3 times per week). For replicates of phenotypical analyses, cells of similar passage number were always used (± 2) to ensure reproducibility of conditions. Insect Sf9 cells were grown in HyClone™ SFX-Insect™ cell culture media (GE Healthcare) at 25 °C with shaking. Cells were split 2 times a week by diluting culture to 0.5-0.7 x10^6 cells/ml.

Genotoxins and inhibitors

Aphidicolin, camptothecin and Mitomycin C were all purchased from Sigma-Aldrich, dissolved in DMSO to a desired stock concentration (20 mM, 20 mM and 4 mM, respectively) and stored at -20 °C; freshly thawed aliquot was always used. Hydroxyurea (Sigma-Aldrich) and 4NQO (Sigma-Aldrich) were prepared freshly before every experiment as a 1 M stock in water and 5 mM stock in ethanol, respectively. Zeocin™ was purchased from InvivoGen. Mirin was purchased from Sigma-Aldrich, dissolved in DMSO to a final concentration of 50 mM and stored at -80 °C.

Plasmid transfections

Transformation of bacmids to insect Sf9 cells was done using TransIT®-LT1 Transfection Reagent (Mirus) according to manufacturer's protocol. Human U2OS cells were transfected using jetPRIME®(Polyplus-transfection®) according to manufacturer's protocol (10 μg plasmid DNA per 10 cm culture dish; 1:2 (w/v) DNA:jetPRIME ratio); medium was replaced after 6-8 hours. HEK 293T cells were transfected using calcium phosphate in no-FCS medium. Briefly, DNA (5 μg each plasmid) was mixed with $CaCl_2$ (final 250 mM) in sterile water. Next, equal volume of 2x HBS (280 mM NaCl, 50 mM HEPES, 1.5 mM Na_2HPO_4 in water) buffer was added while the sample was vortexed at low speed. The mixture was incubated at RT for 20 minutes and added to the cells drop-wise. After 6-8 hours, the medium was changed.

RNA-interference

Short interfering RNA duplexes were designed using Sfold (http://sfold.wadsworth.org/), unless otherwise stated, and synthesised at Microsynth. U2OS cells were transfected with siRNAs using DharmaFECT1 Tranfection Reagent (Dharmacon). Tranfection mix equal to 1:10 of culture medium volume was prepared in Opti-MEM™ (Gibco) by mixing siRNA (final 40 nM) with the transfection reagent (0.55 μl per 100 μl of the mix, irrespective of the number of siRNAs used); the mixture was incubated at RT for 10 minutes and added to the cells. The growth medium was replaced after 24 hours. Sequences of siRNAs used in the study are listed in the Figure 11.

9 Generation of cell lines

Flp-In T-REx

HeLa Flp-In™ T-REx™ (Thermo Fisher) cell lines over-expressing YFP-tagged WRNIP1 isoforms were generated by transfecting an empty cell line with the respective FlpIn-compatible vector and a vector encoding the Flp-recombinase. Two days after the transfection, cells were put under

siRNA	Sequence (5' - 3')	Conditions
siControl	AGGUAGUGUAAUCGCCUUG dTdT	48 h
siHLTF	UUAGAGAACCGGCCUUACU dTdT	2 x 24h
siMRE11#1	GAGCAUAACUCCAUAAGUA dTdT	24 h
siMRE11#2	GGAGGUACGUCGUUUCAGA dTdT	24 h
siRAD51	GACUGCCAGGAUAAAGCUU dTdT	24 h
siWRNIP1	UUAGAACAGACCAACAUUU dTdT	48 h
siZRANB3	UCAGAAAGACACCUCCAAA dTdT	48 h

Figure 11: List of siRNAs in this study

the antibiotic selection with Hygromycin B (Invivogen) and Blasticidin (Invivogen), according to the manufacturer's recommendations. The medium was changed twice a week to ensure proper selection.

WRNIP1 knock-out cell lines

WRNIP1 knockout cells were generated using CRISPR-Cas9 technology. First, short guide RNA targeting the first exon of WRNIP1 was designed using free online tools – MIT CRISPR Design (Massachusetts Institute of Technology, USA) and CCTop (Centre for Organismal Studies, Heidelberg). The sgRNA with the highest score in both prediction algorithms was chosen: 5' - CGTGTCAGGACGCATCGTGT (CGG) - 3'. Next, a pEsgRNA vector (DU46129, MRC Dundee) bearing chosen sgRNA was generated by site-directed mutagenesis according to the approach described in (Munoz et al., 2014). Then, HeLa Flp-In T-REx or U2OS cells were co-transfected with the pEsgWRNIP1 and the Cas9 expression (DU45731, MRC Dundee) vectors and cultured for 48 hours. Cells were then seeded at low density in a 96-well plate to generate monoclonal cultures. Genomic DNA was extracted from the rest of the transfected cells using a standard phenol-chloroform isolation method. CRISPR-Cas9-targeted region was amplified by PCR using oBP07+31 primer pair, the amplicon was digested with EaeI restriction enzyme (New England Biolabs) and reactions were analysed by agarose gel electrophoresis.

10 Baculoviruses

Bacmid generation

Bacmids were generated using the Bac-to-Bac® Baculovirus Expression System (Invitrogen) approach. Briefly, pFastBac-based vector was transfected into DH10bac competent cells. Transfor-

mants were grown for 48 h under selective pressure that includes antibiotics, IPTG and X-gal. All-white transformants were analysed by PCR according to the manufacturer's design. Positive clones were grown in suspension and the bacmids were isolated using the QIAmp DNA Mini Kit. If necessary, bacmids were analysed by PCR using the same approach as for transformant colonies. Bacmids were stored at 4 °C.

Baculovirus generation

To produce baculoviruses, bacmids were first transfected into Sf9 cells. The cells were seeded in a 6-well plate at a density 0.9 x10^6 cells/ml and left to adhere for 30 min prior to the transfection. The transfection mix was prepared by combining 1-2 μg bacmid DNA with the transfection reagent at 1:3 (w:v) ratio in 250 μl of the SFX medium. The mix was incubation at RT for 20 min and added to the growth medium. Cells were incubated at 25 °C for 96 hours. Afterwards, the medium was recovered and filtered through 0.22 μm filter. Next, 1.25 ml of the resulting P1 baculovirus stock was used to infect 5 ml of Sf9 cells seeded at 1 x10^6 in a cell culture flask. After 4 days, the growth medium was recovered and filtered. The titer of the P2 stock was checked by infecting 2 x10^6 adhered Sf9 cells with increasing amount of the baculovirus (0-100 μl), followed by 48 h incubation to allow for protein expression. Next, the cells were collected by scraping, lysed as described above, and levels of the protein of interest were analysed by Western blotting. Minimal volume of the baculovirus that resulted in maximal protein expression was assumed as a volume giving multiplicity of infection (MOI) equal to 1 per 2 x10^6 cells. To amplify the baculovirus, Sf9 cell were seeded at 1 x10^6 cells/ml in a desired volume, infected with P2 virus stock at MOI = 0.1, incubated for 96 h and processed as described above. To ensure optimal stability, all baculovirus stock were supplied with 2% FBS (Gibco) and stored at 4 °C avoiding exposure to light.

11 Proteins isolation and purification

Lysis

Unless otherwise stated, human and insect cells were lysed by incubating PBS-washed cell pellets with 5 PCV (packed-cell volume) of the Lysis Buffer (50 mM Na-phosphate pH 7.0, 150 mM NaCl, 10% glycerol, 0.1% NP-40, 1 mM TCEP, 0.5 mM EDTA), supplied with protease inhibitors cocktail (Roche) and, optionally, 0.1% Benzonase® (Sigma-Aldrich) or PhosSTOP™ (Roche), for 30 min. on ice with intermittent vortexing. Next, the lysate was spun down at 17,200 x g for 30 min at 4 °C. The supernatant was collected. If needed, concentration of the lysate was analysed using Bradford assay.

Preparative purification of proteins from insect cells

All WRNIP1 variants, ZRANB3 and HLTF were purified from insect Sf9 cells. Liquid culture at a density 2x10^6 cells/ml was infected with the baculovirus at MOI = 1. Cells were incubated with shaking at 25 °C for 48 hours and then harvested and lysed as described above. Resulting lysate was spun down at 4 °C in the Sorval™ WX+ ultracentrifuge (Thermo Scientific) equipped with the T-865 rotor at 37500 rpm for 1 hour. The supernatant was collected and filtered through 0.45 μm and 0.22 μm filters. The resulting cell lysate was incubated with 0.01 volumes of equilibrated ANTI-FLAG® M2 beads (Sigma-Aldrich) for 2 hours at 4 °C with rotation. Afterwards, the beads were washed 3 times 10 min. in 10 ml of the Lysis Buffer at 4 °C with rotation. Then, beads were washed additional 3 times with the Storage Buffer (Lysis Buffer minus EDTA for WRNIP1; Lysis Buffer minus EDTA and NP-40 for ZRANB3 and HLTF). Afterwards, bound proteins were eluted with 5 beads volumes of the Storage Buffer supplemented with the 3xFLAG® Peptide (Sigma-Aldrich) at 200 ng/ul for 2 hours, at 4 °C, with rotation. Afterwards, WRNIP1 was aliquoted, snap-frozen and stored at -80 °C. ZRANB3 and HLTF were concentrated on a Amicon® Ultra Centrifugal Filters (Merck Millipore) and loaded on a Superdex™ 200 10/300 GL size-exclusion chromatography column coupled to the AKTA Pure Fast Protein Liquid Chromatography system (GE Healthcare). Fractions were analysed by SDS-PAGE and those containing the protein of interest eluting at a volume corresponding to its monomer were aliquoted, snap-frozen and stored at -80 °C.

Calibration of the Superdex 200 column was done using Low- and High-Molecular Weight Gel Filtration Calibration Kits (GE Healthcare).

Isolation from human cells

Isolation of WRNIP1 was done by over-expression of Flag-tagged proteins in HEK 293T cells, followed by the Flag-immunoprecipitation (Flag-IP). The cDNA transfection and cell lysis were done as described above. For the Flag-IP, cell lysates were incubated with ANTI-FLAG® M2 beads (Sigma-Aldrich), followed by washing in Lysis and Storage buffers and elution in the same fashion as described for the purification from insect cells.

Endogenous WRNIP1 complexes were isolated from U2OS cells. Cell extracts were prepared as described above and cleared with 15 μl of the Protein G Sepharose® Fast Flow beads (PGS) for 30 min at 4 °C with rotation. This step was done to remove any contaminants binding non-specifically to the beads. Afterwards, pre-cleared extracts were mixed with 1 μg of the anti-WHIP (G-2) antibody and incubated for 2 h at 4 °C with rotation. Next, 15 μl of fresh PGS beads was added and the mixture was incubated for an additional 4 h at 4 °C with rotation. Beads were then washed 3 times with 1 ml of the Lysis Buffer and boiled in 5 volumes of the 1X Laemmli sample buffer.

Protein analysis by Western blotting

For the protein analysis by Western blotting, samples were boiled in Laemmli sample buffer and separated by SDS-PAGE run at 180 V for 1 h or 100 V for 2 h. Proteins were then transferred onto a nitrocellulose or a PVDF membrane (GE Healthcare) at 100 V for 1-2 hours. Afterwards, membranes were blocked in the 5% milk-TBST (Tris-buffered saline supplemented with 0.01% Tween®20) solution for 30 minutes and incubated with a primary antibody solution (1:1000) overnight at 4 °C. Then, membranes were briefly washed with TBST and incubated with an appropriate secondary antibody (1:5000) for 2 h at RT. The membranes were then washed several times with TBST and the signal was developed using the Clarity™ Western ECL Blotting Substrate (Bio-Rad) or the SuperSignal™ West Femto Maximum Sensitivity Substrate (Thermo Scientific).

Primary antibodies used for protein detection: β-Actin-HRP (sc-47778, Santa Cruz Biotechnology), ATR pS428 (28535, Cell Signaling Technology), CHK1 pS345 (2348; Cell Signaling Technology), CHK2 pT68 (2661, Cell Signaling Technology), DNA-PKcs (ab1832, Abcam), Flag M2 (F1804, Sigma-Aldrich), HA-tag (A01244-100, GeneScript), H2A.X pS139 (9718, Cell Signaling Technology), HLTF (GTX114776, GeneTex), KAP1 pS824 rabbit (A300-767A; Bethyl Laboratories), MRE11 (NB100-142, Novus Biologicals), NEDD8 (ALX-210-194-R200, Enzo Life Sciences), (PCNA (sc-56, Santa Cruz Biotechnology), RAD51 (sc-8349; Santa Cruz Biotechnology, Inc.), RecQL-1 (sc-166388; Santa Cruz Biotechnology), RNF20 (ab32629, Abcam), β-Tubulin (sc-9104, Santa Cruz Biotechnology), WHIP G-2 (sc-377402, Santa Cruz Biotechnology), WHIP N-17 (sc-55437, Santa Cruz Biotechnology), ZRANB3 (23111-1-AP, proteintech).

12 Assays in cells

Immunofluorescence microscopy of cells

Cells were seeded onto a 22 mm round coverslips and induced with 1 μg/ml doxycycline. After 48 h, cells were washed with PBS, fixed with 3.7% formaldehyde in PBS for 10 min. and washed 3-times with PBS. Next, cells were permeabilised in 0.5% Triton/PBS for 15 min. at RT, followed by washing with PBS and water. Finally, the slides were mounted with 5 μl Vectashield® with DAPI. Cells were imaged using the Leica microscope, model DM6B, coupled to the DMC 2900 digital camera.

Clonogenic survival assay

Cells were seeded in a 24-well plate at a 300 cells/well density and allowed to attach for 6 hours. Next, genotoxins were added directly to the growth medium. After 24 hours, the cells were re-

leased into a drug-free medium and allowed to grow for 10-12 days. Next, cells were washed with 1x PBS, fixed with ice-cold methanol for 10 minutes and incubated for 10 min at RT with the staining solution (0.5% Crystal Violet in 25% methanol). The staining solution was removed, cell were washed with tap water and air-dried before scanning on a flatbed scanner (Epson Perfection V850 Pro). The extent of growth was then quantified using the ColonyArea ImageJ plugin (Guzman et al., 2014). The graphs were prepared in the GraphPad Prism7, using mean values from 3 independent experiments, each consisting of 3 technical replicates (wells).

DNA fibre spreading

Prior to the analysis of DNA fibres, the cells were seeded in a 12-well plate at a density which will ensure that the culture is 70-80% confluent at the day of the labelling. Directly before labelling, cells were washed 3 times with pre-warmed 1x PBS (phosphate-buffered saline). Next, the cells were incubated with the medium containing 0.04 mM CldU (5-Chloro-2'deoxyuridine, Sigma-Aldrich), followed by washing with pre-warmed PBS (3 times, brief). Subsequently, cells were incubated with the medium containing 0.34 mM IdU (5'-Iodo-2'deoxyuridine, Sigma-Aldrich) and a genotoxin, if indicated. Afterwards, cells were washed with PBS as previously and harvested by trypsinisation. The cells were counted, diluted to 2.5 x10^5 cells/ml and mixed with the unlabelled cells at 1:1 ratio. Then, 3 μl of cells suspension was spotted onto a glass slide, 7 μl of Fibre Lysis buffer was added (200 mM Tris-Cl pH 7.4, 50 mM EDTA, 0.5% SDS in a sterilised water; filtered) and the drop was pipetted up and down 5 times, avoiding drop expansion. Slides were incubated at RT for 9 minutes and tilted manually at an angle that allowing the drop to slide smoothly down to the bottom of the slide. Next, the slides were air dried and fixed at 4 °C overnight in the 3:1 mix of methanol and glacial acetic acid. The slides were then washed in 1x PBS (2 x 3 min) and DNA was denatured in the 2.5 M HCl for 1 h at RT. The slides were washed in 1x PBS (2 x 3 min) and subsequently blocked in a freshly prepared IF Blocking buffer (1x PBS containing 2% Bovine serum albumin and 0.1% Tween®20; filtered) for 40 min at RT. Next, 60 μl of the primary antibodies mix (mouse α-BrdU/IdU (347580, Becton Dickinson) at 1:80, rat α-BrdU/CldU (ab6326, Abcam) at 1:500, in the IF Blocking buffer) was added on top of the slide and the slide was covered with a cover slip. The slides were incubated at RT for 2.5 h, Next, the cover slips carefully removed and the slides were washed with PBST (1x PBS containing 0.2% Tween®20; 5 x 3 min), followed by incubation with the secondary antibodies mix (Alexa^{4}88-conjugated α-mouse (A-11001, Invitrogen) at 1:300 and Cy^3-conjugated α-rabbit (712-165-153, Jackson ImmunoResearch) at 1:300, in the IF Blocking buffer) and washing in the same way as for the primary antibodies. Subsequently, the slides were air dried in dark and mounted with 20 μl of the ProLong™ Gold Antifade Mountant (Invitrogen). The slides were stored at 4 °C. DNA fibres were visualised (60X objective,

IX81, Olympus coupled to a CCD camera, Hammatsu) and scored using ImageJ; for each biological replicate 100-200 molecules were scored, the IdU:CldU ratio was calculated for each fibre and the median value was extracted. Statistical analysis on median values from three independent biological replicates was done in the GraphPad Prism7 software using one-way ANOVA.

13 Mass spectrometry analysis of WRNIP1 interactome

Sample preparation

Protein complexes that were subjected to the mass spectrometry analysis were prepared as described above, with the exception for the samples that were cross-linked. The cross-linking was done by incubating cells with PBS containing 1 mM DSP (3,3-Dithio-bis-(sulfosuccinimidyl)propionate, EMD Millipore) for 30 min. at 37 °C. The reaction was quenched for 15 min. at room temperature by the addition of Tris-HCl to a final concentration of 20 mM. Cells were then washed with PBS and collected by scraping. Cell pellets were resuspended in 5 PCV of the Lysis Buffer from which reducing agent – TCEP – was omitted. The Lysis Buffer was supplied with proteases inhibotors and Benzonase nuclease, as described above. Mixtures were incubated for 30 min. on ice and sonicated in a water bath sonicator Bioruptor (Diagenode) until the solutions were clear. Lysates were spun down, supernatants collected and normalised using the Bradford assay. Afterwards, protein complexes were isolated by the Flag-IP as described above, except in all steps the reducing agent was omitted. After the elution, cross-links were reversed by the addition of DTT (ditiotreitol) to a final concentration of 50 mM and 1-hour incubation at 37 °C. The samples were analysed by mass spectrometry at the Functional Genomics Center Zurich.

Sample analysis by mass spectrometry

Samples were precipitated with an equal volume of 20% trichloroacetic acid (TCA; Sigma-Aldrich) and washed twice with cold acetone. The dry pellets were dissolved in 45 ml buffer (10 mM Tris [pH 8.2], 2 mM CaCl2) and 5 ml trypsin (100 ng/ml in 10 mM HCl) for digestion, which was carried out in a microwave instrument (Discover System; CEM) for 30 min at 5 W and 60 °C. Samples were dried in a SpeedVac (Savant). For liquid chromatography (LC)-tandem mass spectrometry (MS/MS) analysis, the samples were dissolved in 0.1% formic acid (Romil) and an aliquot ranging from 5% to 25% was analyzed on a nanoAcquity UPLC System (Waters) connected to a Q Exactive mass spectrometer (Thermo Scientific) equipped with a Digital PicoView source (New Objective). Peptides were trapped on a Symmetry C18 trap column (5 mm, 180 mm 3 20 mm; Waters) and separated on a BEH300 C18 column (1.7 mm, 75 mm 3 150 m; Waters) at a flow rate of 250 nl/min

using a gradient from 1% solvent B (0.1% formic acid in acetonitrile; Romil)/99% solvent A (0.1% formic acid in water; Romil) to 40% solvent B/60% solvent A within 90 min. Mass spectrometry settings for the data-dependent analysis were as follows: (1) precursor scan range, mass-to-charge ratio (m/z) of 350–1,500; resolution, 70,000; maximum injection time, 100 ms; and threshold, 3e6; and (2) fragment ion scan range, 200–2,000 m/z; resolution, 35,000; maximum injection time, 120 ms; and threshold, 1e5.

Proteins were identified using the Mascot search engine (version 2.4.1; Matrix Science). Mascot was set up to search the Swiss-Prot database assuming the digestion enzyme trypsin. Mascot was searched with a fragment ion mass tolerance of 0.030 Da and a parent ion tolerance of 10.0 ppm. Oxidation of methionine was specified in Mascot as a variable modification. Scaffold (Proteome Software) was used to validate MS/MS-based peptide and protein identifications. Peptide identifications were accepted if they achieved a false discovery rate (FDR) of less than 0.1% by the scaffold local FDR algorithm. Protein identifications were accepted if they achieved an FDR of less than 1.0% and contained at least two identified peptides.

14 Biochemical assays

DNA substrates

All the oligonucleotides used for DNA substrates preparation were synthesised by Microsynth and are listed together with DNA structures in the Figure 11. Oligonucleotide X01 served as a basis for all substrates used in this study and was therefore labelled on the 5'-end either by FAM (fluorescein amidite) during the synthesis or by the kinase-mediated reaction with ATP γ-^{32}P. The radioactive labelling was done in 10 μl reactions containing 1 μM X01, 10 U T4 Poluynucleotide Kinase (Thermo Scientific™), PNK buffer (Thermo Scientific™) and 25 μCi ATP γ-^{32}P. The reaction was incubated at 37 °C for 30 min, followed by purification on two illustra MicroSpin G-25 columns (GE Healthcare).

Annealing of DNA substrates was done in a buffer containing 10 mM Tris-HCl pH 8.0, 50 mM NaCl and 10 mM $MgCl_2$. Oligonucleotides were mixed, incubated for 5 min at 95 °C and then allowed to cool down to room temperature. The final concentration of resulting DNA substrates was 100 nM for FAM-labelled substrates (10X stock) and 50 nM (50X stock) for the radioactive substrates. The substrates were stored at -20 °C.

DNA binding

DNA binding was done in 10 μl reactions containing 1 μl of a DNA substrate (final concentrations: 1 nM for radioactive and 10 nM for fluorescent substrates) and 9 μl of protein-storage buffer mix.

A

Name	Sequence (5' - 3')
X01	GACGCTGCCGAATTCTACCAGTGCCTTGCTAGG ACATCTTTGCCCACCTGCAGGTTCACCC
X01c	GGGTGAACCTGCAGGTGGGCAAAGATGTCCTA GCAAGGCACTGGTAGAATTCGGCAGCGTC
X02	TGGGTGAACCTGCAGGTGGGCAAAGATGTCCA TCTGTTGTAATCGTCAAGCTTTATGCCGTT
X02.1/2	TGGGTGAACCTGCAGGTGGGCAAAGATGTCC
XO3	GAACGGCATAAAGCTTGACGATTACAACAGATC ATGGAGCTGTCTAGAGGATCCGACTATCGA
XO3.1/2	CATGGAGCTGTCTAGAGGATCCGACTATCGA
XO4	ATCGATAGTCGGATCCTCTAGACAGCTCCATGTA GCAAGGCACTGGTAGAATTCGGCAGCGT
XO4.1/2	TAGCAAGGCACTGGTAGAATTCGGCAGCGT
XO1.1/2	GGACATCTTTGCCCACCTGCAGGTTCACCC
XO1c.MM	GGGTGAACCTGCAGGTGGGCAAAGATGTCCC AGCAAGGCACTGGTAGAATTCGGCAGCGTC
XO1c.MM2	GGGTGAACCTGCAGGTGGGCAAAAATGTCCTA GCAAGGCACTGGTAGAATTCGGCAGCGTC
XO2c.MM	GAACGGCATAAAGCTTGACGATTACAACAGAT GGACATTTTTGCCCACCTGCAGGTTCACCC

B

Substrate	Composition
ssDNA	X01
dsDNA	X01, X01c
3' overhang	X01, X04.1/2
5' overhang	X01, X02.1/2
splayed arms	X01, X04
3' flap	X01, X03.1/2, X04
5' flap	X01, X02.1/2, X04
replication fork	X01, X02.1/2, X03.1/2, X04
4-way junction	X01, X02, X03, X04
branch migration replication fork	X01, X02.1/2, X01c.MM, X01.1/2
branch migration 4-way junction	X01, X01c.MM2, X02, X02c.MM

Figure 12: Oligonucleutides-based DNA substrates (A) List of oligonucleotides used for substrate annealing. (B) List of DNA structures and their constituents.

Reactions were incubated on ice for 30 min., followed by the addition of loading buffer (unfolding: 0.1% SDS, 10 mM EDTA, 2% Ficoll, Bromophenol Blue; native: 3.5% Ficoll, 10 mM Tris-Cl pH 7.5) and analysis by native gel electrophoresis using 0.5X TBE 5% polyacrylamide gels.

ATPase activity assay

ATPase activity assay was done in 5 μl reactions containing 5 mM $MgCl_2$, 0.01 mM ATP, 0.033 μM ATP γ-^{32}P analysed protein and, optionally, 50 nM of a DNA substrate. In the control sample, protein was replaced by the respective storage buffer. Reactions were incubated at 37 °C for 30 minutes and then stopped by the addition of EDTA to a final concentration of 50 mM. Two 1-μl samples were spotted on a PEI-Cellulose F thin-layer chromatoghraphy plates (Merck-Millipore) and the plates were resolved in a mixture of 0.15 M LiCl and 0.15 M formic acid. Resolved plates were air-dried and analysed by autoradiography.

Branch migration and fork reversal assays

Branch migration assay was done in 10 μl reactions containing 1 nM DNA substrate (radioactively-labelled), 100 μg/ml BSA (New England Biolabs), 1 mM ATP, 0.5 mM $MgCl_2$ and the protein(s) of interest. Reactions were carried out at 37 °C. Reactions were deproteinized for 20 min at 37 °C with 2 mg/ml Proteinase K and 0.4% SDS and resolved by native PAGE through 8% polyacrylamide gels in TBE.

In vitro fork reversal was done in a similar fashion, except the deproteinised reactions were analysed by electrophoresis through 1% agarose in TBE buffer containing 0.5 mg/ml ethidium bromide.

15 Bioinformatics

Multiple-sequence alignment

Primary sequence alignment was done using Clustal Omega algorithm with default settings, accessed through the Uniprot website (www.uniprot.org). Accession numbers of aligned proteins were: Q96S55-1 (*H. sapiens*), K7BSN9 (*P. troglodytes*), Q91XU0 (*M. musculus*), P40151 (*S. cerevisiae*), P0AAZ4 (*E. coli*).

Structure prediction and analysis

Prediction of three-dimensional structures of both isoforms (Q96S55-1 and Q96S55-2) was done using Phyre2 (Protein Homology/analogy Recognition Engine V 2.0) algorithm and the models were analysed using UCSF Chimera and PyMOL.

RESULTS

16 Analysis of WRNIP1 isoforms

Due to alternative splicing, WRNIP1 transcripts are processed into two distinct mRNA isoforms. Since the available literature regarding WRNIP1 does not mention the existence of two isoforms nor provides any information as to which one was analysed, we decided to include both of them in our analyses to identify differences and their potential significance for protein function.

16.1 In silico analysis of WRNIP1 isoforms

First, a brief in silico analysis was performed. Primary sequence alignment of human WRNIP1's long isoform to the protein's homologues from other species showed that the missing stretch of 25 amino acids is highly conserved and lies within the ATPase domain of the protein (Figure 13A). To check whether this stretch changes the architecture of the catalytic pocket, the three-dimensional structure models were analysed. The models were generated by prediction algorithm, based on the solved structure of the bacterial homologoue of WRNIP1, MgsA (Page et al., 2011). MgsA lacks the N-terminal third, therefore the predicted models are N-terminally truncated. As shown in the Figure 13B, both isoforms, referred to from now on as WRNIP1L (long, 72 kDa) and WRNIP1S (short, 69 kDa), show a similar overall fold, except the C-terminal part, putatively responsible for oligomerisation (Crosetto et al., 2008). Although the additional stretch of 25 amino acids lies within the ATPase domain in close proximity to the motifs responsible for ATP hydrolysis, it does not significantly distort the catalytic pocket (Figure 13C).

16.2 Analysis of WRNIP1 isoforms in cells

Available transciptomics data suggest that, at least at the mRNA level, the long isoform is the predominant one across various healthy and cancer tissue types. Before commencing our analyses in cells, we wanted to check which isoform is present in our model system – U2OS cells. In order to do so, bulk mRNA from U2OS cells was amplified into cDNA by RT-PCR, followed by PCR with WRNIP1-specific primers. Products corresponding to both isoforms were detected, however in dramatically different amounts (Figure 14A). Since only an end-point RT-PCR was performed, we could not infer precise quantitative information, however the result clearly shows that the long isoform is predominant in U2OS cells.

When analysed by Western blotting, endogenous WRNIP1 runs as a single band at around 90 kDa level. To check which isoform the band corresponds to, the two WRNIP1 isoforms were ectopically expressed in U2OS cells depleted of endogenous protein by siRNA targeting the 3'UTR

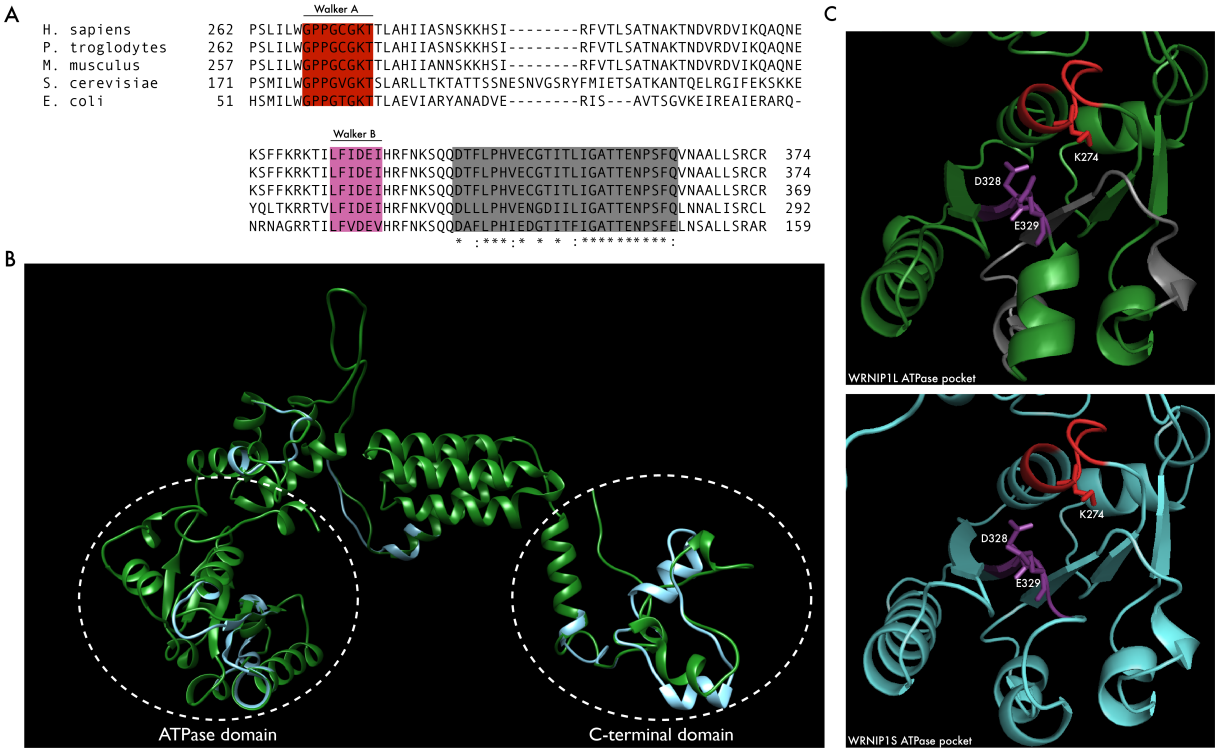

Figure 13: In silico analysis of WRNIP1 isoforms. (A) Alignment of WRNIP1L primary sequence from multiple species. The 25-aa insertion is shown in grey. Asterisk indicates complete residue conservation, colon indicates conservation of amino acid chemical character. AAA+ ATPase motifs are shown in red and violet. (B) Superimposition of predicted structures of WRNIP1L (green) and WRNIP1S (light blue). Relevant domains are indicated with dashed elipses. (C) Comparison of the catalytic pockets of the two WRNIP1 isoforms. Residues relevant for ATPase activity are indicated, color coding as in (A) and (B).

(Figure 14B). Both isoforms were strongly over-expressed compared to the endogenous WRNIP1, and WRNIP1L was present at higher levels than WRNIP1S, which was observed reproducibly in all experiments that involved expression of the two proteins. Their 3 kDa size difference allowed to separate the two isoforms and compare their migration patterns to the endogenous protein, showing that the endogenous WRNIP1 band corresponds to the long isoform. In two other commonly used cell lines – RPE-1 and HEK 293T – endogenous WRNIP1 displays the same migration pattern (Figure 14C).

Endogenous WRNIP1 localises to the nucleus, where it shows diffuse pan-nuclear staining (The Human Protein Atlas). Some reports also suggest formation of small focal structures in unperturbed conditions (Crosetto et al., 2008). To verify localisation of WRNIP1 isoforms, HeLa FlpIn T-REx cell lines expressing YFP-tagged proteins were generated and analysed by fluorescence microscopy (Figure 14D). Both isoforms localised to the nucleus, however, while ^{YFP}WRNIP1S showed only pan-nuclear staining, ^{YFP}WRNIP1L additionally formed big bright foci.

To summarise, WRNIP1L seems to be the predominant, if not the only isoform present in the cell. Also, an in silico analysis indicates that WRNIP1S and WRNIP1L have a similar overall fold

and the additional 25-aa fragment does not seem to alter the ATPase domain in a significant way. The strikingly different localisation of the two isoforms suggests that there may be a functional difference.

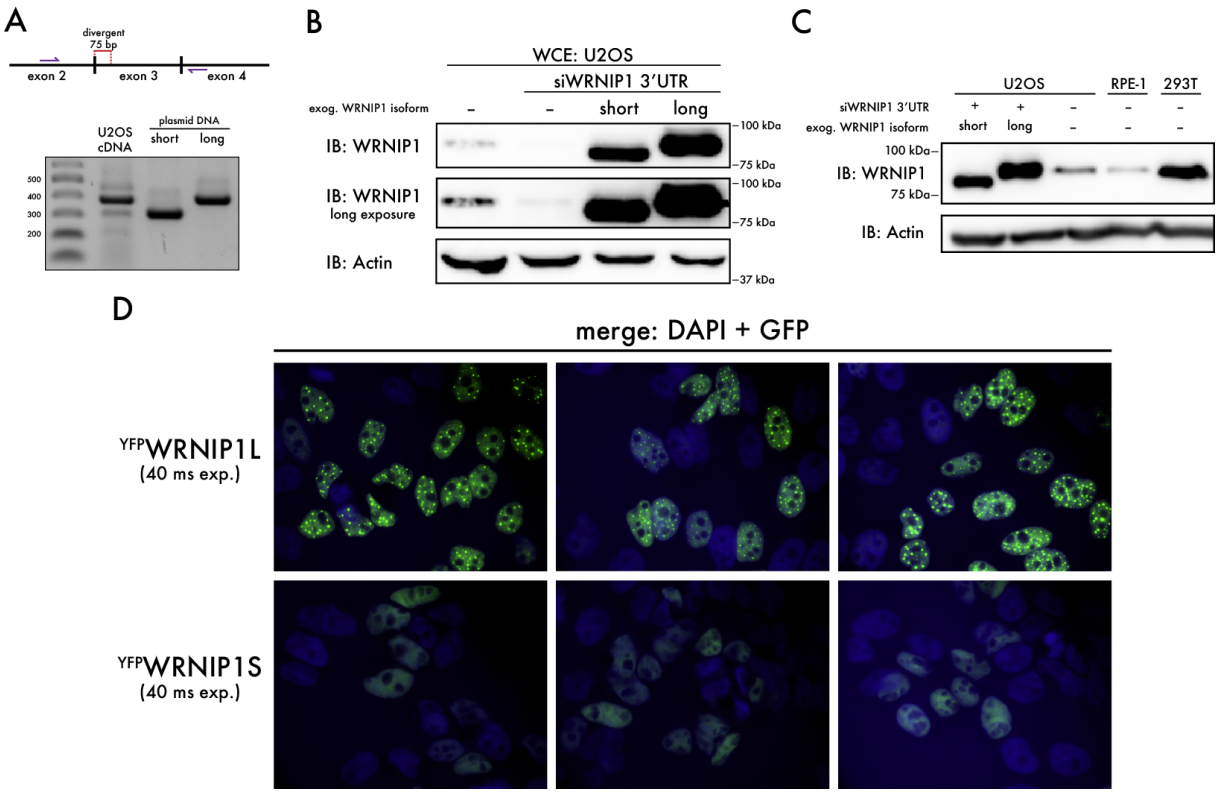

Figure 14: Analysis of WRNIP1 isoforms in cells. (A) Experimental design and result of the end-point RT-PCR analysis of WRNIP1 transcripts from U2OS cells. (B) and (C) Comparison of ectopically expressed WRNIP1 isoforms to the endogenous protein. (D) Representative fluorescence microscopy images of cell lines over-expressing YFP-tagged WRNIP1 isoforms.

17 Purification of WRNIP1

WRNIP1 was shown to oligomerise, both in cells (Crosetto et al., 2008) and in vitro (Tsurimoto et al. (2005), ichi Kawabe et al. (2006)), reportedly assembling into homo-octamers, as assessed by size-exclusion chromatography and glycerol-gradient ultracentrifugation (Tsurimoto et al., 2005).

17.1 Purification of WRNIP1 variants

For the purpose of this study, we decided to purify a series of WRNIP1S/L variants, including wild-type, UBZ-mutant and two ATPase-domain mutants, having a K274A mutation that affects the binding of an ATP molecule or an E329Q mutation that allows for binding of ATP, but impairs its hydrolysis (Figure 15A). The tag of choice was a Flag-tag, due to its small size, robustness and already proven efficacy in WRNIP1 purification (Tsurimoto et al., 2005).

WRNIP1 variants were expressed in insect Sf9 cells and purified according to the procedure depicted in Figure 15B. This simple and fast procedure yielded recombinant protein of high concentration and purity (Figure 15C). Purified WRNIP1 migrated as two bands, with the minor, higher one representing the protein modified with a single ubiquitin moiety. The band representing ubiquitylated WRNIP1 was absent in the UBZ-mutant, which is in line with reports suggesting that WRNIP1 undergoes coupled mono-ubiquitylation, i.e. ubiquitylation that requires an intact UBZ domain. Of note, purification of WRNIP1S variants was less robust, yielding protein preparations of lower concentration and purity.

17.2 WRNIP1 purifies as a high-molecular weight complex

To assess whether purified WRNIP1 forms oligomers, as reported in the literature, analytical gel filtration was done (Figure 15D). Both WRNIP1 isoforms eluted as high-molecular weight (M_W) complexes, with the elution volume similar to the 669-kDa thyroglobulin size marker. The size of monomeric WRNIP1 is 72 and 69 kDa for the long and short isoform, respectively, therefore the apparent size of the complex exceeds the theoretical weight for an octamer. However, size exclusion-based resolution of molecules depends on the radius of an analysed molecule, rather than its factual size, thus providing only an estimate of the molecular weight. Interestingly, WRNIP1S gave an additional small peak at 12.65 ml, which, according to the standard curve, corresponds to a 70-kDa molecule. It could either represent monomeric WRNIP1S or the aforementioned contaminant of similar size (Figure 15C). To further investigate WRNIP1's oligomeric state, non-denaturating Western blotting was performed (Figure 15E). The bulk of the protein migrated as high-M_W complexes, in line with the gel filtration results. Longer exposure times revealed also lower-M_W populations of WRNIP1, but these were present only in WRNIP1S and, to a lesser extent, in K274A-WRNIP1L preparations. Similar to the gel filtration chromatography, the size estimation in native-PAGE is imprecise, since the electrophoretic migration depends on the protein's charge in its native state and cannot be directly related to size markers. Nevertheless, my data clearly show that WRNIP1 predominantly assembles high-order oligomers, which is in line with published data.

18 Biochemical activities of WRNIP1

Several groups have attempted to study WRNIP1's activities in vitro. It was found that the protein binds DNA, although there is no consensus about its substrate preference (Yoshimura et al. (2009), Kanamori et al. (2011)). WRNIP1 was also found to have a ssDNA annealing activity (Hishida et al., 2001) and stimulate DNA Polymeraseδ (Tsurimoto et al., 2005), however both of these functions

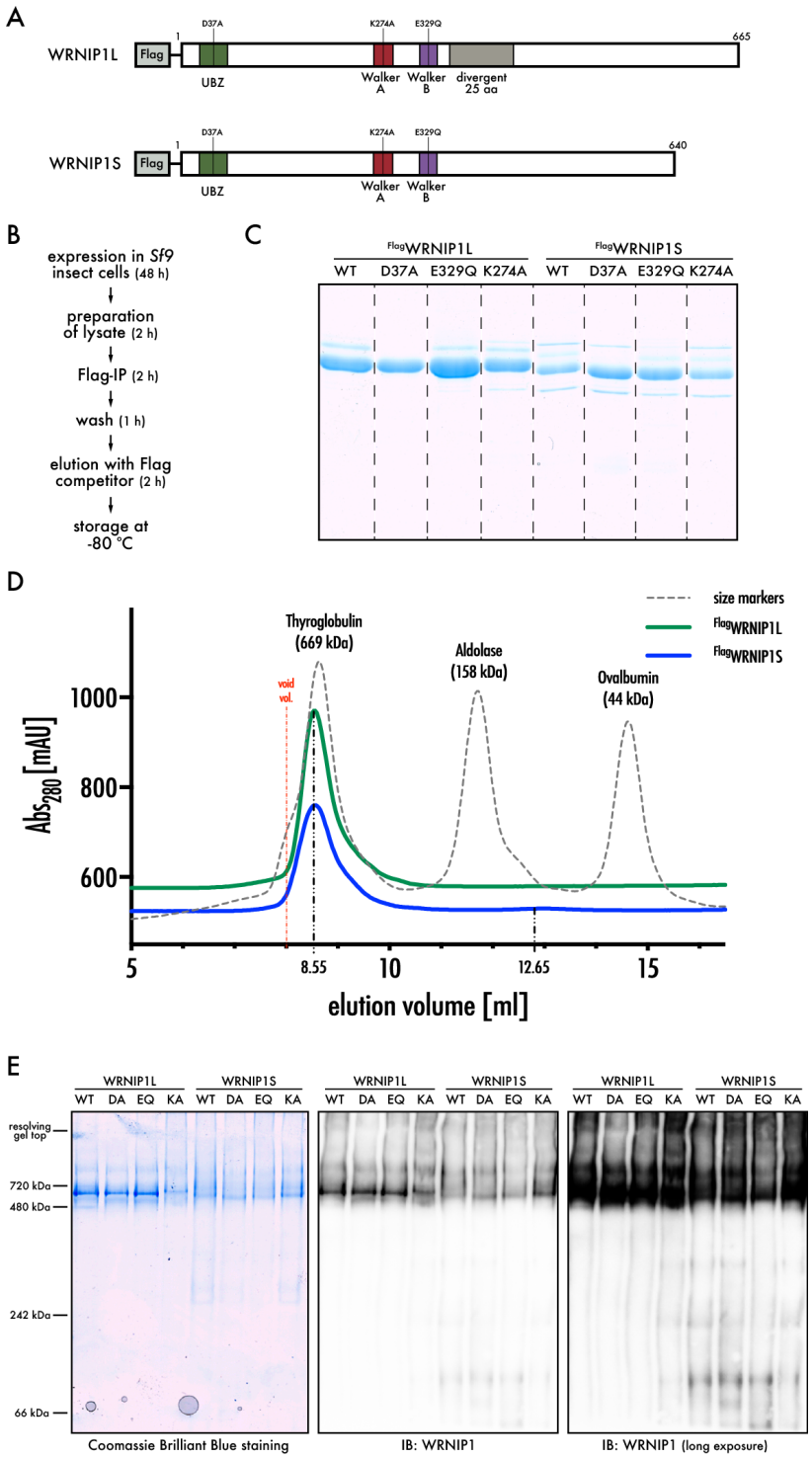

Figure 15: Purification of WRNIP1. (A)) Schematic of WRNIP1 isoforms with indicated mutations that were introduced. (B) Strategy of purification. (C) Commassie-stained SDS gel showing all purified proteins. Equal volumes were analysed. Dashed lines indicate excised irrelevant lanes. (D) Chromatogram of Superdex200 size-exclusion analysis of purified wild-type WRNIP1 isoforms. (E) Analysis of purified WRNIP1 proteins by native PAGE.

were inhibited, rather than driven, by the presence of ATP, leaving the question about WRNIP1's enzymatic activity still open.

18.1 WRNIP1 binds DNA with a preference for 4-way junctions

Since we suspected a role for WRNIP1 at stalled replication forks, we tested whether it is able to bind to structures that can arise during replication fork remodeling, such as three- or four-way junctions. In EMSA (electrophoretic mobility shift assay) with a series of oligonucleotide-based DNA substrates, WRNIP1 showed a clear preference for structures having a branch-point, such as splayed arms or 3- or 4-way junctions (Figure 16A). Closer analysis done by titration of WRNIP1 into a fixed amount of branched substrates showed that WRNIP1 has the highest preference for a 4-way junction substrate, a structure that resembles a reversed replication fork. Due to the fact that WRNIP1 forms high-M_W oligomers it was difficult to analyse its protein-DNA complexes by electorphoresis. The observed smearing could be caused by low gel percentage or by dynamic complex assembly-disassembly cycles. Also, the shifted DNA band was often retained in the well, which may be attributed either to the size of the protein-DNA complexes or the presence of protein aggregates. To address this issue, the procedure was optimised. The improved protocol gave interesting results: apart from the bands retained in the wells of the gel, observed for most substrates and both isoforms, there was a population of fast-migrating WRNIP1-DNA complexes seen only for the 4-way junction substrate and WRNIP1S, but not WRNIP1L (Figure 16B). Further analysis showed that all WRNIP1S variants and K274A-WRNIP1L follow the same behaviour (Figure 16C).

Above data shows that WRNIP1 has the ability to bind to DNA structures that can arise during stalled fork remodeling. Interestingly, only WRNIP1 preparations that putatively contain monomeric WRNIP1 (Figure 15E) showed specific binding to a 4-way junction substrate that mimics a reversed replication fork.

18.2 WRNIP1 has no branch migration and a weak ATPase activity

Since WRNIP1's ATPase domain is homologous to the one found in bacterial replication fork remodeling enzyme RuvB, we wondered whether WRNIP1 could have similar activity. To establish whether WRNIP1 is able to directly remodel replication fork intermediates, DNA branch migration activity was assayed, using 3- or 4-way junction substrates in which the branching point can be moved, mimicking fork reversal and fork restoration reactions, respectively. Such an activity is a feature of fork remodeling helicases and translocases that were introduced earlier. Neither of WRNIP1 isoforms could catalyse branch migration of three- or four-way junction, in contrast to the DNA translocase ZRANB3 (Figure 17A).

Due to the failure to detect any branch migration activity, the ATPase activity of WRNIP1 was

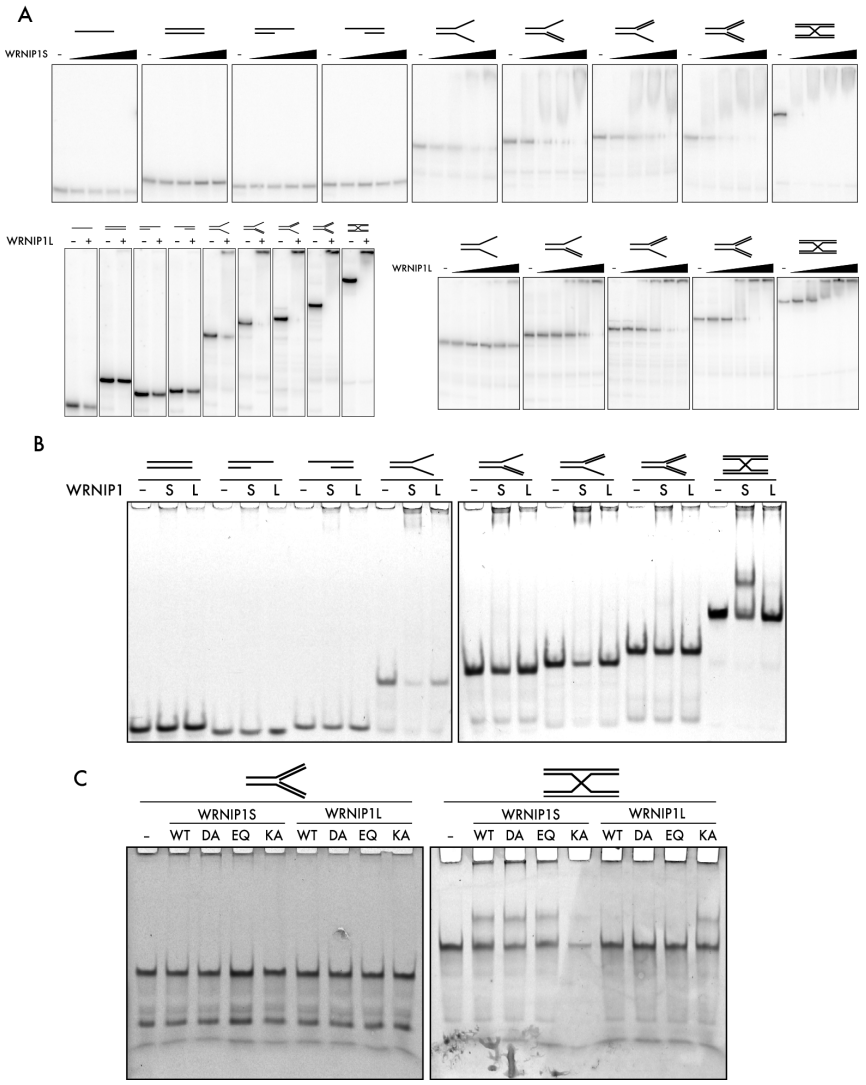

Figure 16: Analysis of WRNIP1's DNA binding abilities by EMSA. (A) Binding of WRNIP1S (upper panel) and WRNIP1L (lower panels) to radioactively labeled DNA substrates under mildly unfolding conditions (0.1% SDS). (B) Binding of wild-type WRNIP1S and WRNIP1L to FAM-labeled DNA substrates under native conditions. (C) Binding of all purified WRNIP1 variants to 3- and 4-way junction substrates under native conditions.

tested, using an assay that measures the release of radioactive gamma-phosphate group from an ATP molecule. Surprisingly, neither WRNIP1 isoform showed any ATPase activity, in striking contrast to another potent DNA translocase, HLTF (Figure 17B).

19 Physical and functional interactions of WRNIP1

WRNIP1 was suggested to interact with several proteins involved in DNA replication or DNA-damage response pathways, such as Polδ, WRN, ZRANB3 or ATMIN (Kanu et al., 2016). To gain further insight into WRNIP1's function, we decided to use an unbiased approach in order to characterise the interaction network of WRNIP1 in cells.

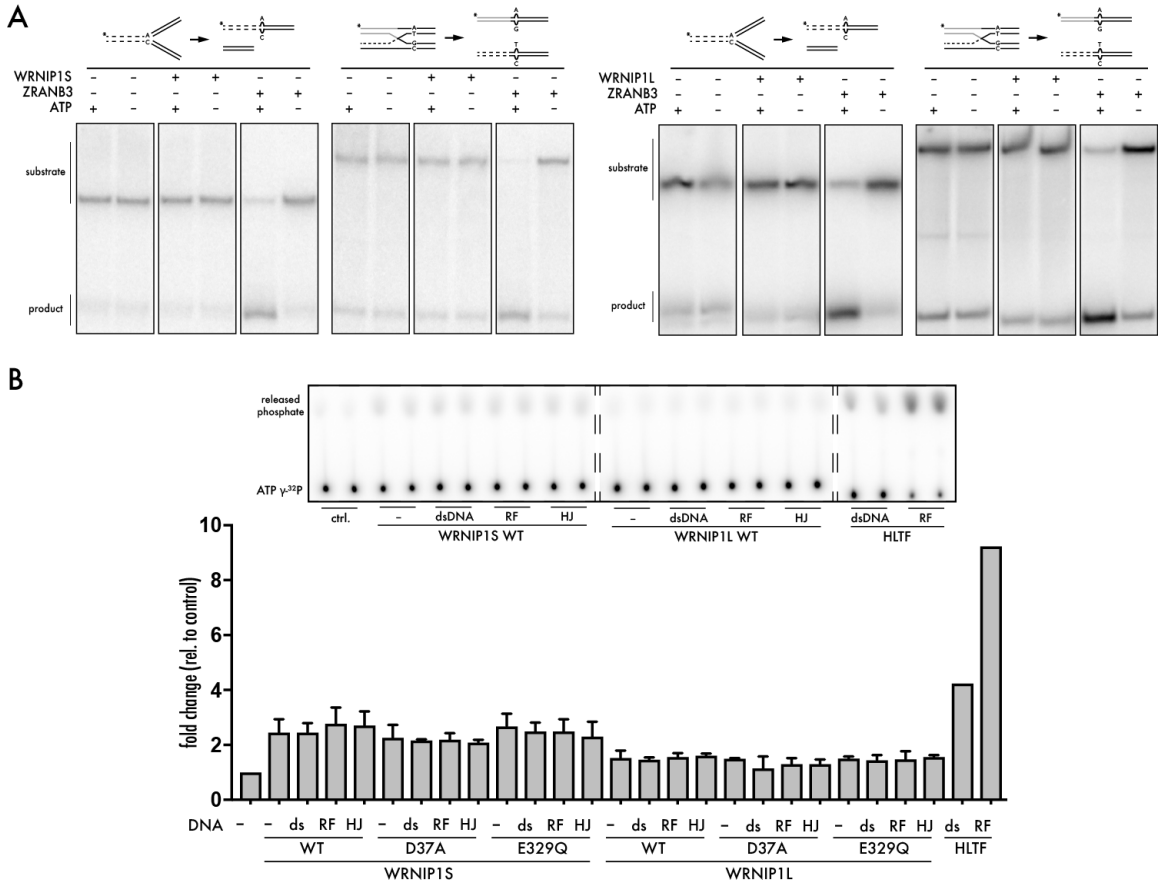

Figure 17: Analysis of WRNIP1's biochemical activities. (A) Branch migration activity of WRNIP1S (left panel) and WRNIP1L (right panel) on radioactively labeled moveable 3- and 4-way junctions. (B) ATPase activity of all purified WRNIP1 variants. Upper panel - representative scan of a TLC plate; lower panel - quantification of the released phosphate group, represented as a fold change relatively to the control sample

19.1 WRNIP1 forms transient interactions at replication forks

Prior to mass spectrometry, Flag- or YFP-tagged WRNIP1 was overexpressed in cells, followed by affinity purification, washing-off of contaminants and elution of residual bound proteins. Surprisingly, apart from the usual contaminants, no meaningful hits were identified, including already established interactors. Although WRNIP1's presence at the replication fork had been shown in several proteomic studies, not a single replisome-associated protein was found in the analysed samples. This result was reproducible irrespective of the cell line (HEK 293T, HEK 293 FlpIn T-REx, HeLa, HeLa FlpIn T-REx), the tag (Flag, YFP) and the subcellular fraction (cytoplasm, nuclear) Even isolation of endogenous WRNIP1 did not give any meaningful data. Finally, as a last resort, in vivo crosslinking was done prior to protein isolation. As seen in the Venn diagram (Figure 18A), this approach turned out to be successful. 937 proteins were identified in the Flag-pull-down sample when protein complexes were cross-linked beforehand, compared to only 262 in

the non-cross-linked sample. A group of 220 proteins was common for both datasets, howeverm the majority of it (187) overlapped with the control set. As expected, a significant number of proteins identified in the cross-linked Flag-WRNIP1L pull-down was also found in the control sample (404), however, more than half of the hits were unique. Importantly, among these were all of the core components of the replisome, suggesting that WRNIP1L localises to the replication fork, which is in line with the literature. Moreover, a number of DNA damage and replication stress response proteins were found, including several that are involved in stalled replication fork-remodeling (HLTF, PARP1, RECQ1, MRE11) or the ubiquitin-system. A full list of meaningful hits reproducibly found in several replicates is given in Figure 18B. Although cross-linking greatly improved the result, it should be kept in mind that such an approach may identify many indirect interaction partners or false-positives that were isolated by simply being in close proximity to WRNIP1.

To validate some of the candidate interacting proteins, endogenous WRNIP1 was isolated from untreated and hydroxyurea-treated U2OS cells. The choice of the dosage and duration of treatment was based on proteomics studies, where WRNIP1 showed the highest abundance shortly after replication fork stalling (Dungrawala et al., 2015). Despite promising mass spectrometry data, none of the tested proteins was immuno-precipitated together with WRNIP1, irrespective of the conditions (Figure 18C). Surprisingly, mass spectrometry data could not be confirmed by Western blotting even when the same samples were analysed (data not shown). It is thus possible that the interactions are too weak or that only a small subpopulation of WRNIP1 exists in multi-protein complexes, eluding detection by most commonly used methods. Of note, none of the reported WRNIP1 interactors, such as WRN (Kawabe et al., 2001), RAD51, BRCA2 (Leuzzi et al., 2016), ATMIN (Kanu et al., 2016) or ZRANB3 (Ciccia et al., 2012) was found.

19.2 WRNIP1 interacts with ZRANB3 in vitro

Given WRNIP1's potential role at stalled replication forks, we were in particular interested to have a closer look at a possible interaction between WRNIP1 and ZRANB3. Previously, the two proteins were found to co-localise at UV-induced damage sites, however only if de-ubiquitylation of PCNA and signaling through PIK kinases were blocked (Ciccia et al., 2012). Moreover, WRNIP1 co-precipitated with tagged-ZRANB3, yet only upon formaldehyde-induced cross-linking in addition to the aforementioned treatments (Ciccia et al., 2012). To further investigate the interaction, both proteins were co-overexpressed in insect cells, followed by immuno-precipitation. Since WRNIP1 is mono-ubiquitylated in a UBZ-dependent manner and ZRANB3's function in response to replication stress depends, among others, on its ubiquitin-binding NZF domain (Ciccia et al. (2012), Vujanovic et al. (2017)), the UBZ-mutant D37A WRNIP1 was included in the

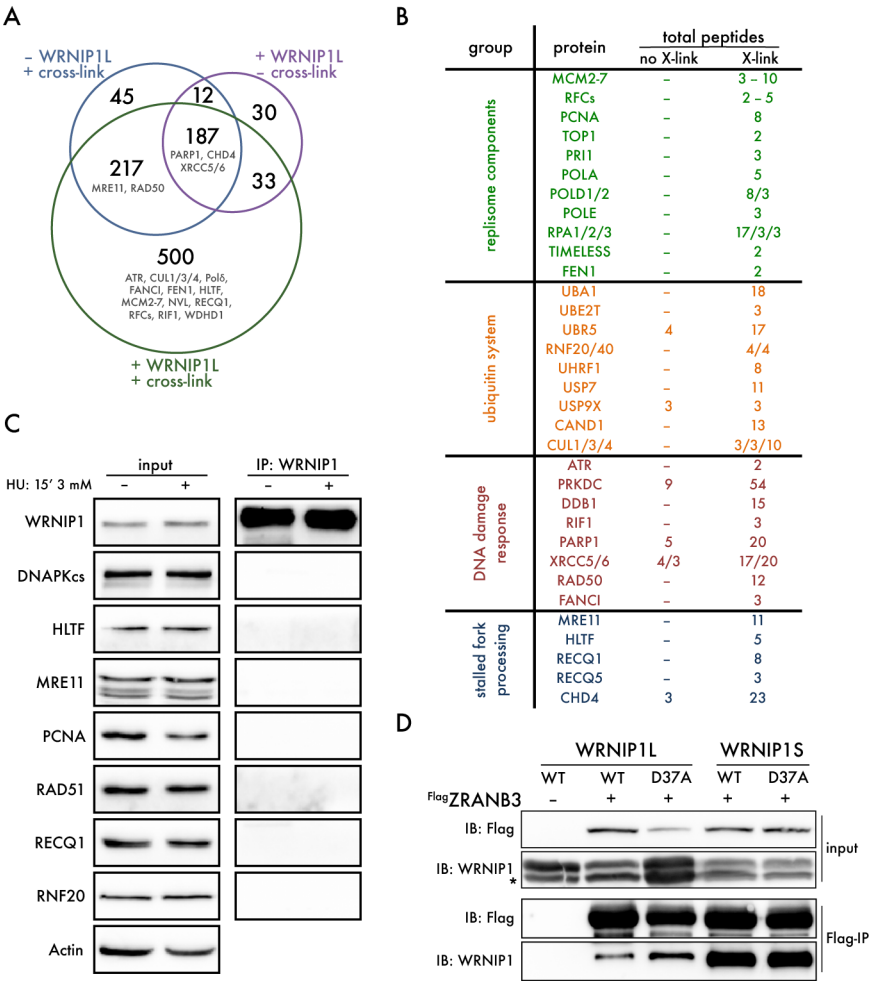

Figure 18: WRNIP1 interactome. (A) Venn diagram of datasets containing proteins identified by mass spectrometry in the three indicated conditions. The numbers indicate number of individual proteins. Sizes of circles are proportional to the amount of identified proteins. (B) List of significant hits reproducibly found in mass spectrometry analyses. (C) Western blotting analysis of endogenous WRNIP1 pull-down from U2OS cells. (D) Western blotting analysis of co-purification of WRNIP1 and ZRANB3 from insect cells. Asterisk indicates WRNIP1 degradation product.

analysis. As seen in Figure 18D, both variants of WRNIP1 co-purified with Flag-ZRANB3 and the interaction was independent of WRNIP1 ubiquitylation. Interestingly, WRNIP1S was reproducibly pulled-down more efficiently than WRNIP1L, despite being expressed at lower levels.

19.3 WRNIP1 influences ZRANB3's branch migration activity

The fact that WRNIP1 interacts with a known replication fork remodeler, but has no intrinsic branch migration activity may indicate that the protein might act as an auxiliary factor that indirectly participates in fork remodeling. To validate this hypothesis, a branch migration assay was performed with oligonucleotide-based substrates, using ZRANB3 in combination with WRNIP1L. Proteins were added at the same time or one of the proteins was pre-incubated with the substrate,

before addition of the other and starting the reaction by ATP (Figure 19A). In all of the tested scenarios, WRNIP1L did not affect product formation by ZRANB3. The same result was obtained for WRNIP1S (data not shown). To exclude the possibility that an effect of WRNIP1 cannot be reliably detected on a short oligonucleotide-based substrate that was used in the assays, a plasmid-based replication fork was then used (Figure 19B, upper panel). Such a substrate had been previously used to assess in vitro fork reversal activity of FANCM (Gari et al., 2008a), HLTF (Blastyak et al., 2010), ZRANB3, SMARCAL1 (Ciccia et al., 2012) and FBH1 (Fugger et al., 2015). As expected, WRNIP1L had no fork reversal activity (Figure 19B, lanes 2-4), in contrast to ZRANB3 (lane 5). Interestingly, titration of WRNIP1L into the reaction with ZRANB3 decreased accumulation of the end product, suggesting that WRNIP1L can inhibit long-range fork reversal by ZRANB3.

20 Function of WRNIP1 in cells

The cellular function of WRNIP1 has been difficult to establish since the moment the protein was identified. Until 2016, when WRNIP1 was shown to be involved in the protection of stalled replication forks, all accumulated observations did not allow to unequivocally characterise the protein's function. Since there was no data on any phenotype caused by WRNIP1 loss, we decided to investigate it with a series of commonly used assays.

20.1 WRNIP1 loss does not alter the response to genotoxic treatment

Loss of a factor involved in the DNA damage- or replication stress response frequently causes altered sensitivity to genotoxic agents. However, loss of WRNIP1 did not cause any significant change of cells survival upon treatment with a panel of genotoxins, which included drugs inducing physical damage, such as CPT, MMC, 4NQO or Zeocin, and compounds known to induce replication stress without modifying the DNA template, such as aphidicolin and HU (Figure 20A).

Two main kinases govern the cellular response to replication stress or DNA damage: ATR and ATM. To assess whether loss of WRNIP1 changes these signaling events, the phosphorylation status of ATM and ATR substrates was checked by Western blotting in response to (Figure 20B) or upon recovery from (Figure 20C) HU-induced replication stress. In both cases the kinetics of CHK1, CHK2 and KAP1 phosphorylation did not change significantly when WRNIP1 was absent. In the case of phospho-H2AX, loss of WRNIP1 seemed to enhance the modification upon longer HU-treatment and slow-down the dissipation of phosphorylation in the recovery phase. Interestingly, upon longer exposure times, it became evident that an up-shifted population of γH2AX, putatively mono-ubiquitylated, follows similar kinetics, i.e. without WRNIP1 the basal level was lower but got relatively more enhanced upon stress, and it persisted after the genotoxin was re-

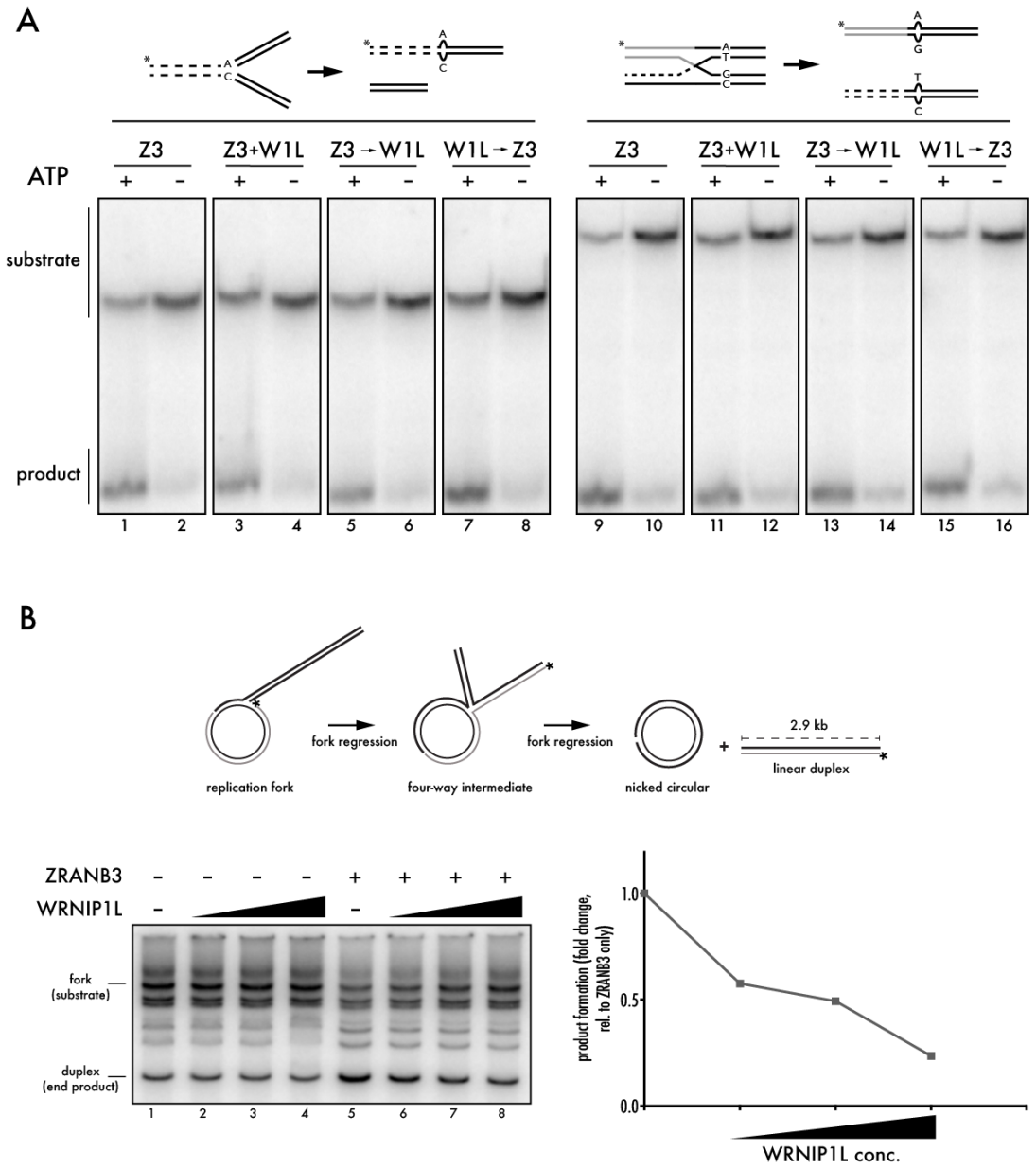

Figure 19: Functional interaction between WRNIP1 and ZRANB3. (A) Branch migration assay analysing the influence of WRNIP1 on ZRANB3 activity. (B) Fork reversal assay on a plasmid-based substrate. Upper panel - schematic of the assay; lower panel - influence of WRNIP1L on ZRANB3 fork reversal activity.

moved. Also, while phosphorylation of ATR did not seem affected, an extra band detected with the pATR S428 antibody around 100 kDa showed a different pattern in WRNIP1-depleted cells compared to the control. There are reports in literature suggesting that antibodies generated against phosphorylated peptides can recognise other substrates having similar motifs, e.g. pMCM3 can be detected by a pATM antibody (Mcmahon et al., 2012). The identity of the phosphorylated protein detected with the pATR antibody is unknown, however the data suggest that WRNIP1 can influence its basal and stress-induced phosphorylation events.

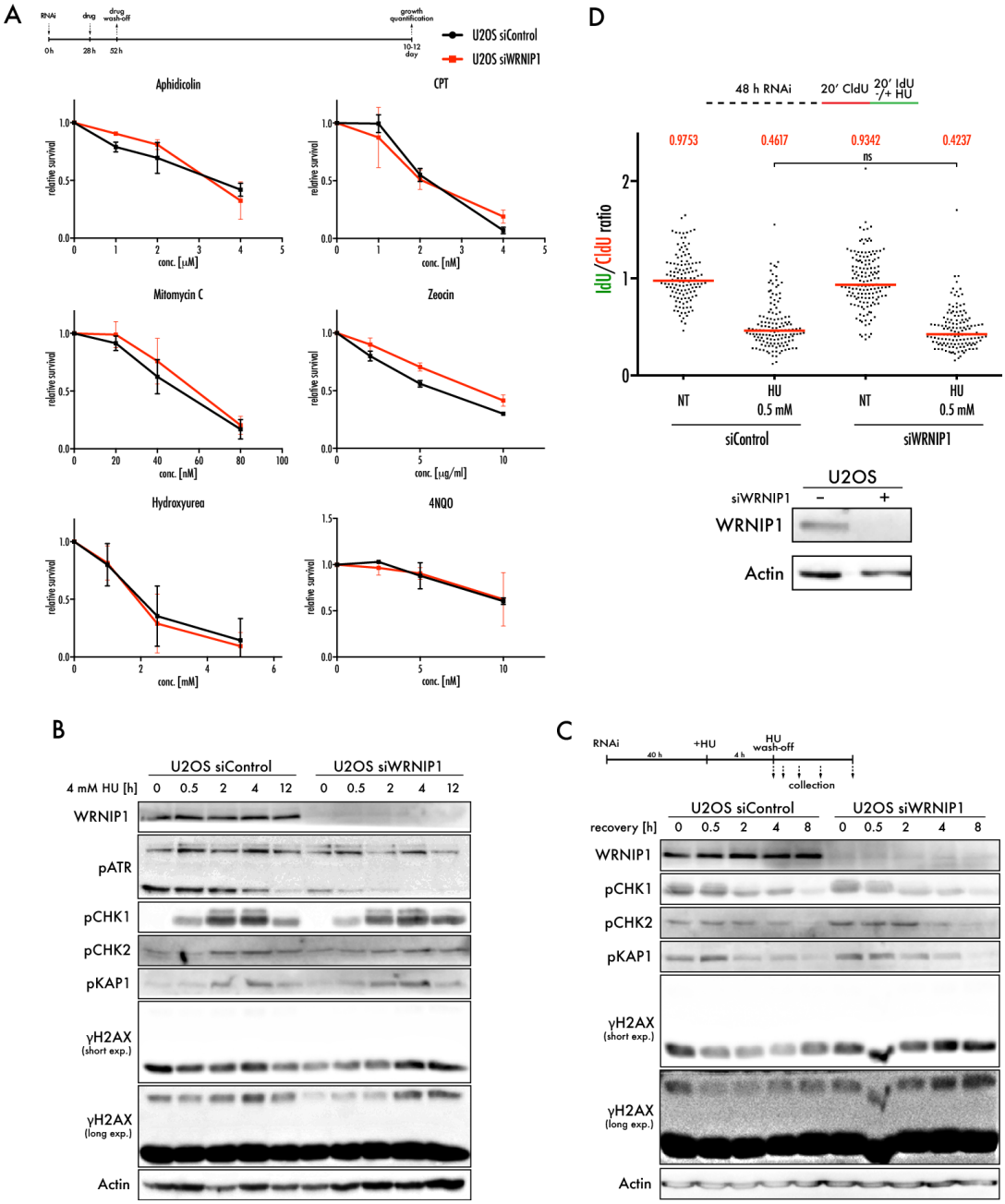

Figure 20: Phenotypical analysis of WRNIP1-deficient U2OS cells. (A) Clonogenic assay. Quantification represents 3 independent biological replicates, each consisting of 3 technical replicates. (B) Western blotting analysis of ATR and ATM signalling activation along hydroxyurea-treatment timecourse. (C) Western blotting analysis of ATR and ATM signalling activation during recovery from hydroxyurea-induced replication stress. (D) Analysis of replication dynamics by DNA fibre spreading. One hundred to two hundred molecules were scored for each condition. Horizontal line indicates median value, also given in red above the graph. Statistical analysis: Mann-Whitney test; ns - non-significant.

20.2 WRNIP1 does not influence replication dynamics upon replication stress

It has been established that global replication fork progression slow-down is an immediate response to a wide variety of genotoxic insults (Zellweger et al., 2015). It was further elucidated

that a challenged replication fork undergoes reversal, which causes the observed decrease in fork speed, when assayed by DNA fibre spreading (Zellweger et al. (2015), Vujanovic et al. (2017)). Based on these findings, replication fork progression upon HU-induced stress was checked in cells depleted of WRNIP1. Cells were sequentially pulse-labeled with halogenated thymidine analogues, additionally supplementing the second label with hydroxyurea at a concentration known to slow-down, but not stall replication fork progression (Figure 20D). WRNIP1 absence did not alter DNA synthesis upon HU treatment, further suggesting that the protein is not required for stress-induced replication fork reversal.

20.3 WRNIP1 protects stalled replication forks from MRE11-dependent degradation downstream of replication fork reversal

Recently, WRNIP1 was found to protect stalled replication forks from MRE11-dependent degradation (Leuzzi et al., 2016). The authors postulated that the protein acts together with BRCA2 to stabilise RAD51 on ssDNA generated at an uncoupled replication fork. Since in the absence of WRNIP1, MRE11-dependent degradation caused only parental ssDNA accumulation, the authors argued that nascent DNA is degraded without prior replication fork reversal. In support of their claim, depletion of RAD51, which should prevent fork reversal, did not rescue fork stability in a WRNIP1-depleted background.

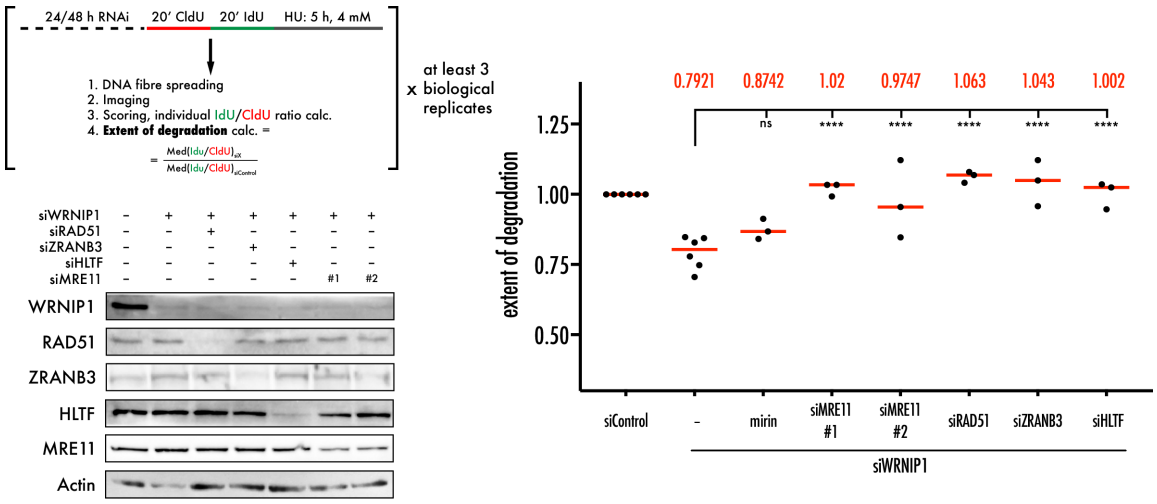

Figure 21: Nascent DNA degradation in WRNIP1-deficient cells. DNA fibre spreading analysis of stalled fork degradation. Upper-left panel - experimental design. Lower-left panel - Western blotting analysis of knock-down efficiency. Right panel - DNA fibre spreading results. Each dot represents an individual biological replicate; at least one hundred molecules were scored in each replicate. Horizontal lines indicate mean value, also given in red above the plot. Statistical analysis: one-way ANOVA; ns, not significant; ****, P<0.0001.

Nevertheless, we decided to revisit these results and, knowing how complex the role of RAD51 at stalled replication forks is, to include other genetic conditions that would block replication fork reversal. In order to do so, cells were pulse-labelled with thymidine analogues, followed by HU-induced replication fork stalling (Figure 21A). After DNA fibre spreading and imaging, the ratio of IdU and CldU track lengths was calculated for each molecule. Next, the "extent of degradation" was calculated for each sample relatively to the control sample. This was done to avoid variations between biological replicates. After acquiring data from at least 3 independent biological replicates, proper statistical tests were performed. The reason for such an experimental design was to confirm reproducibility of the results and enable a meaningful statistical analysis. As shown in Figure 21B, depletion of WRNIP1 caused nascent DNA degradation upon replication fork stalling. However, in contrast to the literature, treatment with mirin, an inhibitor of MRE11, did not rescue replication fork protection. On the other hand, depleting MRE11 by two different siRNA duplexes did revert the degradation phenotype. A similar rescue result was obtained when replication fork reversal was prevented by complete depletion of RAD51 or either of the fork reversing enzymes ZRANB3 and HLTF.

To summarise, in line with the literature, WRNIP1 depletion causes MRE11-dependent degradation of nascent DNA at a stalled replication fork. In contrast to the published model however, my data clearly indicates that WRNIP1 exerts its protective function downstream of replication fork reversal.

20.4 WRNIP1 knockout cells do not show nascent DNA degradation

To complement the studies in cells, WRNIP1 knock-out cell lines were generated using CRISPR-Cas9 technology. The short guide RNA was designed to target the first exon of WRNIP1, as seen on the schematic (Figure 22A). The initial validation of the knockout was done by restriction-digest of the targeted locus amplified from genomic DNA. The NHEJ-mediated processing of the Cas9-generated double-strand break would lead to the loss of a restriction site, enabling an easy estimation of knockout efficiency (Figure 22A). Using this approach, WRNIP1 knock-out HeLa FlpIn T-REx and U2OS cell lines were generated in which WRNIP1 was completely absent (Figure 22B).

To determine whether the cell lines recapitulate the results obtained with transient knock-down of the protein, stalled fork degradation was assessed, using standard DNA fibre spreading assay (Figure 22C). Surprisingly, both WRNIP1 knock-out cell lines were completely devoid of stalled fork degradation and therefore were not used for any further analyses.

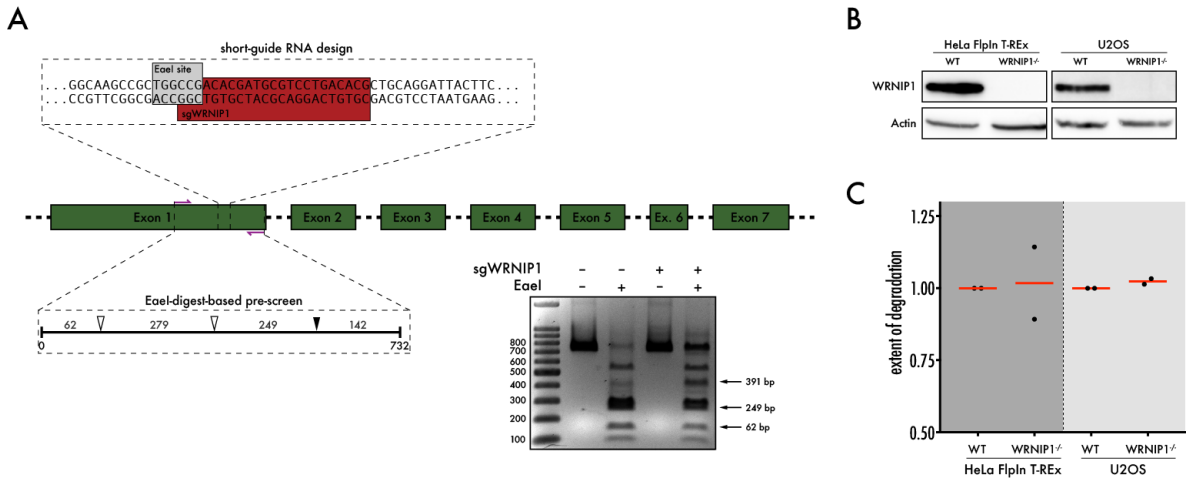

Figure 22: Generation and analysis of WRNIP1 knockout cell lines. (A) Schematic of WRNIP1-targeting short guide RNA design and experimental approach for knockout efficiency assessment. (B) Western blotting analysis of WRNIP1 knock-out HeLa FlpIn T-REx (left) and U2OS (right) cell lines. (C) Stalled replication fork degradation analysis in WRNIP1 knockout cells. Experimental design was the same as in Figure 21A, except here, two biological replicates were analysed. Horizontal red lines indicate mean value.

20.5 WRNIP1 is modified in cells by ubiquitin and ubiquitin-like modifiers

WRNIP1 was found to be modified by SUMO and ubiquitin, with the latter modification depending entirely on an intact UBZ domain (Bish and Myers, 2007). Using mass spectrometry, the authors were able to suggest several lysines that could be ubiquitylated, however no follow-up studies were done. Although the UBZ domain was implicated in targeting WRNIP1 to sites of replication stress, it remains unclear whether it is WRNIP1's ability to bind ubiquitin chains via the UBZ domain or UBZ-dependent ubiquitylation of the protein itself that drives the function. We decided to investigate this further in an attempt to identify the modified residues in WRNIP1 and to elucidate the role of PTMs in WRNIP1's function.

Apart from the abovementioned report, WRNIP1 was found in a number of proteomic screens aimed at the identification of post-translationally modified proteins. All sites for potential ubiquitylation, SUMOylation, NEDDylation and phosphorylation are depicted in Figure 23A. Additionally, GPS-SUMO prediction algorithm (http://sumosp.biocuckoo.org/) identified several putative SUMO-interacting motifs within WRNIP1, marked in the schematic in light brown.

First, in order to confirm the presence of ubiquitylation, Flag-tagged WRNIP1 was co-expressed with HA-tagged ubiquitin in human cells. Western blotting of isolated WRNIP1 clearly showed that the protein was indeed ubiquitylated in a UBZ-dependent manner (Figure 23B, upper panel). To identify the modified residue, several lysine-mutants were generated, chosen based on how frequent they were found in proteomic studies. All WRNIP1L variants were expressed and isolated from human cells, followed by Western blotting or in-gel staining (Figure 23B, lower panel).

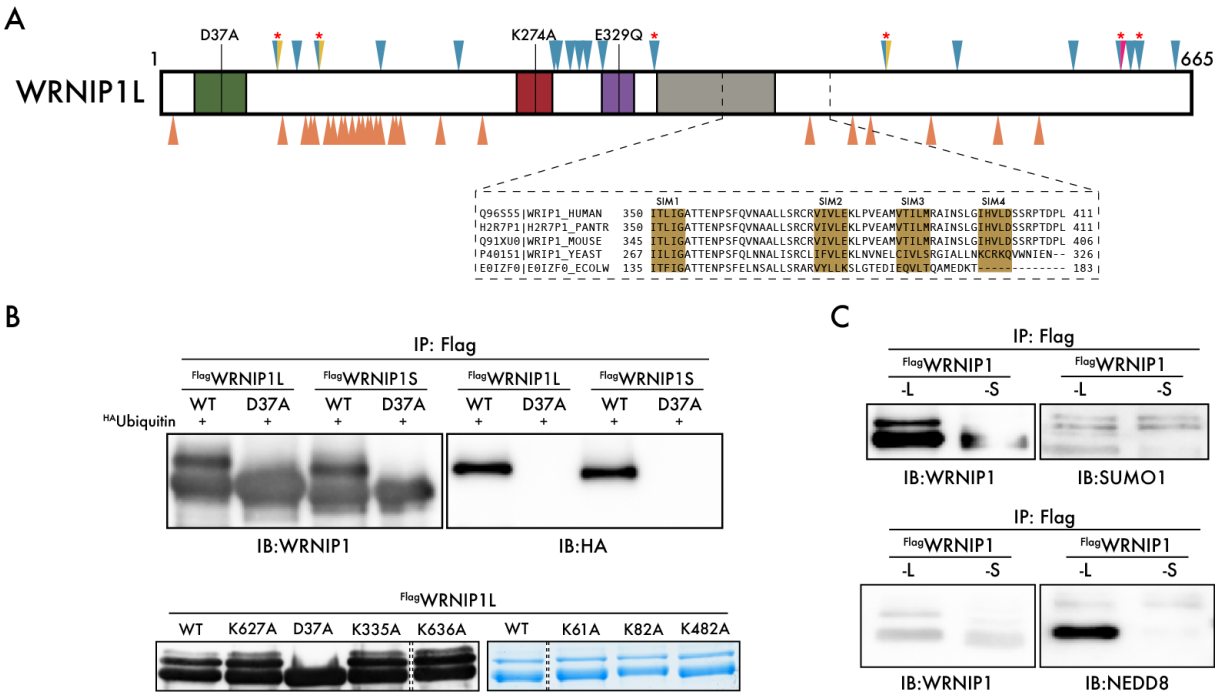

Figure 23: Post-translational modifications of WRNIP1. (A) Schematic depicting ubiquitylation (blue triangles), SUMOylation (yellow triangles), NEDDylation (pink triangle) and phosphorylation (orange triangles below). Predicted SUMO-interacting motifs (SIM) are indicated in light brown in the inset. Modifications were found on the PhosphoSitePlus database or predicted by GPS-SUMO (SUMOylation and SIM) and NeddyPreddy (NEDDylation). Generated mutants shown in (B) are marked with red asterikses. (B) Analysis of WRNIP1 ubiquitylation. Upper panel - Western blotting analysis of Flag-WRNIP1 isolated from cells co-expressing Flag-WRNIP1 and HA-Ubiquitin. Lower panel - Western blotting (left) or SDS-PAGE analysis of indicated mutant Flag-WRNIP1L. Dashed lines indicate excised irrelevant lanes. (C) Analysis of SUMOylation (upper panel) and NEDDylation (lower panel) of WRNIP1 in cells.

Unfortunately, none of the mutants could recapitulate complete lack of modification seen for the UBZ-mutant (D37A) or any reduction in the amount of modified protein. In line with the literature, WRNIP1 was also SUMOylated (Figure 23C, upper). Interestingly, WRNIP1, especially the long isoform, was also modified by NEDD8 - another ubiquitin-related peptide (Figure 23C, lower). Interestingly, NEDDylation was detected mainly in the lower band, suggesting that WRNIP1 could be constitutively modified in cells.

DISCUSSION

21 Results discussion

21.1 WRNIP1 protects replication forks after their stress-induced reversal by binding to the resulting 4-way junction

In this project, we aimed at investigating the role of WRNIP1 in the replication stress response and elucidating the underlying mechanism. Recently, the protein was found to protect stalled replication forks from MRE11-dependent degradation, however the mechanistic data were still missing (Leuzzi et al., 2016). Here, we employed in vitro analysis of WRNIP1 activity and investigated further its cellular function, which led us to a model, in which WRNIP1 protects replication forks after their stress-induced remodeling, by binding specifically to 4-way junctions that result from stalled fork reversal (Figure 24).

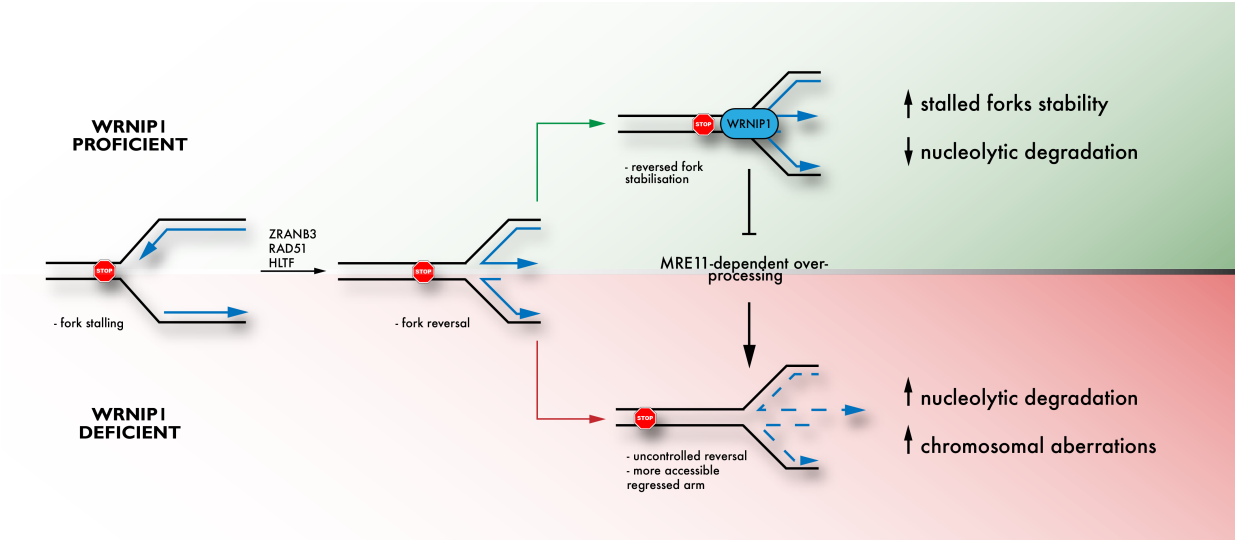

Figure 24: Proposed model. See text for details

Our proposed model stands in disagreement with published data. The study mentioned above concluded that stalled replication forks are not reversed prior to MRE11-dependent degradation in the absence of WRNIP1, since knock-down of RAD51, which should prevent fork reversal, did not rescue fork protection (Leuzzi et al., 2016). In contrast, we reproducibly saw that fork resection in WRNIP1-deficient cells can be avoided completely by RAD51 depletion (Figure 21). The simplest explanation for this discrepancy could be the efficiency of RAD51 knockdown, which in our case was full, while only partial in the case of the other study. RAD51 has a crucial, but complex, role in replication fork reversal and protection. It was recently shown that the RAD51

T131P mutant, which cannot form stable nucleofilaments (Wang et al., 2015), is still able to mediate fork reversal, but is incapable of fork protection (Mijic et al., 2017). It is therefore plausible that incomplete RAD51 knockdown would leave enough protein to remodel stalled forks, but not enough to avoid their over-processing by nucleases. To corroborate our findings, we have also blocked replication fork reversal by depleting the fork remodeling ATPases ZRANB3 and HLTF, both of which were recently shown to prevent fork degradation in a BRCA2-deficient background (Taglialatela et al. (2017), Mijic et al. (2017)). In the case of WRNIP1-depleted cells, knockdown of either ZRANB3 or HLTF led to a complete rescue of fork protection (Figure 21), further showing that WRNIP1 acts downstream of replication fork reversal. These findings will be next corroborated by performing a direct visualisation of replication intermediates by electron microscopy, as was recently done for BRCA2 (Mijic et al., 2017).

In the next steps, it will be interesting to analyse which functional domains of WRNIP1 are necessary for its protective function. Preliminary data from complementation studies were inconclusive, possibly due to the fact that ectopic expression of WRNIP1 leads to an extreme overproduction of the protein, which may be counter-productive due to WRNIP1's apparent propensity to form stable oligomers, as discussed later.

Surprisingly, preventing stalled fork degradation by RNAi-mediated depletion of MRE11, but not inhibition by mirin could rescue replication fork stability in WRNIP1-deficient background; in agreement with literature, mirin fully rescued stalled fork protection in BRCA2-deficient cells (data not shown). The different effect of RNAi-mediated knock-down and inhibition with mirin could be due to the fact that the inhibitor blocks only the exonuclease activity of MRE11 (**?**)Shibata2014), leaving the endonuclease activity intact. MRE11 initiates end-resection by nicking dsDNA away from the end, generating an entry point for its 3'-5' exonucleolytic activity (Stracker and Petrini, 2011), it is therefore possible that WRNIP1 prevents nucleolytic degradation of a stalled replication fork at an early stage, which putatively depends on the endonucleolytic activity of MRE11. To validate this hypothesis, we will make use of more available MRE11 inhibitor PFM01, which specifically targets the endonuclease activity of the protein (Shibata et al., 2014).

Unexpectedly, even though WRNIP1 is needed for stalled fork protection, it is dispensable for cell survival upon genotoxic treatment (Figure 20A). Evidently, more sensitive assays should be employed to assess WRNIP1's importance for the maintenance of genomic stability, e.g. analysis of chromosomal aberrations by metaphase spreads. Moreover, to our surprise, we were unable to reproduce the fork degradation phenotype in WRNIP1 knock-out cell lines (Figure 22C). Possibly, long culturing of the cells, which is required to isolate knock-out clones, led to adaptation of cells to the absence of WRNIP1. It is known that cells may eventually adapt to unfavourable circumstances by, e.g. secondary mutations or upregulation of compensatory pathways. For instance, it was recently shown that HR-deficient tumours might acquire chemoresistance to PARP inhibitor

by the loss of PTIP, a factor that normally promotes stalled fork degradation. This leads to stabilisation of replication forks in spite of the absence of BRCA2 (Chaudhuri et al., 2016). While we do not plan on investigating the WRNIP1 knock-out cell lines any further, it is evident that inducing a complete absence of an important factor may dramatically rewire cellular pathways, therefore studies involving knock-out cells should be always complemented with RNAi-based transient knock-down.

While our initial hypothesis assumed that WRNIP1 could have a direct role in replication fork remodeling, we did not detect branch migration, or any DNA metabolising activity (Figure 17), indicating that WRNIP1 does not actively remodel replication forks. This notion was corroborated by experiments in cells, where we showed that depletion of WRNIP1 does not influence replication fork progression upon replication stress, in contrast to the absence of enzymes involved in fork regression, such as RAD51 (Zellweger et al., 2015), ZRANB3 (Vujanovic et al., 2017) and HLTF (Kile et al., 2015).

On the other hand, WRNIP1 shows DNA binding abilities, with a strong preference for 4-way junctions (Figure 16). This result led us to hypothesise that WRNIP1 may stabilise reversed replication forks, rather than actively generating them. Interestingly, WRNIP1 decreased the efficiency with which ZRANB3 is able to reverse plasmid-based replication forks in vitro (Figure 19B). The first experiment was done in an end-point fashion, however the assay also allows for monitoring the extent of fork reversal. It will be therefore interesting to investigate whether WRNIP1 causes accumulation of forks with regressed arms of specific length, preventing too extensive reversal. Also, while so far we only investigated the functional interaction between WRNIP1 and ZRANB3, we will expand our analyses to another fork reversing enzyme – HLTF.

The above observations allow us to speculate that WRNIP1 is an early responder to replication fork stalling and remodeling. Based on WRNIP1's DNA binding abilities and preference for 4-way junctions, we propose that the protein binds to replication forks that have been regressed by the co-operative action of RAD51 and ZRANB3 or HLTF, thus preventing excessive fork reversal and nucleolytic over-processing. A similar model was recently described for the maintenance of telomere integrity, when TRF2, a component of the Shelterin complex, was found to protect t-loops against cleavage, by binding to the branch-point at its base (Schmutz et al., 2017).

21.2 Potential mechanism for WRNIP1-BRCA2 epistasis in the protection of stalled replication forks

WRNIP1 was found to act in the same protective pathway as BRCA2 (Leuzzi et al., 2016). Recent data suggest that BRCA2 is not necessary for preventing stalled fork degradation at an early timepoint (30 min after fork stalling), but becomes indispensable later (120 min after fork stalling)

(Lemaçon et al., 2017). Interestingly, WRNIP1's abundance at replication forks increases rapidly right after fork stalling, peaks at the 15 min time-point, and then decreases (Dungrawala et al., 2015). It is therefore plausible that the protein is crucial for preventing nucleolytic degradation immediately after fork reversal and then "hands over" to BRCA2, which is in turn required for fork protection when replication stress persists. A time-resolved fork degradation assay will be done to validate this hypothesis.

21.3 WRNIP1 preferentially binds 4-way DNA junctions and is active as a monomer or a low-order oligomer

We found that WRNIP1 binds DNA in vitro, with a preference for 4-way junction substrates that mimic Holliday junctions or reversed replication forks. At first, we observed a much broader substrate specificity, i.e. WRNIP1 was found to bind to any structure that had a branching point (Figure 16A). However, we realised that our experimental conditions probably caused unfolding of the protein by the action of SDS, which may have caused either unspecific protein-DNA complexes or exposed WRNIP1's DNA-interaction surface, which was otherwise shielded by oligomerisation or aggregation of the protein. The latter hypothesis is more plausible, since not all DNA substrates were bound by WRNIP1 and there was a clear preference for a 4-way junction. Indeed, when the DNA binding assay was performed in native conditions, we observed that only the 4-way junction was shifted, interestingly only by wild type WRNIP1S and not WRNIP1L (Figure 16B). To determine whether the ability to bind 4-way junctions was unique to the short isoform, we tested all other purified WRNIP1 variants for DNA binding. Surprisingly, apart from all WRNIP1S mutants, also K274A WRNIP1L was able to shift the 4-way junction substrate (Figure 16C), suggesting that, in principle, both isoforms have the same DNA binding ability. To explain this discrepancy, we analysed all WRNIP1 preparations. Closer examination by the use of native-PAGE coupled to Western blotting revealed that, apart from the major high M_W WRNIP1 population, there is an additional, much less abundant form of a higher electrophoretic mobility, suggesting a smaller size (Figure 15E). Interestingly, the latter population was present only in WRNIP1 preparations that were able to specifically bind to 4-way junctions (Figure 16C). These results raise the interesting possibility that WRNIP1, while mostly present in stable higher-order oligomers, binds DNA only as a monomer or lower-order oligomer.

In 2005, WRNIP1's size was analysed by gel filtration and glycerol-gradient ultracentrifugation, and it was determined that the protein assembles into homo-octamers (Tsurimoto et al., 2005). This notion has never been challenged, since oligomerisation was expected from a protein belonging to the AAA+ ATPase family. However, members of this family usually form hexameric rings, with some exceptions, most notably RFC (pentameric) or the apoptosome (heptameric); an

octameric human AAA+ ATPase has never been reported (rev. in Wendler et al. (2012)). Also, the authors' conclusion about the oligomeric state of WRNIP1 is surprising, since their data from glycerol-gradient ultracentrifugation clearly indicates that the protein sediments faster than alcohol dehydrogenase (141-151 kDa), but slower than catalase (232 kDa), and disagrees with their gel filtration results that shows WRNIP1 eluting at a similar volume as thyroglobulin (669 kDa). Interestingly, fractionation of cell extracts by size-exclusion chromatography revealed that the endogenous WRNIP1 eluted in two populations – one of high M_W (600-700 kDa) and another of lower M_W (100-200 kDa) (Crosetto et al. (2008), Tan et al. (2017)). The second study also shows that in the conditions that activate WRNIP1 the lower M_W complexes become more abundant. Interestingly, such a behaviour has been already reported, e.g. for RAD51, whose oligomers have to be disrupted to enable loading of the protein onto DNA (rev. in Lord and Ashworth (2007)), or RAD18, which under unperturbed conditions exists as oligomers/aggregates that are disrupted when the protein needs to be activated in the response to DNA damage (Zeman et al., 2014). Although data regarding WRNIP1 suggest that the protein may follow a similar behaviour, the hypothesis was never put forward, therefore we plan to investigate it by analysing a non-oligomerising mutant of WRNIP1 and by checking the oligomeric state of WRNIP1 that is bound to chromatin, in a similar manner as has been recently done for the replisome-associated redox sensor PRDX2 (Somyajit et al., 2017). As noted, not all of our WRNIP1 preparations contain the lower M_W population, i.e. WRNIP1L WT, D37A and E329Q seem to form exclusively high-order oligomers (Figure 15E). A possible explanation could be the fact that, according to the predicted structures (Figure 13B), the two isoforms differ in the folding of the C-terminus, which is reportedly responsible for oligomerisation of the protein (Crosetto et al., 2008). It is thus possible that WRNIP1S self-associates more weakly than WRNIP1L. As for the ATP-binding mutant WRNIP1L K274A, it has been observed that mutations in the ATP-binding pocket of AAA+ ATPases (as is the case for K274A mutant) may compromise their ability to form oligomers (rev. in Wendler et al. (2012)).

21.4 WRNIP1 interactome

To gain more insight into WRNIP1's cellular function, we wanted to identify its yet undiscovered interaction partners. This turned out to be a difficult task since WRNIP1 seemingly did not interact with any protein involved in DNA metabolism or DNA damage response, irrespective of the strategy we used (different tags, IP of endogenous protein, cell fractionation, different cell lines). The only meaningful data was acquired when cross-linking was included in the protocol (Figure 18A). Identification of many replisome components indicated that, in our experimental conditions, WRNIP1 does associate with replication forks, which is in line with the literature ((Alabert et al., 2014), Dungrawala et al. (2015)); we were unable to show WRNIP1's association with the

replisome by iPOND (data not shown). Interestingly, several proteins involved in the transactions at stalled replication forks were also found in the dataset, such as MRE11, HLTF, RECQ1, PARP1 or CHD4 (Figure 18B). However, we could not recapitulate any of the interactions by WRNIP-IP and Western blotting (Figure 18C). The reason for this could be either the fact that cross-linking is prone to give false positive results, or the transient and weak nature of WRNIP1 interactions. We think that the latter is more plausible, since also the reported interactions of WRNIP1 with Polη (Yoshimura et al., 2014) or ZRANB3 (Ciccia et al., 2012) are either very weak or seen only upon severe treatment of cells. Also, mass spectrometry or IP approaches never identified ZRANB3, although we were able to clearly show the interaction when the two proteins were expressed in a heterologous system (Figure 18D). Surprisingly, in our mass spectrometry datasets we have never found WRN, RAD51 or BRCA2, all of which were reported to interact with WRNIP1. In the case of the interaction with WRN, the analysis was done on purified proteins (Kawabe et al., 2001), suggesting that the complex may be too transient to be detected in cell lysates. As for the lack of interaction with BRCA2 or RAD51, the difference is hard to explain, since we have tried to recapitulate this result using exactly the same protocol as in the reported study (Leuzzi et al., 2016), however no interaction was found (data not shown).

Our interactome study suggests that WRNIP1 does not seem to form stable complexes in cells. We hypothesised that one way to explain such an uncommon behaviour would be if WRNIP1 were a protein chaperone. Chaperones, that are most commonly oligomeric proteins, bind to their substrates, which triggers ATP hydrolysis and, in turn, remodeling of the interaction partner, followed by a rapid dissociation of the complex. Many AAA+ ATPases are chaperones, with the most notable examples being HSP (Heat Shock Protein) proteins or p97/VCP (rev. in Saibil (2013)). The latter protein has a well-established role in the DNA damage response, e.g. it was shown to extract Polη from DNA after TLS (Davis et al., 2012) or Ku70/80 after NHEJ (van den Boom et al., 2016). Interestingly, p97 is targeted to its polyubiquitylated substrates by adaptor proteins, such as DVC1, which has a UBZ domain that mediates substrate recognition (Davis et al., 2012). Since WRNIP1 has an AAA+ ATPase domain, reportedly forms oligomers and binds polyubiquitin chains via its UBZ motif, we hypothesise that it may have a similar function as p97-DVC1. Apart from the lack of stable protein-protein interactions, this could also explain the very weak, DNA-independent ATPase activity. To address the latter, we have attempted mass spectrometry analysis using WRNIP1 mutants that are unable to hydrolyse ATP (K274R or E329Q), however it did not improve the result (data not shown).

An alternative, or complementary, explanation for the limited success of our interactome analysis could be the aforementioned possibility that WRNIP1 is inactive in its oligomeric state. Since in most of the experiments we have over-expressed WRNIP1 to extremely high levels, it is plausible that the majority of the protein self-associates and does not engage in protein-protein inter-

actions. In this view, it would be interesting to check which form of WRNIP1 – high or low M_W – interacts with ZRANB3. The fact that WRNIP1S is reproducibly pulled-down with ZRANB3 more efficiently than WRNIP1L, despite being expressed at lower level, suggests that the low M_W population engages in interactions, however this would need to be confirmed by e.g. native PAGE of analytical gel filtration. Also, the most recent study shows that, in the conditions promoting formation of a complex between WRNIP1, TRIM14 (Tripartite motif 14) and PPP6C phosphatase, the low M_W (100-200 kDa) population of WRNIP1 is more abundant (Tan et al., 2017).

21.5 Post-translational modifications of WRNIP1

Lastly, we were interested in elucidating the role of WRNIP1 modifications for its cellular function. It is well established that the protein is ubiquitylated in a UBZ-dependent manner (Bish and Myers, 2007). We were able to recapitulate this result by showing that the WRNIP1 UBZ mutant (D37A) is not modified by ubiquitin anymore (Figure 23B). This observation is reminiscent of a phenomenon called "coupled monoubiquitylation", where the modification of a protein depends on its ubiquitin-binding motif. One model explaining this, proposes that the substrate protein binds to a ubiquitylated E3 ubiquitin ligase, which enables the modification of the substrate protein (rev. in Haglund and Stenmark (2006)). The co-existence of a UBD and mono-ubiquitylation can provide an elegant auto-inhibitory mechanism, where an intra-molecular interaction between the two is formed. Such a negative-feedback loop was described for Polymerase η, which inhibits its unscheduled interaction with PCNA in unperturbed conditions. On the other hand, when the TLS pathway has to be initiated, ubiquitylation of Polη is lost and the protein can use its UBD to interact with PCNA and perform its function (Bienko et al., 2010). Another UBZ-containing protein, RAD18, was also shown to be mono-ubiquitylated which inhibited its cellular functions (Zeman et al., 2014). In this case, the authors found that the inhibitory effect was due to the binding of RAD18-Ub to the unmodified protein, tethering RAD18 into large, inactive aggregates. Genotoxic treatment caused de-ubiquitylation, allowing RAD18 to form functional complexes with its interaction partners HLTF and SHPRH. Out of the two presented mechanisms, the first one seems to be more plausible for WRNIP1, since the WRNIP1 UBZ mutant forms the same high M_W complexes as the wild type protein. If the intra-molecular UBD-ubiquitin interaction indeed inhibited the formation of complexes with interaction partners, preventing ubiquitylation should lead to the identification of more WRNIP1 interactors. This was however not the case – the dataset obtained for WRNIP1 D37A was not significantly different than the one of the wild type protein (data not shown). On the other hand, the WRNIP1 UBZ mutant was also over-expressed to extremely high levels, which may have potentially caused issues, as discussed above. So far, the inability of WRNIP1 UBZ mutants to localise to sites of DNA damage was explained by a compromised

recognition of polyubiquitylated PCNA (Crosetto et al. (2008), Nomura et al. (2012), Kanu et al. (2016)). However, it is also possible that the lack of UBZ-dependent ubiquitylation contributes to the phenotype. Therefore, we wanted to identify the modified lysines and generate a WRNIP1 mutant that cannot be ubiquitylated, but still has a functional UBZ domain. Based on available proteomics data, we have mutated several lysine residues, however none of the mutants could recapitulate the complete lack of modification seen for the UBZ mutant (Figure 23B). This is not surprising, since it is known that adjacent lysine residues can compensate and get modified, which was shown for e.g. Polymeraseη that had to be mutated at 4 sites to abrogate monoubiquitylation (Bienko et al., 2010). Therefore, we are planning to generate multiple-lysine mutants and analyse the function of unmodified WRNIP1 in the replication stress response. Interestingly, a recent study has identified WRNIP1 as one of less than 100 substrates of the BRCA1 E3 ubiquitin ligase (Kim et al., 2017). To investigate this further, we plan to check the ubiquitylation status of WRNIP1 in BRCA1-depleted cells.

As for the other potential modifications of WRNIP1, namely SUMOylation, NEDDylation or phosphorylation (Figure 23A), more basic experiments have to be done to confirm their existence, e.g. de-modification of WRNIP1 isolated from human cells with the respective enzymes. Only then it would be interesting to investigate further to find modified residues and the potential function of these modifications. The same holds true for the putative SIMs that were found by prediction algorithms. While the high evolutionary conservation of primary sequence is promising, first, the ability of WRNIP1 to bind SUMO moieties has to be confirmed.

22 Concluding remarks and outlook

In this study, we have investigated further the role of WRNIP1 in the protection of stalled replication forks against MRE11-dependent deleterious over-processing. We have suggested a molecular mechanism of the protective function, which is unprecedented, despite the ever-growing list of factors that are necessary to avoid stalled replication fork over-resection. Our in vitro analysis of WRNIP1's function and oligomeric state challenges the existing evidence and provides a possible explanation as to why the characterisation of WRNIP1's functions and activities has been so difficult thus far.

On the other hand, our data necessitates more experiments to elucidate the function of WRNIP1 further or to confirm preliminary observations. I believe that the most crucial future experiments involve:

1. Direct visualisation of replication intermediates – this analysis will be done to validate my DNA fibre data indicating that in WRNIP1 absence MRE11-dependent degradation targets reversed replication forks. The analysis will be performed in collaboration with Prof. Massimo Lopes group.

2. Rescue of fork protection by complementation with WRNIP1 alleles – this analysis will define which functional domains or features of WRNIP1 are necessary for the protein's function in replication fork protection. To do so, conditions where WRNIP1 is expressed at physiological level have to be established.

3. Epistasis with BRCA2 – to validate our model suggesting that WRNIP1 is needed for fork protection immediately after replication fork reversal, fork degradation time-course experiments will be done.

4. Purification of low M_W WRNIP1 – our DNA-binding data and yet-unnoticed published observations indicate that WRNIP1 may be active as a low-order oligomer or a monomer. Since it is known that the C-terminal part of the protein is necessary for oligomerisation, truncations will be introduced in order to force WRNIP1 out of the putatively inactive oligomers. Such mutants will be analysed in vitro for DNA binding and for influence on replication fork reversal.

5. WRNIP1's influence on replication fork reversal in vitro – first, the initial data suggesting that WRNIP1 inhibits ZRANB3's fork reversal activity will be confirmed. Then, a more detailed analysis of the extent of reversal in the presence of WRNIP1 will be done to validate our hypothesis that WRNIP1 binds to early-stage reversed forks. Finally, the same analysis will be done with HLTF.

6. Oligomerisation status of WRNIP1 in cells – to validate our hypothesis about WRNIP1 being active as a monomer or a low-order oligomer, the oligomeric status of the protein will be checked by analytical size-exclusion chromatography or native-PAGE of subcellular fractions and/or in response to genotoxic treatment.

7. Modification of WRNIP1 - WRNIP1 seems to be a heavily modified protein, therefore a comprehensive study of its PTMs is impossible within the scope of this project. However, since WRNIP1 is a putative substrate for BRCA1, I believe that it would be interesting to follow this lead and check whether or not WRNIP1's function depends on this important tumour suppresor.

References

Aguilera, A. and Gómez-González, B. (2008). Genome instability: a mechanistic view of its causes and consequences. *Nature Reviews Genetics*, 9(3):204–217.

Alabert, C., Bukowski-Wills, J.-C., Lee, S.-B., Kustatscher, G., Nakamura, K., de Lima Alves, F., Menard, P., Mejlvang, J., Rappsilber, J., and Groth, A. (2014). Nascent chromatin capture proteomics determines chromatin dynamics during DNA replication and identifies unknown fork components. *Nature Cell Biology*, 16(3):281–293.

Alberts, B., Bray, D., Lewis, J., Raff, M., Roberts, K., and Watson, J. (2002). *Molecular Biology of the Cell*. Garland, 4th edition. Available from https://www.ncbi.nlm.nih.gov/books/NBK21054/.

Badu-Nkansah, A., Mason, A. C., Eichman, B. F., and Cortez, D. (2016). Identification of a substrate recognition domain in the replication stress response protein zinc finger ran-binding domain-containing protein 3 (ZRANB3). *Journal of Biological Chemistry*, 291(15):8251–8257.

Bansbach, C. E., Bétous, R., Lovejoy, C. A., Glick, G. G., and Cortez, D. (2009). The annealing helicase SMARCAL1 maintains genome integrity at stalled replication forks. *Genes and Development*, 23(20):2405–2414.

Barber, L. J., Youds, J. L., Ward, J. D., McIlwraith, M. J., O'Neil, N. J., Petalcorin, M. I. R., Martin, J. S., Collis, S. J., Cantor, S. B., Auclair, M., Tissenbaum, H., West, S. C., Rose, A. M., and Boulton, S. J. (2008). RTEL1 Maintains Genomic Stability by Suppressing Homologous Recombination. *Cell*.

Bartkova, J., Hořejší, Z., Koed, K., Krämer, A., Tort, F., Zieger, K., Guldberg, P., Sehested, M., Nesland, J. M., Lukas, C., Ørntoft, T., Lukas, J., and Bartek, J. (2005). DNA damage response as a candidate anti-cancer barrier in early human tumorigenesis. *Nature*, 434(7035):864–870.

Berti, M., Chaudhuri, A. R., Thangavel, S., Gomathinayagam, S., Kenig, S., Vujanovic, M., Odreman, F., Glatter, T., Graziano, S., Mendoza-Maldonado, R., Marino, F., Lucic, B., Biasin, V., Gstaiger, M., Aebersold, R., Sidorova, J. M., Monnat, R. J., Lopes, M., and Vindigni, A. (2013). Human RECQ1 promotes restart of replication forks reversed by DNA topoisomerase I inhibition. *Nature Structural & Molecular Biology*, 20(3):347–354.

Berti, M. and Vindigni, A. (2016). Replication stress: getting back on track. *Nature Structural & Molecular Biology*, 23(2):103–109.

Bétous, R., Couch, F. B., Mason, A. C., Eichman, B. F., Manosas, M., and Cortez, D. (2013). Substrate-Selective Repair and Restart of Replication Forks by DNA Translocases. *Cell Reports*, 3(6):1958–1969.

Bétous, R., Mason, A. C., Rambo, R. P., Bansbach, C. E., Badu-Nkansah, A., Sirbu, B. M., Eichman, B. F., and Cortez, D. (2012). SMARCAL1 catalyzes fork regression and holliday junction migration to maintain genome stability during DNA replication. *Genes and Development*, 26(2):151–162.

Bienko, M., Green, C. M., Sabbioneda, S., Crosetto, N., Matic, I., Hibbert, R. G., Begovic, T., Niimi, A., Mann, M., Lehmann, A. R., Dikic, I., Mann, M., Lehmann, A. R., and Dikic, I. (2010). Regulation of Translesion Synthesis DNA Polymerase η by Monoubiquitination. *Molecular Cell*, 37(3):396–407.

Bish, R. A. and Myers, M. P. (2007). Werner helicase-interacting protein 1 binds polyubiquitin via its zinc finger domain. *Journal of Biological Chemistry*, 282(32):23184–23193.

Blackford, A. N., Schwab, R. A., Nieminuszczy, J., Deans, A. J., West, S. C., and Niedzwiedz, W. (2012). The DNA translocase activity of FANCM protects stalled replication forks. *Human Molecular Genetics*, 21(9):2005–2016.

Blastyak, A., Hajdu, I., Unk, I., and Haracska, L. (2010). Role of Double-Stranded DNA Translocase Activity of Human HLTF in Replication of Damaged DNA. *Molecular and Cellular Biology*, 30(3):684–693.

Branzei, D. and Foiani, M. (2010). Maintaining genome stability at the replication fork. *Nature Reviews Molecular Cell Biology*, 11(3):208–219.

Brun, J., Chiu, R. K., Wouters, B. G., and Gray, D. a. (2010). Regulation of PCNA polyubiquitination in human cells. *BMC research notes*, 3:85.

Byun, T. S., Pacek, M., Yee, M. C., Walter, J. C., and Cimprich, K. A. (2005). Functional uncoupling of MCM helicase and DNA polymerase activities activates the ATR-dependent checkpoint. *Genes and Development*, 19(9):1040–1052.

Cejka, P. (2015). DNA end resection: Nucleases team up with the right partners to initiate homologous recombination. *Journal of Biological Chemistry*, 290(38):22931–22938.

Chaudhuri, A. R., Callen, E., Ding, X., Gogola, E., Duarte, A. A., Lee, J.-E., Wong, N., Lafarga, V., Calvo, J. A., Panzarino, N. J., John, S., Day, A., Crespo, A. V., Shen, B., Starnes, L. M., de Ruiter, J. R., Daniel, J. A., Konstantinopoulos, P. A., Cortez, D., Cantor, S. B., Fernandez-Capetillo, O., Ge, K., Jonkers, J., Rottenberg, S., Sharan, S. K., and Nussenzweig, A. (2016). Replication fork stability confers chemoresistance in BRCA-deficient cells. *Nature*, 535(7612):382–387.

Chu, W. K., Payne, M. J., Beli, P., Hanada, K., Choudhary, C., and Hickson, I. D. (2015). FBH1 influences DNA replication fork stability and homologous recombination through ubiquitylation of RAD51. *Nature Communications*, 6:5931.

Ciccia, A. and Elledge, S. J. (2010). The DNA Damage Response: Making It Safe to Play with Knives. *Molecular Cell*, 40(2):179–204.

Ciccia, A., Nimonkar, A. V., Hu, Y., Hajdu, I., Achar, Y. J., Izhar, L., Petit, S. A., Adamson, B., Yoon, J. C., Kowalczykowski, S. C., Livingston, D. M., Haracska, L., and Elledge, S. J. (2012). Polyubiquitinated PCNA Recruits the ZRANB3 Translocase to Maintain Genomic Integrity after Replication Stress. *Molecular Cell*, 47(3):396–409.

Collis, S. J., Ciccia, A., Deans, A. J., Horejsi, Z., Martin, J. S., Maslen, S. L., Skehel, J. M., Elledge, S. J., West, S. C., and Boulton, S. J. (2008). FANCM and FAAP24 Function in ATR-Mediated Checkpoint Signaling Independently of the Fanconi Anemia Core Complex. *Molecular Cell*, 32(3):313–324.

Cortez, D. (2015). Preventing replication fork collapse to maintain genome integrity. *DNA Repair*, 32:149–157.

Couch, F. B., Bansbach, C. E., Driscoll, R., Luzwick, J. W., Glick, G. G., Bétous, R., Carroll, C. M., Jung, S. Y., Qin, J., Cimprich, K. A., and Cortez, D. (2013). ATR phosphorylates SMARCAL1 to prevent replication fork collapse. *Genes and Development*, 27(14):1610–1623.

Crosetto, N., Bienko, M., Hibbert, R. G., Perica, T., Ambrogio, C., Kensche, T., Hofmann, K., Sixma, T. K., and Dikic, I. (2008). Human Wrnip1 is localized in replication factories in a ubiquitin-binding zinc finger-dependent manner. *Journal of Biological Chemistry*, 283(50):35173–35185.

Davis, E. J., Lachaud, C., Appleton, P., Macartney, T. J., Näthke, I., and Rouse, J. (2012). DVC1 (C1orf124) recruits the p97 protein segregase to sites of DNA damage. *Nature Structural & Molecular Biology*, 19(11):1093–1100.

Dungrawala, H., Bhat, K. P., Le Meur, R., Chazin, W. J., Ding, X., Sharan, S. K., Wessel, S. R., Sathe, A. A., Zhao, R., and Cortez, D. (2017). RADX Promotes Genome Stability and Modulates Chemosensitivity by Regulating RAD51 at Replication Forks. *Molecular Cell*, 67(3):374–386.e5.

Dungrawala, H., Rose, K. L., Bhat, K. P., Mohni, K. N., Glick, G. G., Couch, F. B., and Cortez, D. (2015). The Replication Checkpoint Prevents Two Types of Fork Collapse without Regulating Replisome Stability. *Molecular Cell*, 59(6):998–1010.

Follonier, C., Oehler, J., Herrador, R., and Lopes, M. (2013). Friedreich's ataxia–associated GAA repeats induce replication-fork reversal and unusual molecular junctions. *Nature Structural & Molecular Biology*, 20(4):486–494.

Fragkos, M., Ganier, O., Coulombe, P., and Méchali, M. (2015). DNA replication origin activation in space and time. *Nature Reviews Molecular Cell Biology*, 16(6):360–374.

Fugger, K., Chu, W. K., Haahr, P., Kousholt, A. N., Beck, H., Payne, M. J., Hanada, K., Hickson, I. D., and Sørensen, C. S. (2013). FBH1 co-operates with MUS81 in inducing DNA double-strand breaks and cell death following replication stress.1. Fugger, K. et al. FBH1 co-operates with MUS81 in inducing DNA double-strand breaks and cell death following replication stress. Nat. Commun. 4,. *Nature communications*, 4:1423.

Fugger, K., Mistrik, M., Danielsen, J. R., Dinant, C., Falck, J., Bartek, J., Lukas, J., and Mailand, N. (2009). Human Fbh1 helicase contributes to genome maintenance via pro- and anti-recombinase activities. *Journal of Cell Biology*, 186(5):655–663.

Fugger, K., Mistrik, M., Neelsen, K. J., Yao, Q., Zellweger, R., Kousholt, A. N., Haahr, P., Chu, W. K., Bartek, J., Lopes, M., Hickson, I. D., and Sørensen, C. S. (2015). FBH1 catalyzes regression of stalled replication forks. *Cell Reports*, 10(10):1749–1757.

Gaillard, H., García-Muse, T., and Aguilera, A. (2015). Replication stress and cancer. *Nature Reviews Cancer*, 15(5):276–289.

Gali, H., Juhasz, S., Morocz, M., Hajdu, I., Fatyol, K., Szukacsov, V., Burkovics, P., and Haracska, L. (2012). Role of SUMO modification of human PCNA at stalled replication fork. *Nucleic Acids Research*, 40(13):6049–6059.

Gari, K., Decaillet, C., Delannoy, M., Wu, L., and Constantinou, A. (2008a). Remodeling of DNA replication structures by the branch point translocase FANCM. *Proceedings of the National Academy of Sciences*, 105(42):16107–16112.

Gari, K., Décaillet, C., Stasiak, A. A. Z., Stasiak, A. A. Z., and Constantinou, A. (2008b). The Fanconi Anemia Protein FANCM Can Promote Branch Migration of Holliday Junctions and Replication Forks. *Molecular Cell*, 29(1):141–148.

Georgescu, R. E., Langston, L., Yao, N. Y., Yurieva, O., Zhang, D., Finkelstein, J., Agarwal, T., and O'Donnell, M. E. (2014). Mechanism of asymmetric polymerase assembly at the eukaryotic replication fork. *Nature Structural & Molecular Biology*, 21(8):664–670.

Guzman, C., Bagga, M., Kaur, A., Westermarck, J., and Abankwa, D. (2014). ColonyArea: An ImageJ plugin to automatically quantify colony formation in clonogenic assays. *PLoS ONE*, 9(3):14–17.

Haglund, K. and Stenmark, H. (2006). Working out coupled monoubiquitination. *Nature cell biology*, 8(11):1218–1219.

Halazonetis, T. D., Gorgoulis, V. G., and Bartek, J. (2008). An Oncogene-Induced DNA Damage Model for Cancer Development. *Science*, 319(5868):1352–1355.

Hanada, K., Budzowska, M., Davies, S. L., van Drunen, E., Onizawa, H., Beverloo, H. B., Maas, A., Essers, J., Hickson, I. D., and Kanaar, R. (2007). The structure-specific endonuclease Mus81 contributes to replication restart by generating double-strand DNA breaks. *Nature Structural & Molecular Biology*, 14(11):1096–1104.

Hanahan, D. and Weinberg, R. A. (2011). Hallmarks of cancer: The next generation. *Cell*, 144(5):646–674.

Hashimoto, Y., Chaudhuri, A. R., Lopes, M., and Costanzo, V. (2010). Rad51 protects nascent DNA from Mre11-dependent degradation and promotes continuous DNA synthesis. *Nature Structural & Molecular Biology*, 17(11):1305–1311.

Higgins, N. P., Kato, K., and Strauss, B. (1976). A model for replication repair in mammalian cells. *Journal of Molecular Biology*, 101(3):417–425.

Higgs, M. R., Reynolds, J. J., Winczura, A., Blackford, A. N., Borel, V., Miller, E. S., Zlatanou, A., Nieminuszczy, J., Ryan, E. L., Davies, N. J., Stankovic, T., Boulton, S. J., Niedzwiedz, W., and Stewart, G. S. (2015). BOD1L Is Required to Suppress Deleterious Resection of Stressed Replication Forks. *Molecular Cell*, 59(3):462–477.

Higgs, M. R. and Stewart, G. S. (2016). Protection or resection: BOD1L as a novel replication fork protection factor. *Nucleus*, 7(1):34–40.

Hishida, T., Iwasaki, H., Ohno, T., Morishita, T., and Shinagawa, H. (2001). A yeast gene, MGS1, encoding a DNA-dependent AAA(+) ATPase is required to maintain genome stability. *Proceedings of the National Academy of Sciences of the United States of America*, 98(15):8283–9.

Hishida, T. and Ohno, T. (2002). Saccharomyces cerevisiae MGS1 is essential in strains de ® cient in the RAD6 -dependent DNA damage tolerance pathway. *The EMBO Journal*, 21(8):2019–2029.

Hoffmann, S., Smedegaard, S., Nakamura, K., Mortuza, G. B., Räschle, M., de Opakua, A. I., Oka, Y., Feng, Y., Blanco, F. J., Mann, M., Montoya, G., Groth, A., Bekker-Jensen, S., and Mailand, N. (2016). TRAIP is a PCNA-binding ubiquitin ligase that protects genome stability after replication stress. *Journal of Cell Biology*, 212(1):63–75.

Huang, J., Liu, S., Bellani, M. A., Thazhathveetil, A., Ling, C., DeWinter, J. P., Wang, Y., Wang, W., and Seidman, M. M. (2013). The DNA Translocase FANCM/MHF Promotes Replication Traverse of DNA Interstrand Crosslinks. *Molecular Cell*, 52(3):434–446.

ichi Kawabe, Y., Seki, M., Yoshimura, A., Nishino, K., Hayashi, T., Takeuchi, T., Iguchi, S., Kusa, Y., Ohtsuki, M., Tsuyama, T., Imamura, O., Matsumoto, T., Furuichi, Y., Tada, S., and Enomoto, T. (2006). Analyses of the interaction of WRNIP1 with Werner syndrome protein (WRN) in vitro and in the cell. *DNA Repair*, 5(7):816–828.

Johnson, R. E., Klassen, R., Prakash, L., and Prakash, S. (2015). A major role of DNA Polymerase Delta in replication of both the leading and lagging DNA strands. *Molecular Cell*, 59(2):95–121.

Kanamori, M., Seki, M., Yoshimura, A., Tsurimoto, T., Tada, S., and Enomoto, T. (2011). Werner interacting protein 1 promotes binding of Werner protein to template-primer DNA. *Biological & pharmaceutical bulletin*, 34(8):1314–1318.

Kanu, N., Zhang, T., Burrell, R. A., Chakraborty, A., Cronshaw, J., DaCosta, C., Grönroos, E., Pemberton, H. N., Anderton, E., Gonzalez, L., Sabbioneda, S., Ulrich, H. D., Swanton, C., and Behrens, A. (2016). RAD18, WRNIP1 and ATMIN promote ATM signalling in response to replication stress. *Oncogene*, 35(30):4009–4019.

Kawabe, Y. I., Branzei, D., Hayashi, T., Suzuki, H., Masuko, T., Onoda, F., Heo, S. J., Ikeda, H., Shimamoto, A., Furuichi, Y., Seki, M., and Enomoto, T. (2001). A Novel Protein Interacts with the Werner's Syndrome Gene Product Physically and Functionally. *Journal of Biological Chemistry*, 276(23):20364–20369.

Kile, A. C., Chavez, D. A., Bacal, J., Eldirany, S., Korzhnev, D. M., Bezsonova, I., Eichman, B. F., and Cimprich, K. A. (2015). HLTF's Ancient HIRAN Domain Binds 3' DNA Ends to Drive Replication Fork Reversal. *Molecular Cell*, 58(6):1090–1100.

Kim, B. J., Chan, D. W., Jung, S. Y., Chen, Y., Qin, J., and Wang, Y. (2017). The Histone Variant MacroH2A1 Is a BRCA1 Ubiquitin Ligase Substrate. *Cell Reports*, 19(9):1758–1766.

Kim, J. H., Kang, Y. H., Kang, H. J., Kim, D. H., Ryu, G. H., Kang, M. J., and Seo, Y. S. (2005). In vivo and in vitro studies of Mgs1 suggest a link between genome instability and Okazaki fragment processing. *Nucleic Acids Research*, 33(19):6137–6150.

Kolinjivadi, A. M., Sannino, V., De Antoni, A., Zadorozhny, K., Kilkenny, M., Técher, H., Baldi, G., Shen, R., Ciccia, A., Pellegrini, L., Krejci, L., and Costanzo, V. (2017). Smarcal1-Mediated Fork Reversal Triggers Mre11-Dependent Degradation of Nascent DNA in the Absence of Brca2 and Stable Rad51 Nucleofilaments. *Molecular Cell*, 67(5):867–881.e7.

Lemaçon, D., Jackson, J., Quinet, A., Brickner, J. R., Li, S., Yazinski, S., You, Z., Ira, G., Zou, L., Mosammaparast, N., and Vindigni, A. (2017). MRE11 and EXO1 nucleases degrade reversed forks and elicit MUS81-dependent fork rescue in BRCA2-deficient cells. *Nature Communications*, 8(1):860.

Leman, A. R. and Noguchi, E. (2013). *The replication fork: Understanding the eukaryotic replication machinery and the challenges to genome duplication*, volume 4.

Leonard, A. C. and Méchali, M. (2013). DNA Replication Origins. *Cold Spring Harb Perspect Biol*, 5(10):a010116.

Leuzzi, G., Marabitti, V., Pichierri, P., and Franchitto, A. (2016). WRNIP 1 protects stalled forks from degradation and promotes fork restart after replication stress. *The EMBO journal*, 35(13):1–15.

Lin, J. R., Zeman, M. K., Chen, J. Y., Yee, M. C., and Cimprich, K. A. (2011). SHPRH and HLTF Act in a Damage-Specific Manner to Coordinate Different Forms of Postreplication Repair and Prevent Mutagenesis. *Molecular Cell*, 42(2):237–249.

Lomonosov, M., Anand, S., Sangrithi, M., Lomonosov, M., and Anand, S. (2003). Stabilization of stalled DNA replication forks by the BRCA2 breast cancer susceptibility protein service Stabilization of stalled DNA replication forks by the BRCA2 breast cancer susceptibility protein. pages 3017–3022.

Lopes, M., Cotta-Ramusino, C., Pellicioli, A., Liberi, G., Plevani, P., Muzi-Falconi, M., Newlon, C. S., and Foiani, M. (2001). The DNA replication checkpoint response stabilizes stalled replication forks. *Nature*, 412(6846):557–561.

Lord, C. J. and Ashworth, A. (2007). RAD51, BRCA2 and DNA repair: a partial resolution. *Nature Structural & Molecular Biology*, 14(6).

Lujan, S. A., Williams, J. S., and Kunkel, T. A. (2016). DNA Polymerases Divide the Labor of Genome Replication. *Trends in Cell Biology*, 26(9):640–654.

Macheret, M. and Halazonetis, T. D. (2015). DNA Replication Stress as a Hallmark of Cancer. *Annual Review of Pathology: Mechanisms of Disease*, 10(1):425–448.

Mailand, N., Gibbs-Seymour, I., and Bekker-Jensen, S. (2013). Regulation of PCNA–protein interactions for genome stability. *Nature Reviews Molecular Cell Biology*, 14(5):269–282.

Manosas, M., Perumal, S. K., Croquette, V., and Benkovic, S. J. (2012). Direct observation of stalled fork restart via fork regression in the T4 replication system. *Science*, 338(6111):1217–1220.

Mazin, A. V., Mazina, O. M., Bugreev, D. V., and Rossi, M. J. (2010). Rad54, the motor of homologous recombination. *DNA Repair*, 9(3):286–302.

Mcmahon, T., Zijl, P. C. M. V., and Gilad, A. A. (2012). ATM Kinase is Activated by Sindbis Viral Vector Infection Christine. *Virus Research*, pages 97–102.

Michel, B. and Sandler, S. J. (2017). Replication restart in bacteria. *Journal of Bacteriology*, 199(13):1–13.

Mijic, S., Zellweger, R., Chappidi, N., Berti, M., Jacobs, K., Mutreja, K., Ursich, S., Ray Chaudhuri, A., Nussenzweig, A., Janscak, P., and Lopes, M. (2017). Replication fork reversal triggers fork degradation in BRCA2-defective cells. *Nature Communications*, 8(1):859.

Moldovan, G. L., Dejsuphong, D., Petalcorin, M. I. R., Hofmann, K., Takeda, S., Boulton, S. J., and D'Andrea, A. D. (2012). Inhibition of homologous recombination by the PCNA-interacting protein PARI. *Molecular Cell*, 45(1):75–86.

Moldovan, G. L., Pfander, B., and Jentsch, S. (2007). PCNA, the Maestro of the Replication Fork. *Cell*, 129(4):665–679.

Motegi, A., Liaw, H.-J., Lee, K.-Y., Roest, H. P., Maas, A., Wu, X., Moinova, H., Markowitz, S. D., Ding, H., Hoeijmakers, J. H. J., and Myung, K. (2008). Polyubiquitination of proliferating cell nuclear antigen by HLTF and SHPRH prevents genomic instability from stalled replication forks. *Proceedings of the National Academy of Sciences of the United States of America*, 105(34):12411–12416.

Mourón, S., Rodriguez-Acebes, S., Martínez-Jiménez, M. I., García-Gómez, S., Chocrón, S., Blanco, L., and Méndez, J. (2013). Repriming of DNA synthesis at stalled replication forks by human PrimPol. *Nature Structural & Molecular Biology*, 20(12):1383–1389.

Munoz, I. M., Szyniarowski, P., Toth, R., Rouse, J., and Lachaud, C. (2014). Improved genome editing in human cell lines using the CRISPR method. *PLoS ONE*, 9(10).

Neelsen, K. J. and Lopes, M. (2015). Replication fork reversal in eukaryotes: from dead end to dynamic response. *Nature Reviews Molecular Cell Biology*, 16(4):207–220.

Neelsen, K. J., Zanini, I. M. Y., Herrador, R., and Lopes, M. (2013). Oncogenes induce genotoxic stress by mitotic processing of unusual replication intermediates. *Journal of Cell Biology*, 200(6):699–708.

Nomura, H., Yoshimura, A., Edo, T., Kanno, S. I., Tada, S., Seki, M., Yasui, A., and Enomoto, T. (2012). WRNIP1 accumulates at laser light irradiated sites rapidly via its ubiquitin-binding zinc finger domain and independently from its ATPase domain. *Biochemical and Biophysical Research Communications*, 417(4):1145–1150.

Page, A. N., George, N. P., Marceau, A. H., Cox, M. M., and Keck, J. L. (2011). Structure and biochemical activities of Escherichia coli MgsA. *Journal of Biological Chemistry*, 286(14):12075–12085.

Pepe, A. and West, S. C. (2014). MUS81-EME2 promotes replication fork restart. *Cell Reports*, 7(4):1048–1055.

Petermann, E. and Helleday, T. (2010). Pathways of mammalian replication fork restart. *Nature Reviews Molecular Cell Biology*, 11(10):683–687.

Petermann, E., Orta, M. L., Issaeva, N., Schultz, N., and Helleday, T. (2010). Hydroxyurea-Stalled Replication Forks Become Progressively Inactivated and Require Two Different RAD51-Mediated Pathways for Restart and Repair. *Molecular Cell*, 37(4):492–502.

Pines, J. (2011). Cubism and the cell cycle: The many faces of the APC/C. *Nature Reviews Molecular Cell Biology*, 12(7):427–438.

Poole, L. A. and Cortez, D. (2017). Functions of SMARCAL1, ZRANB3, and HLTF in maintaining genome stability. *Critical Reviews in Biochemistry and Molecular Biology*, 0(0):1–19.

Ray Chaudhuri, A., Hashimoto, Y., Herrador, R., Neelsen, K. J., Fachinetti, D., Bermejo, R., Cocito, A., Costanzo, V., and Lopes, M. (2012). Topoisomerase I poisoning results in PARP-mediated replication fork reversal. *Nature Structural & Molecular Biology*, 19(4):417–423.

Ribeyre, C., Zellweger, R., Chauvin, M., Bec, N., Larroque, C., Lopes, M., and Constantinou, A. (2016). Nascent DNA Proteomics Reveals a Chromatin Remodeler Required for Topoisomerase I Loading at Replication Forks. *Cell Reports*, 15(2):300–309.

Saibil, H. (2013). Chaperone machines for protein folding, unfolding and disaggregation. *Nature Reviews Molecular Cell Biology*, 14(10):630–642.

Saldivar, J. C., Cortez, D., and Cimprich, K. A. (2017). The essential kinase ATR: ensuring faithful duplication of a challenging genome. *Nature Reviews Molecular Cell Biology*, 18(10):622–636.

Saugar, I., Parker, J. L., Zhao, S., and Ulrich, H. D. (2012). The genome maintenance factor Mgs1 is targeted to sites of replication stress by ubiquitylated PCNA. *Nucleic Acids Research*, 40(1):245–257.

Schlacher, K., Christ, N., Siaud, N., Egashira, A., Wu, H., and Jasin, M. (2011). Double-strand break repair-independent role for BRCA2 in blocking stalled replication fork degradation by MRE11. *Cell*, 145(4):529–542.

Schlacher, K., Wu, H., and Jasin, M. (2012). A Distinct Replication Fork Protection Pathway Connects Fanconi Anemia Tumor Suppressors to RAD51-BRCA1/2. *Cancer Cell*, 22(1):106–116.

Schmutz, I., Timashev, L., Xie, W., Patel, D. J., and de Lange, T. (2017). TRF2 binds branched DNA to safeguard telomere integrity. *Nature Structural & Molecular Biology*, 24(9).

Seigneur, M., Bidnenko, V., Ehrlich, S. D., and Michel, B. (1998). RuvAB acts at arrested replication forks. *Cell*, 95(3):419–430.

Shibata, A., Moiani, D., Arvai, A., Perry, J., Harding, S., Genois, M.-M., Maity, R., vanRossum Fikkert, S., Kertokalio, A., Romoli, F., Ismail, A., Ismalaj, E., Petricci, E., Neale, M., Bristow, R., Masson, J.-Y., Wyman, C., Jeggo, P., and Tainer, J. (2014). DNA Double-Strand Break Repair Pathway Choice Is Directed by Distinct MRE11 Nuclease Activities. *Molecular Cell*, 53(1):7–18.

Simandlova, J., Zagelbaum, J., Payne, M. J., Chu, W. K., Shevelev, I., Hanada, K., Chatterjee, S., Reid, D. A., Liu, Y., Janscak, P., Rothenberg, E., and Hickson, I. D. (2013). FBH1 helicase disrupts RAD51 filaments in vitro and modulates homologous recombination in mammalian cells. *Journal of Biological Chemistry*, 288(47):34168–34180.

Sogo, J. M., Lopes, M., and Foiani, M. (2002). Fork Reversal and ssDNA Accumulation at Stalled Replication Forks Owing to Checkpoint Defects. *Science*, 297(5581):599–602.

Somyajit, K., Gupta, R., Sedlackova, H., Neelsen, K. J., Ochs, F., Rask, M.-b., Choudhary, C., and Lukas, J. (2017). Redox-sensitive alteration of replisome architecture safeguards genome integrity. *Science*, 358(November):797–802.

Stracker, T. H. and Petrini, J. H. J. (2011). The MRE11 complex: starting from the ends. *Nature Reviews Molecular Cell Biology*, 12(2):90–103.

Suzuki, N., Rohaim, A., Kato, R., Dikic, I., Wakatsuki, S., and Kawasaki, M. (2016). A novel mode of ubiquitin recognition by the ubiquitin-binding zinc finger domain of WRNIP1. *FEBS Journal*, 283(11):2004–2017.

Taglialatela, A., Alvarez, S., Leuzzi, G., Sannino, V., Ranjha, L., Huang, J.-W., Madubata, C., Anand, R., Levy, B., Rabadan, R., Cejka, P., Costanzo, V., and Ciccia, A. (2017). Restoration of Replication Fork Stability in BRCA1- and BRCA2-Deficient Cells by Inactivation of SNF2-Family Fork Remodelers. *Molecular Cell*, 68(2):414–430.e8.

Tan, P., He, L., Cui, J., Qian, C., Cao, X., Lin, M., Zhu, Q., Li, Y., Xing, C., Yu, X., Wang, H. Y., and Wang, R.-F. (2017). Assembly of the WHIP-TRIM14-PPP6C Mitochondrial Complex Promotes RIG-I-Mediated Antiviral Signaling. *Molecular Cell*, 68(2):293–307.e5.

Thangavel, S., Berti, M., Levikova, M., Pinto, C., Gomathinayagam, S., Vujanovic, M., Zellweger, R., Moore, H., Lee, E. H., Hendrickson, E. A., Cejka, P., Stewart, S., Lopes, M., and Vindigni, A. (2015). DNA2 drives processing and restart of reversed replication forks in human cells. *Journal of Cell Biology*, 208(5):545–562.

Toledo, L., Neelsen, K. J., and Lukas, J. (2017). Replication Catastrophe: When a Checkpoint Fails because of Exhaustion. *Molecular Cell*, 66(6):735–749.

Toledo, L. I., Altmeyer, M., Rask, M. B., Lukas, C., Larsen, D. H., Povlsen, L. K., Bekker-Jensen, S., Mailand, N., Bartek, J., and Lukas, J. (2014). ATR prohibits replication catastrophe by preventing global exhaustion of RPA. *Cell*, 156(1-2):374.

Tsurimoto, T., Shinozaki, A., Yano, M., Seki, M., and Enomoto, T. (2005). Human Werner helicase interacting protein 1 (WRNIP1) functions as novel modulator for DNA polymerase. *Genes to Cells*, 10(1):13–22.

Urban, V., Dobrovolna, J., and Janscak, P. (2017). Distinct functions of human RecQ helicases during DNA replication. *Biophysical Chemistry*, 225:20–26.

van den Boom, J., Wolf, M., Weimann, L., Schulze, N., Li, F., Kaschani, F., Riemer, A., Zierhut, C., Kaiser, M., Iliakis, G., Funabiki, H., and Meyer, H. (2016). VCP/p97 Extracts Sterically Trapped Ku70/80 Rings from DNA in Double-Strand Break Repair. *Molecular Cell*, 64(1):189–198.

Vujanovic, M., Krietsch, J., Raso, M. C., Terraneo, N., Zellweger, R., Schmid, J. A., Taglialatela, A., Huang, J. W., Holland, C. L., Zwicky, K., Herrador, R., Jacobs, H., Cortez, D., Ciccia, A., Penengo, L., and Lopes, M. (2017). Replication Fork Slowing and Reversal upon DNA Damage Require PCNA Polyubiquitination and ZRANB3 DNA Translocase Activity. *Molecular Cell*, 67(5):882–890.e5.

Wang, A. T., Kim, T., Wagner, J. E., Conti, B. A., Lach, F. P., Huang, A. L., Molina, H., Sanborn, E. M., Zierhut, H., Cornes, B. K., Abhyankar, A., Sougnez, C., Gabriel, S. B., Auerbach, A. D., Kowalczykowski, S. C., and Smogorzewska, A. (2015). A Dominant Mutation in Human RAD51 Reveals Its Function in DNA Interstrand Crosslink Repair Independent of Homologous Recombination. *Molecular Cell*, 59(3):478–490.

Wendler, P., Ciniawsky, S., Kock, M., and Kube, S. (2012). Structure and function of the AAA+ nucleotide binding pocket. *Biochimica et Biophysica Acta (BBA) - Molecular Cell Research*, 1823(1):2–14.

Weston, R., Peeters, H., and Ahel, D. (2012). ZRANB3 is a structure-specific ATP-dependent endonuclease involved in replication stress response. *Genes and Development*, 26(14):1558–1572.

Yang, Y., Liu, Z., Wang, F., Temviriyanukul, P., Ma, X., Tu, Y., Lv, L., Lin, Y. F., Huang, M., Zhang, T., Pei, H., Chen, B. P., Jansen, J. G., De Wind, N., Fischhaber, P. L., Friedberg, E. C., Tang, T. S., and Guo, C. (2015). FANCD2 and REV1 cooperate in the protection of nascent DNA strands in response to replication stress. *Nucleic Acids Research*, 43(17):8325–8339.

Yeeles, J. T. P., Deegan, T. D., Janska, A., Early, A., and Diffley, J. F. X. (2015). Regulated eukaryotic DNA replication origin firing with purified proteins. *Nature*, 519(7544):431–435.

Yoshimura, A., Kobayashi, Y., Tada, S., Seki, M., and Enomoto, T. (2014). WRNIP1 functions upstream of DNA polymerase η in the UV-induced DNA damage response. *Biochemical and Biophysical Research Communications*, 452(1):48–52.

Yoshimura, A., Seki, M., Kanamori, M., Tateishi, S., Tsurimoto, T., Tada, S., and Enomoto, T. (2009). Physical and functional interaction between WRNIP1 and RAD18. *Genes & genetic systems*, 84(2):171–178.

Yusufzai, T. and Kadonaga, J. T. (2008). HARP Is an ATP-Driven Annealing Helicase. *Science*, 322(5902):748–750.

Yusufzai, T. and Kadonaga, J. T. (2010). Annealing helicase 2 (AH2), a DNA-rewinding motor with an HNH motif. *Proceedings of the National Academy of Sciences of the United States of America*, 107(49):20970–20973.

Yusufzai, T., Xiangduo, K., Kyoko, Y., and Kadonaga, J. T. (2009). The annealing helicase HARP is recruited to DNA repair sites via an interaction with RPA. *Genes and Development*, 23(20):2400–2404.

Zellweger, R., Dalcher, D., Mutreja, K., Berti, M., Schmid, J. A., Herrador, R., Vindigni, A., and Lopes, M. (2015). Rad51-mediated replication fork reversal is a global response to genotoxic treatments in human cells. *Journal of Cell Biology*, 208(5):563–579.

Zeman, M. K. and Cimprich, K. A. (2014). Causes and consequences of replication stress. *Nature cell biology*, 16(1):2–9.

Zeman, M. K., Lin, J. R., Freire, R., and Cimprich, K. A. (2014). DNA damage-specific deubiquitination regulates Rad18 functions to suppress mutagenesis. *Journal of Cell Biology*, 206(2):183–197.

Zhang, J., Dai, Q., Park, D., and Deng, X. (2016). Targeting DNA replication stress for cancer therapy. *Genes*, 7(8).

Zhang, J., Dewar, J. M., Budzowska, M., Motnenko, A., Cohn, M. A., and Walter, J. C. (2015). DNA interstrand cross-link repair requires replication-fork convergence. *Nature Structural & Molecular Biology*, 22(3):242–247.